The University of Kansas


Technical Report

# Designing a Multichannel Sense-and-Avoid Radar for Small UASs

Mikhail Zakharov

ITTC-FY2014-TR-70093-02

February 2014

Project Sponsor: NASA

*Abstract*

This thesis presents the design, analysis and test results of a 1.445 GHz Frequency-Modulated Continuous Wave (FMCW) collision-avoidance radar for Unmanned Aircraft Systems (UASs). This radar system is being developed by the department of Electrical Engineering (EE) in coordination with the Aerospace Engineering (AE) department and is intended to provide situational awareness for a 40% Yak-54 model aircraft by providing range, radial velocity and angle-of-arrival (AoA) information for nearby targets. A target's range and Doppler is determined by employing a two-dimensional (2-D) Fast Fourier Transform (FFT) on the received signal which maps the target to a specific range-Doppler bin. An array of receiving antennas is used to determine a target's elevation and azimuth angles by exploiting the received signal's phase difference at each individual antenna.

# Table of Contents

## Table of Figures

# Introduction

## Background

Unmanned Aircraft Systems have gained much attention over the last several years. A significant increase in research is being seen in the development and advancement of UASs for environmental and agricultural purposes. UASs are more commonly used in countries like Japan and Canada, where the airspace is subject to fewer rules and regulations as opposed to the United States where the use of UASs for commercial applications is currently unlawful. The Federal Aviation Administration (FAA) does, however, allow certified operators to conduct UAS flights, but only outside of restricted airspace [1]. Although UASs come in various shapes and sizes, they can usually be classified under one of the following two types of categories: Fixed wing and rotary wing UASs. Fixed wing UASs are capable of flying at high speeds for a considerable length of time but are subject to stalling. Large and heavy fixed wing UASs will usually require a landing strip for takeoff and landing. Rotary wing (copter) UASs have the benefit of being able to hover and fly at low speeds and altitude, and they can take off and land vertically, thus eliminating the need for a runway [8].

### Motivation

#### *Economic Motivation*

Agricultural farming is currently undergoing a transformation into what is known as Precision Agriculture. In traditional farming, when an herbicidal problem, for example, is detected locally the idea is to try to prevent the problem from spreading by subjecting the whole field to herbicide control. But is it necessary to have the entire field covered with some controlling agent if it can be known beforehand the exact locations where this problem persists and attend to the problem only where it is necessary? Precision agriculture is focused on solving problems locally rather than globally. This method consequently reduces the amount of time and resources needed such as herbicides, pesticides, fertilizers etc… for agricultural farming. Quick surveys of crop fields from UASs not only permit farmers to closely monitor their field's condition but allow for a quick response if needed.

Apart from agricultural applications, UASs can enhance the effectiveness of search and rescue missions as well as humanitarian response to natural disasters, especially where human safety is in question. Traffic control, scientific research, and law enforcement are other examples of applications which would profit from UASs.

Tens of thousands of miles of pipelines are used throughout the U.S. to transport oil and gas [2]. Disruptions in the flow of these resources can have significant ramifications. Constant surveillance of pipelines is important in reducing any risks posed to the pipeline network, such as damage or disruptions caused by natural phenomenon. Current aerial pipeline patrol services require manned aircraft. Replacing human piloted planes with UASs can allow for better surveillance in areas that require low altitude flights or are hard to reach due to challenging terrain.

*Safety Motivation*

Current FAA regulations require that public operators obtain a Certificate of Authorization (COA) for UAS flights. Such authorizations usually limit UAS flights to visual meteorological conditions, daytime hours and prohibit flying over populated areas [1]. To truly realize the previously mentioned benefits, UASs must not be constrained by the COA limits, but rather be eventually integrated into the National Air Space (NAS). The key obstacle for UAS integration into the NAS is guaranteeing that UAS operations do not pose any danger to people and property in the air and on the ground. The Federal Aviation Administration, which regulates civil aviation, requires that UASs meet its minimum standards for Sense and Avoid (SAA). According to the FAA's UAS roadmap for integrating UAS into the NAS, the current SAA technology is immature and cannot substitute for the see-and-avoid as well as visual sighting that manned flights benefit from [4].

# Chapter 1: Sense-and-Avoid Radar for Small UASs

## 1.1 Requirements

The Aerospace Engineering (AE) department at the University of Kansas (KU) is developing an autonomous flight system for small UASs. One of the functionalities of this system is to be able to reroute a flight path if the current course is on a path to collision with either a static or dynamic target. To properly reroute a flight course, it is necessary that the range and direction to the target as well as its velocity be known. Therefore, the requirements of the radar that will provide the necessary information to the autonomous flight controller are largely driven by the requirements established by the AE department that will enable their autonomous flight system to effectively function. For example, simulations performed at the AE department, have revealed that a 40% Yak-54 being on a head on collision path with another Yak-54 can still avoid air-collision even if the two planes get within 100 m, assuming that both are traveling at their maximum speed of 36 m/s [3]. To create a safety margin, the minimum distance between the UAS and any target was increased to 300 m. Requirements for the sense-and-avoid radar are summarized in Table 1.1.

**Table 1.1 Sense-and-avoid radar requirements.**

| Parameter | Value |
|---|---|
| **Target Detection Range** | 300 m to 800 m |
| **Range Resolution** | 10 m |
| **Angular Coverage** | ±15° elevation<br>±180° azimuth |
| **Angle Accuracy** | ±3° |
| **Update Rate** | 10 Hz |

The radar system that is being developed must be able to detect targets from 300 m to 800 m, provide a range resolution of at least 10 m, be able to identify targets ±180°azimuthally and ±15°in elevation while providing ±3°of angular accuracy and being able to update the afore mentioned parameters at a rate of 10 Hz. Although the radar can only estimate radial velocity, the tangential velocity component which is required to completely characterize a target's velocity vector can be determined through additional signal processing that is currently being investigated.

## 1.2 Selecting Radar Type

Choosing the type of radar depends on if and how well that radar technology can achieve its application's requirements. This section will examine some pros and cons of two radar types, namely pulse radar and Frequency Modulated Continuous Wave (FMCW) radar sometimes referred to as broadband radar.

### 1.2.1 Pulse and FMCW Radar Characteristics

Both radar types are capable of providing a target's range, Doppler and bearing information, but differ in the method used for extracting that information. For example, Figure 1.1 shows the transmitted waveform as well as the received signal due to a point target for a pulse radar. The duration between the first and second pulse is the pulse repetition period (PRP) and the duration of every pulse is $T_P$. Pulse radars can also be characterized by their duty factor, $D$ as shown in Equation 1.1, which typically ranges from 1% to 20%.

$$\boldsymbol{D} = \frac{T_P}{PRP} \ [unitless] \tag{1.1}$$

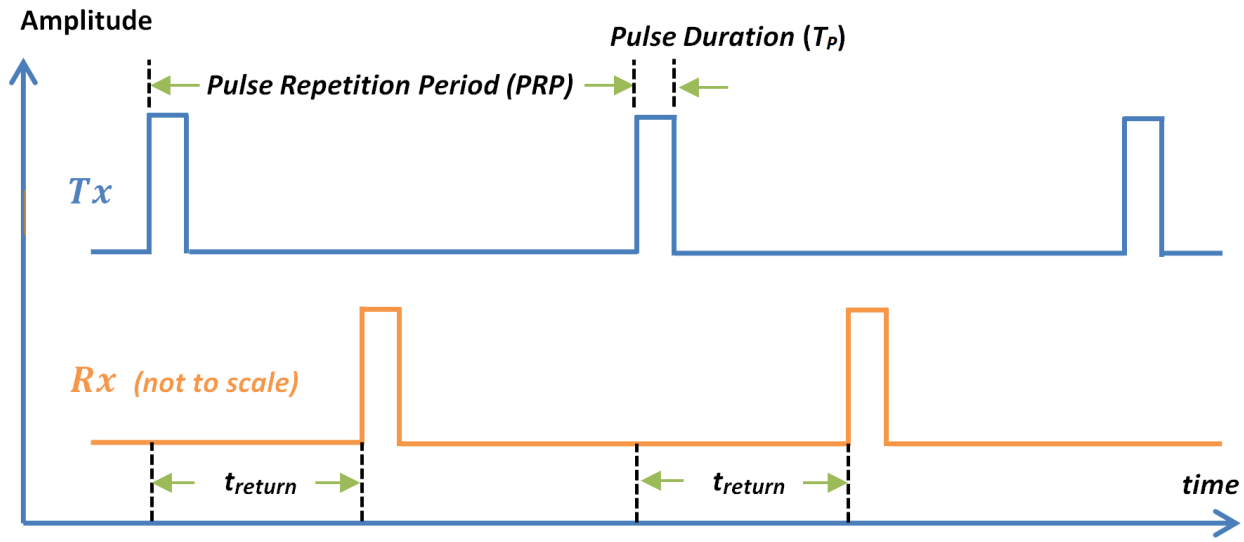


**Figure 1.1 Determining range with a pulse radar.**

The range to the target can be determined by timing the duration that it takes for the transmitted signal's echo to return (shown as $t_{return}$) and using Equation 1.2 to solve for range, where $c$ represents the speed of light in free space and will do so for the remainder of this text. Note that a factor of 2 is necessary to account for the round trip time. The farther the target is away from the radar the greater the return time will be.

$$\boldsymbol{Range} = \frac{c * t_{return}}{2} \ [m] \tag{1.2}$$

An FMCW radar shown in Figure 1.2, transmits a frequency-modulated wave (a sawtooth wave in this case) only the roundtrip time is found by taking the difference in frequency ($\Delta f$) between the current transmit and receive waveforms and using Equation 1.3 to solve for $t_{return}$, where $B$ and $SRP$ are the bandwidth and the duration of one period of the sawtooth wave, respectively.

$$t_{return} = \Delta f \frac{SRP}{B} \ [s] \tag{1.3}$$

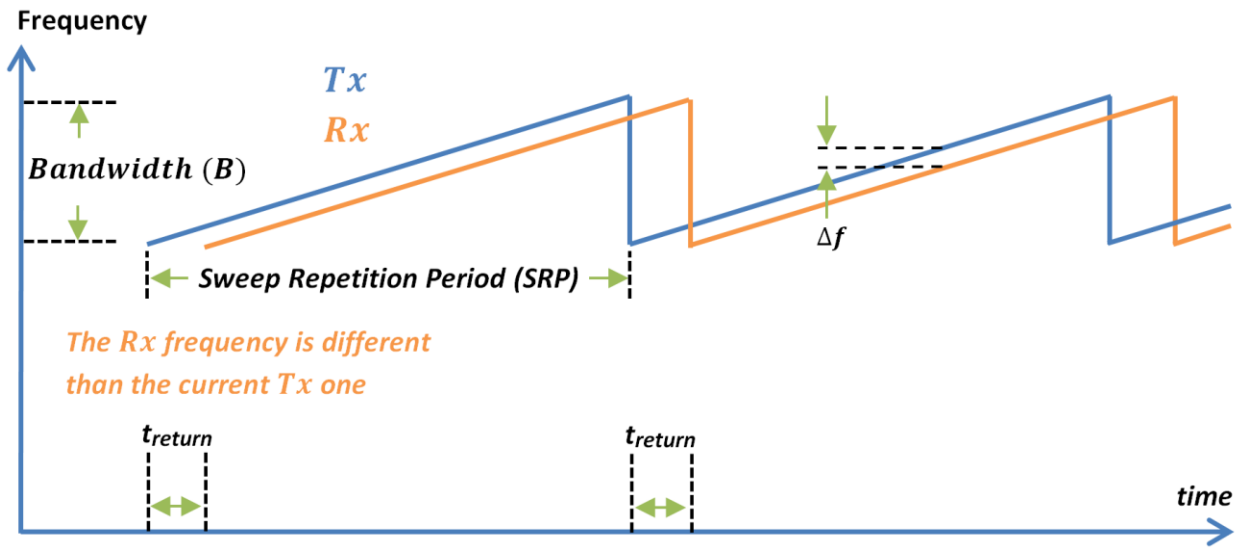


**Figure 1.2 Determining range with an FMCW radar.**

Equation 1.2 can then be used to determine range. The farther the target is away from this type of radar the greater the frequency difference ($\Delta f$) will be. Note that the pulse radar transmits a finite pulse whereas the FMCW radar transmits continuously.

Another key difference between the two technologies is that a pulse radar can use one antenna to both transmit and receive since the radar cannot simultaneously transmit and receive. Having one antenna that serves as both a receiver and transmitter can reduce the size of the radar, but this comes at a cost because the radar cannot receive while transmitting and thus will be blinded for a period of time equal to the pulse duration. A FMCW radar, on the other hand, transmits continuously and thus requires an additional antenna to receive, but does not suffer from minimum target (blind) range.

### *Power Consideration*

Because pulse radars do not transmit continuously, the average power transmitted does not equal the peak power (i.e., instantaneous power of the pulse). For example, a typical radar used for short range detection might have a 100 ns pulse duration ($T_P$) and a pulse repetition frequency (PRF) of 3 kHz. If the radar radiates on average 300 mW of power, then for the duration of every pulse the radar must transmit 1 kW of power according to Equation 1.4. Such high power pulses usually require a magnetron which can be fairly large and bulky in size. Also, magnetrons cannot be turned on instantly but require some amount of time to warm up [5].

$$\boldsymbol{P_{Tx}} = \frac{P_{AVG}}{T_P * PRF} \ [W] \tag{1.4}$$

For an FMCW radar, the peak transmit power is equal to the average transmit power since the radar transmits continuously. Therefore, to transmit 300 mW of average power, a (continuous) signal of 300 mW would need to be transmitted. For such low signal power, a small solid-state amplifier will suffice.

One way of reducing the peak transmit power in a pulse radar while keeping the average power constant would be to increase the pulse duration. There is, however, an upper limit on the pulse duration resulting from the unavoidable blind range due to the radar not being able to receive while transmitting. The blind range cannot be greater than the minimum required detection range of 300 m. Solving Equation 1.2 for $t_{return}$ and using the minimum detection range results in a return time of 2 μs. Therefore, the maximum pulse duration due to blind range can be 2 μs. Increasing the PRF can also reduce the peak transmit power. The upper PRF limit is determined by the maximum detectable range since the radar cannot begin transmitting another pulse until the previous pulse's echo (due to a target at maximum range) is received. Solving Equation 1.2 for $t_{return}$ and using the maximum detection range of 800 m, results in about 5.3 μs which is also the minimum PRP, and whose inverse is the maximum PRF, a value of 187.5 kHz. Using the maximum pulse duration of 2 μs and the maximum PRF of 187.5 kHz in Equation 1.4 results in a transmit power of 800 mW. This peak transmit power is about 2.7 times greater than the peak (and average) transmit power of 300 mW for the FMCW technology. It is worth mentioning that if for any reason the required minimum detection range is reduced, then the ratio between the pulse and FMCW radars' peak transmit powers will be greater than 2.7.

*Transmit Signal Bandwidth*

Another important difference that must be considered is the amount of bandwidth required for short range detection. For pulse radars that transmit a tone, the bandwidth of the pulse is (approximately) inversely proportional to the pulse duration as shown in Equation 1.5. Therefore, increasing the pulse duration will

$$\boldsymbol{B} \cong \frac{1}{T_P} \ [Hz] \quad (for\ pulse\ radar\ only) \tag{1.5}$$

consequently decrease the bandwidth of the pulse. For example, increasing the pulse duration to 2 μs (as was done in the previous section for the sake of reducing the peak transmit power) will reduce the bandwidth to about 500 kHz. As will be shown later, the required range resolution will necessitate the bandwidth of the transmit signal to be much greater than 500 kHz. To circumvent this problem, pulse compression can be exploited. With pulse compression, the bandwidth of the transmit signal depends not on the pulse duration, but rather on the bandwidth of the actual signal being transmitted. For example, if

a frequency-modulated sawtooth wave whose bandwidth is 15 MHz is transmitted for the duration of 2 μs, then the transmitted signal's bandwidth will be 15 MHz and not 500 kHz.

Pulse compression is also used in FMCW radars (as its name implies) because the bandwidth of the transmit signal doesn't correspond to the SRP (i.e., the duration of each pulse) but to the bandwidth of the frequency-modulated wave. For example, the sawtooth wave that is transmitted as was shown in Figure 1.2, has a bandwidth that is equal to the difference between the highest and lowest frequencies.

*Range and Doppler Resolution*

In radar terminology, range resolution is defined as the smallest distance between two targets that can still be discerned as two separate targets. Equation 1.6 shows the relationship between range resolution ($\Delta R$) and bandwidth ($B$).

$$\Delta \boldsymbol{R} = \frac{c}{2B} \ [m] \tag{1.6}$$

Based on this equation, at least 15 MHz of bandwidth is necessary to achieve the required range resolution of 10 m. Recall that this would require a pulse radar to use pulse compression if the peak transmit power is also to be minimized.

Doppler frequency resolution relates to the smallest difference in frequency between two signals that can still be distinguished as two separate signals. Frequency resolution is inversely related to the observation time ($t$) as shown in Equation 1.7.

$$\Delta \boldsymbol{f_D} \cong \frac{1}{t} \ [Hz] \tag{1.7}$$

For both radar types, the observation time will be 100 ms due to the 10 Hz update rate requirement. This results in a Doppler resolution of 10 Hz.

*Leakage Signal*

One of the major drawbacks of FMCW radars is the presence of the leakage signal. Since this technology receives while transmitting, the transmitted signal is always present at the receiving antenna. For monostatic radars, where the receiver and transmitter are in close proximity of each other, the received leakage signal strength can be many orders of magnitude larger than the signal of interest. Not mitigating the leakage signal can result in poor dynamic range and even lead to receiver saturation.

Since an FMCW radar constantly transmits, it is easier to track rather than a pulse radar. However, this is actually a benefit since the radar being proposed in this paper is not meant for an evasive purpose but for commercial and civil applications.

*Summary*

It was found that a FMCW radar is better suited for short range target detection because it is not limited by blind range unlike the pulse radar. The FMCW technology was also found to transmit almost three times less signal power than its counterpart resulting in a lower peak transmit power. However, using a FMCW radar will require resolving the problematic leakage signal.

## 1.3 FMCW Radar Theory

FMCW radars, as their name implies, transmit a frequency modulated signal. The type of modulation scheme used largely depends on the application. Some examples of modulation patterns are sawtooth modulation (linear frequency-modulation), triangular modulation, square-wave modulation [frequency-shift keying (FSK)] and stepped modulation (staircase)]. The sawtooth modulation technique was chosen for this prototype radar. This linear frequency-modulated signal is oftentimes referred to as a "chirp".

### 1.3.1 Accounting for the Doppler Shift

When a linear frequency-modulated signal is transmitted, the signal undergoes a delay proportional to the target's distance. If there is no relative motion between the radar and the object (i.e. the radial velocity is zero), the received echo is the exact replica of the transmitted signal only time delayed by $t_{return}$, as was shown in Figure 1.2. This time delay offsets the received signal such that there is an instantaneous difference in frequency when comparing the transmitted and received signals. This difference in frequency, also known as the beat frequency, is shown as $\Delta f$ in Figure 1.2 and is related to the distance between the radar and target through Equation 1.8. Note that Equation 1.8 is just a substitution of Equation 1.3 into Equation 1.2. It should be mentioned that the beat frequency is constant only between the time the echo (orange) is received and when a new frequency sweep (blue) beings.

$$\boldsymbol{Range} = \frac{c * \Delta f * SRP}{2B} \ [m] \tag{1.8}$$

The method used for finding the beat frequency as well as mapping the frequency to a specific range will be explained later.

When there is relative motion between the radar and an object, the reflected signal will undergo a frequency shift due to the Doppler Effect. This shift is most commonly referred to as the Doppler shift

and is shown as $f_D$ in Figure 1.3. For objects moving away from the radar, the entire spectrum of the echo signal will decrease by the Doppler shift amount, and for objects moving toward the radar, the echo signal's spectrum will increase by the Doppler shift.

The process in the receiver that determines the beat frequency has no way of knowing whether the difference in frequency is due to range or a combination of range and the Doppler shift. The beat frequency denoted by $\Delta f'$ is used in Figure 1.3 to signify the presence of a Doppler shift. Therefore, when distance is being calculated from the beat frequency, the Doppler shift ($f_D$) will introduce an error because the beat frequency used in Equation 1.8 isn't due entirely to range. When a Doppler shift is present, the resulting range can be determined using Equation 1.9.

$$\boldsymbol{Range'} = \frac{c * (\Delta f \pm f_D) * SRP}{2B} \quad [m] \tag{1.9}$$

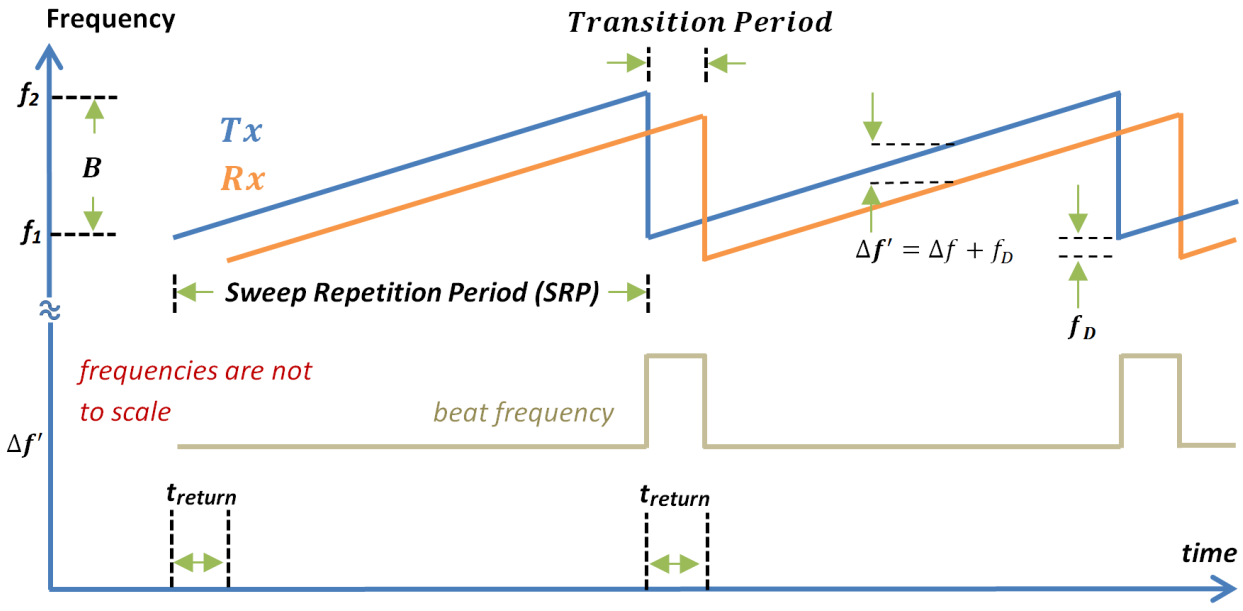


Figure 1.3 Transmit and receive waveforms due to a point target in an FMCW radar.

The error in range due to the Doppler shift can be calculated using Equation 1.10.

$$\boldsymbol{Range\ Error} = \pm\frac{c * f_D * SRP}{2B} \quad [m] \tag{1.10}$$

### 1.3.2 Range Error Due to the Doppler Shift

To calculate the maximum possible error in range caused by the Doppler shift, we must know the maximum Doppler shift that can occur between the radar and the object. We must also determine what the bandwidth and SRP of the signal are. Equation 1.12 shows how the Doppler shift can be calculated based on radial velocity, $v_r$ and the signal's wavelength ($\lambda$).

$$\boldsymbol{\lambda} = \frac{c}{f} \ [m] \tag{1.11}$$

$$\boldsymbol{f_D} = -\frac{2v_r}{\lambda} \ [Hz] \tag{1.12}$$

It is known that the maximum speed of the 40% Yak-54 is approximately 36 m/s. If another Yak-54 were to fly toward the radar mounted Yak-54 head on, then the radial velocity will be 72 m/s. The chirp has a center frequency of 1.445 GHz (for reasons that will be discussed later). With these values, the maximum Doppler frequency is found to be 694 Hz. The bandwidth of the chirp is dictated by the required range resolution (see Equation 1.6). Recall that to satisfy the 10 m range resolution requirement, the bandwidth of the chirp must be at least 15 MHz. Using 694 Hz as the maximum Doppler shift, 15 MHz for bandwidth, and 200 μs for SRP (for reasons that will be mentioned later) in Equation 1.11 results in a range error of ± 1.39 m, a value that is well below the required range resolution of 10 m. Therefore, the error due to the Doppler shift may be considered insignificant. Otherwise, given the knowledge of both $\Delta f$ and $f_D$, this error could be removed.

### 1.3.3 Digital Signal Processing

*Extracting Range Information*

It has been established that computing the radar's range to a target consists of finding the beat frequency and applying Equation 1.9. Hereon, the term "beat signal" will be used to relate to the video signal having the beat frequency characteristic. One method of determining the beat frequency is to sample the beat signal and then perform a fast Fourier transform (FFT) over the sampled sequence. Sampling the beat signal over the transition period (see Figure 1.3) should be avoided since during that time frame it is not proportional to range. When using some sort of memory storage, it is common to form a data matrix with the sampled values as depicted in Figure 1.4. The sampled voltage values for successive frequency sweeps will be stored in adjacent columns. The beat frequency shown as a golden colored waveform is also depicted as a sinusoid in the time domain being sampled. The total number of rows (or samples) in a column will depend on the sampling frequency as well as the duration of the frequency sweep. The number of columns in this matrix will depend on the number of frequency sweeps required by the

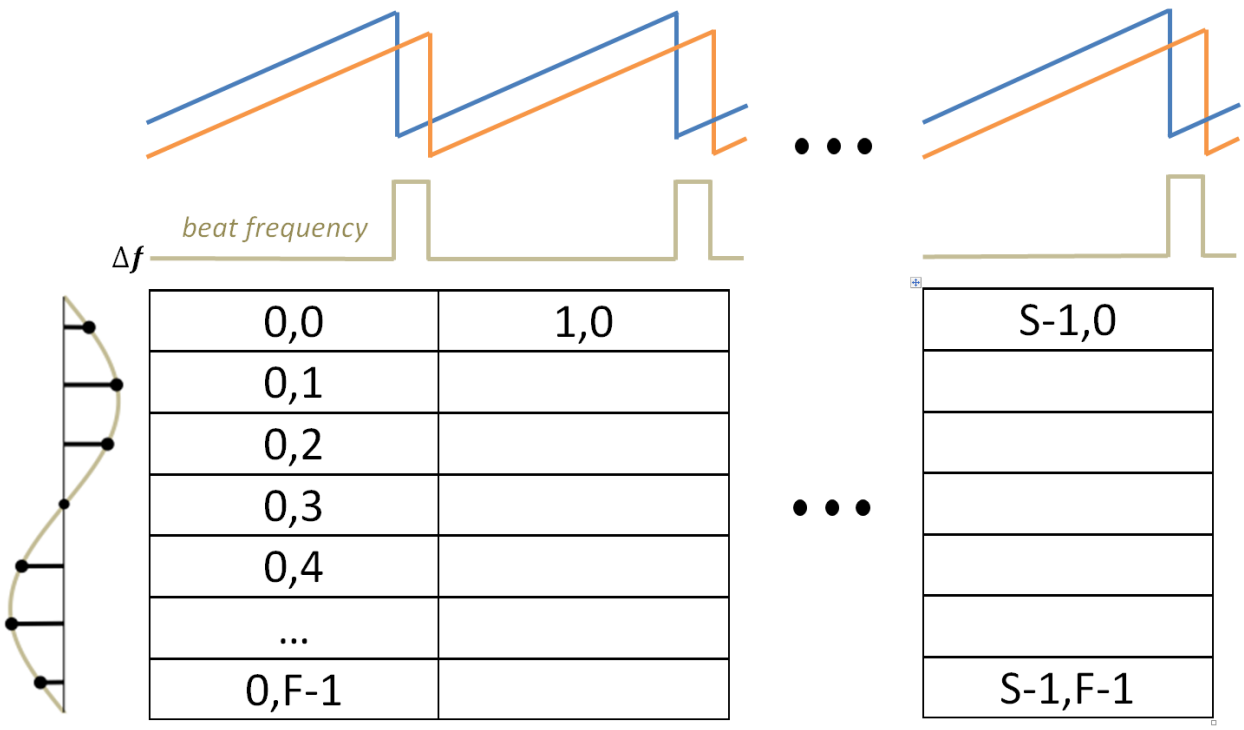


**Figure 1.4 A data matrix used for organizing samples of the beat signal.**

processing system before the data is processed, after which the process repeats. Data in a column are commonly referred to as the "fast time" data because a column of data is filled within one frequency sweep. Conversely, row data is referred to as the "slow time" data since only one value in any given row is stored for every frequency sweep. Every cell in the data matrix is labeled with a pair of indices that correspond to a particular column and row.

*Extracting Doppler Information*

It was brought to attention in a previous section that the receiver has no way of determining how much of the beat frequency is due to the Doppler shift and how much is due to range. Fortunately, when a data matrix is filled with samples of the beat signal, it is possible through signal processing to not only recover range information but the Doppler frequency as well. To better understand how this can be achieved, consider the following illustration in Figure 1.5. A linear frequency-modulated signal is transmitted and impinges upon a point target a distance of $R$ away. Note that the smallest (starting) frequency of the transmitted wave first impinges on the target because we are considering an up-chirp. As such, the echo (orange) being received will increase in frequency with respect to time, as well. Assuming that there is no radial velocity between the radar and the target implies that range $R$ will remain constant. The amount of phase change ($\Phi$) that the signal undergoes as it propagates through free space depends on the signal's

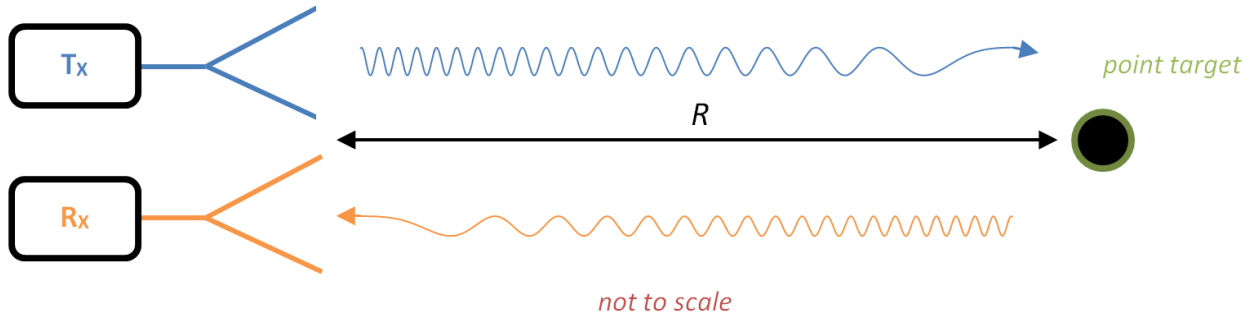


Figure 1.5 FMCW range and Doppler detection.

wavenumber $k$ and can be found using Equation 1.13, where the total distance that a signal covers will be twice the range ($R$) since the receiver and transmitter are collocated.

$$\boldsymbol{\Phi} = k * 2R\,, \qquad k = \frac{2\pi}{\lambda}$$

$$= \frac{4\pi R}{\lambda}\,[rad] \tag{1.13}$$

Thus, in essence, the total amount of phase change depends on range. This means that if at time zero the echo is received, then for a constant range the initial (time zero) phase difference between the current transmit and receive signals will always be the same regardless of the initial phase of the transmitted signal. Furthermore, this initial phase difference (at time zero) is the initial phase of the beat frequency and will be periodic every SRP. Also, since range is constant, the received echo will always undergo a constant attenuation through free space resulting in the amplitude of the beat frequency being a constant, and consequently a constant amplitude beat signal. The matrix would be unique in this case, because the values making up any given row will be identical. If the FFT of any row is taken, then the result will be zero frequency (DC) since the values in any given row are constant.

Consider the case where the target is moving toward (or away from) the radar. The initial phase of the beat frequency due to the first chirp will be some number based on the instantaneous range, and the first sample of the beat signal (of the first chirp) will be some value. Because range is now changing with time, the initial phase of the beat frequency due to the second chirp will not be *exactly* the same as that of the first chirp, and the initial phase due to the third chirp will not be the same as that of the second chirp and so on. By definition, the change in phase with respect to time is the Doppler frequency. Therefore, taking the FFT of a row will result in the Doppler frequency.

Performing a two-dimensional (2-D) FFT over the data matrix (once horizontally and once vertically across all rows and columns) will generally result in a complex data matrix. Taking the magnitude

squared of each bin results in a 2-D magnitude plot that maps the received signal energy into a single range-Doppler bin. Both axes will have units of Hz, only one axis will correspond to range and the other to Doppler. If multiple targets are within the radar's detection range, then multiple peaks will show up on the 2-D plot. Once the coordinates (i.e. range-Doppler bins) of all peaks are known, Equations 1.9 and 1.12 can be used to back calculate the range and radial velocity, respectively of any target.

### 1.3.4 Coherent Integration

In simple (low-cost) radio frequency (RF) receivers that do not employ high level signal processing, the signal-to-noise ratio (SNR) is greatest at the input to a receiver, and gets progressively worse as the signal propagates through the receiver, due to additive thermal noise of the components that make up the receiver. To get a sense of what the SNR might be at the input to the receiver, consider a target 800 m away, having a radar cross section (RCS) of 1 $m^2$, and with a center frequency of 1.445 GHz. The amount of attenuation that the transmitted signal experiences can be found using Equation 1.14, with the assumptions that the transmit and receive antennas are the same, that their polarizations are matched and that they are lossless. This equation is often called the radar range equation. In this equation, RCS and antenna gain are represented by $\sigma$ and $G$, respectively.

$$\boldsymbol{P_R} = \frac{P_T G^2 \lambda^2 \sigma}{(4\pi)^3 R^4} \ [W] \quad (two\ way) \tag{1.14}$$

If the antenna gain is unity and the transmitted signal power is 25 dBm (~316 mW), then the received power is approximately -138 dBm (see Appendix A.1).

Noise power at the input to the receiver can be calculated using Equation 1.15, where $k$ is the Boltzmann constant, $T$ is the temperature in Kelvin of the environment toward which the receiving antenna is directed, and $B$ is the bandwidth of the signal.

$$\boldsymbol{P_N} = kTB \ [W] \tag{1.15}$$

Recall that to satisfy the 10 m range resolution requirement, the bandwidth of the chirp must be at least 15 MHz. Using this bandwidth and a temperature of 290 K (assuming that the environment is homogenous and that the input antenna noise temperature is 290 K) the resulting noise power is found to be about -102 dBm (see Appendix A.2). The SNR can now be calculated with Equation 1.16, a value of -31 dB.

$$\boldsymbol{SNR(dB)} = 10Log_{10}\left(\frac{P_R}{P_N}\right) \ [unitless] \tag{1.16}$$

The SNR is significantly lower than the typical 10 dB required for detection. Also, the SNR will decrease even further by an amount equal to the receiver's noise figure (in dB) which will be discussed later. Performing integrations of the measured data is a way of increasing the SNR. Signal integration is the process of summing the contents of several samples and results in SNR improvement. Incoherent integration is a type of integration that only uses a signal's amplitude information and can improve SNR by a factor of the square root of the number of integrations. Coherent integration is a type that in the summation process takes into account the sample-to-sample phase change in addition to the samples' magnitude. Coherent integration can increase the SNR by a factor equal to the number of integrations performed. However, for this FMCW radar, there is a limit on how much the SNR can be improved which is equal to the transmitted signal's time-bandwidth product ($TBP$) as shown in the following equation, where $\tau$ is the duration of the signal (also the SRP) and $B$ is the signal's spectral width (bandwidth).

$$\boldsymbol{TBP} = \tau B \; [unitless] \tag{1.17}$$

It has been shown previously that 15 MHz of bandwidth is required to obtain a range resolution of 10 m and from the system's requirements the duration of every update is 100 ms (10 Hz). Since the coherent integration process will be performed on data sampled for 100 ms, this length of time will be the signal's duration used in the previous equation. Using these values, the resulting $TBP$ is about 62 dB. Therefore, the coherent integration process can be used to increase the SNR by 62 dB at most.

The number of cells (voltage samples) in the data matrix will depend on how much SNR improvement is needed, since SNR increases by a factor equal to the number of coherent integrations. For example, if a data matrix consists of 800 rows and 500 columns, then 400,000 (56 dB) integrations (the product of the two numbers) will be performed which will increase SNR by about 56 dB. It is worth mentioning that the actual SNR improvement will be less than 56 dB by about 6 dB due to the Hanning windowing process that is used prior to performing the 2-D FFT, which is beyond the scope of this paper.

Since the number of integrations is dependent only on the number of samples in the matrix, the matrix could be of any dimension so long as the total number of cells is equal to the necessary number of integrations required to achieve a certain SNR improvement. However, a 2-D FFT can be computed faster if the data matrix is more square (i.e, the number of rows equals the number of columns). The number of rows in the data matrix will depend on the sampling frequency as well as the frequency sweep duration (and thus implicitly on the total number of sweeps in 100 ms). The number of columns in the matrix will depend only on the number of sweeps in one observation period (100ms). Therefore, to minimize the FFT processing time, the number of sweeps in one observation period must be selected such

that the matrix is made more square-like. It is important to know that although a matrix with only one column might still have the necessary number of samples (rows) to attain a specific SNR improvement, the Doppler frequency (in the slow time) cannot be determined with just one sample (column).

### 1.3.5 Leakage Signal

All FMCW radars have one problem in common and that is the leakage signal which is present in the received signal. This problem arises from the nature of FMCW operation in that the radar transmits and receives simultaneously. In a monostatic case, the distance separating the transmitting antenna can be very small resulting in a powerful received leakage signal. For example, if both antennas are identical, lossless and have unity gain, then Equation 1.18 can be used to determine the received leakage signal power. Note that this equation has an $R^2$ dependence and differs from Equation 1.14 because the wave propagates in one direction only.

$$\boldsymbol{P_R} = \frac{P_T G^2 \lambda^2}{(4\pi)^2 R^2} \ [W] \quad (one\ way) \tag{1.18}$$

If the transmit and receive antennas are spaced one meter apart and the transmit power is 25 dBm, then the received power is calculated to be approximately -11 dBm (see Appendix A.3). Recall that the strength of the echo signal at a range of 800 m was previously calculated to be -138 dBm which makes it 127 dB weaker than the leakage signal. Therefore, the leakage signal's power will need to be considered when selecting components in the receiver design. Not addressing the leakage signal can lead to undesired radar performance due to receiver saturation.

Since the leakage signal arrives at the receiving antenna much earlier than the return echo, the beat frequency due to the leakage signal will be much smaller than that of the echo. Also, the radial velocity between the transmit and receive antennas is always zero, which means that after a 2-D FFT, the leakage signal's beat frequency will always have a zero Doppler coordinate.

## 1.4 Angle-of-Arrival Estimation Theory

In a spherical coordinate system, three coordinates are needed to uniquely represent the location of a point namely $r, \theta\ and\ \varphi$. Similarly, the location of a target relative to the radar can be determined if the range to the target as well as the elevation and azimuth angles are known. Therefore, estimating the received echo's angle-of-arrival (AoA) is a necessary step in localizing a target. Unlike range which can be determined with a single antenna, angle measurements require multiple antennas.

### 1.4.1 Elevation Angle Detection

Consider the setup shown in Figure 1.6 where two antennas $A$ and $B$ are separated by half a wavelength (i.e. the center-to-center spacing $d$ is $\lambda/2$) and placed along the vertical axis with the origin half-way in between the two antennas. In this analysis, it will be assumed that the intruder is a point target and that it is in the radar's far field. This assumption will allow the received (i.e. reflected) wave to be characterized by a plane wave. The received signal's wave front first impinges on antenna $A$ and then on antenna $B$. $\Phi_A$ and $\Phi_B$ are the relative phases of the received signal at antennas $A$ and $B$, respectively. Note that the wave had to travel a distance $l$ after it impinged on antenna $A$, before hitting antenna $B$. The signal's phase at antenna $B$ is greater than that of antenna $A$ by the product of the distance $l$ and the wave's wave number ($2\pi/\lambda$).

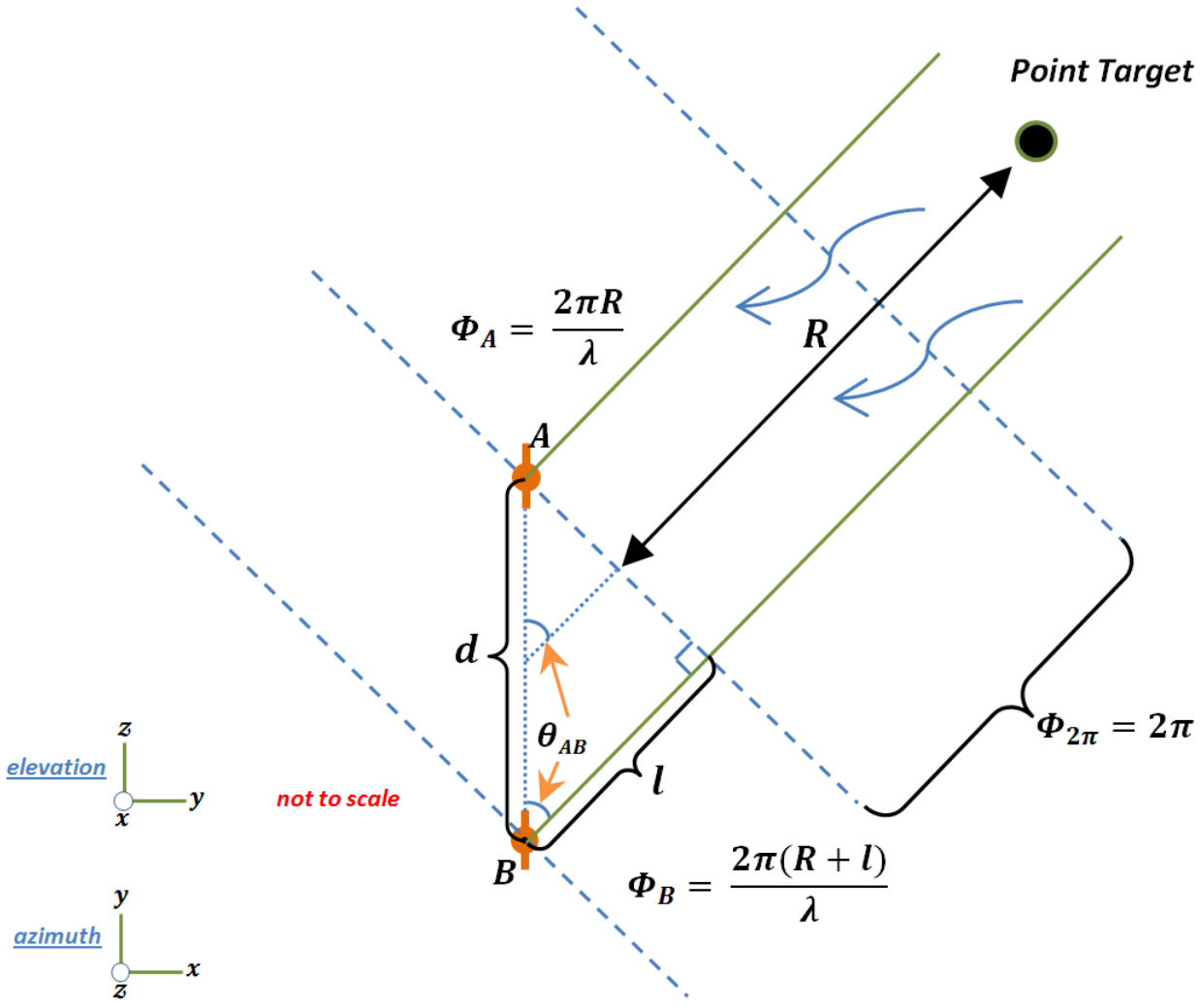


**Figure 1.6 Receiving antenna geometry for measuring elevation angle.**

The elevation AoA shown as $\theta_{AB}$ can be found with an inverse *cosine* operation using the following equation, where $l$ is the only unknown.

$$\boldsymbol{\theta_{AB}} = cos^{-1}\left(\frac{l}{d}\right) \tag{1.19}$$

Recall from a previous section that the phase of the received echo depends solely on the range to the target and can be found using Equation 1.13. Solving Equation 1.13 for range $R$ and replacing this symbol with $l/2$ (since $l$ is a one way distance), provides an equation that can be used to solve for the unknown length $l$.

$$\boldsymbol{l} = \frac{\lambda * \Delta\Phi_{BA}}{2\pi} \tag{1.20}$$

where, $\Delta\Phi_{BA}$ in this case is the difference between the phases of the received echo.

$$\boldsymbol{l} = \frac{\lambda(\Phi_B - \Phi_A)}{2\pi} \tag{1.21}$$

Substituting this into Equation 1.19 yields,

$$\boldsymbol{\theta_{AB}} = cos^{-1}\left(\frac{\frac{\lambda(\Phi_B - \Phi_A)}{2\pi}}{d}\right) \tag{1.22}$$

If the two antennas are separated by one-half wavelength, the previous equation reduces to the following:

$$\boldsymbol{\theta_{AB}} = cos^{-1}\left(\frac{(\Phi_B - \Phi_A)}{\pi}\right) \tag{1.23}$$

Note that the AoA is now a function of the phases of the received signal. Recall that after the 2-D FFT, the data matrix will generally consist of complex voltages. Every bin that makes up the matrix will be composed of a real and imaginary number. The phase of the complex number in the bin that corresponds to a particular target will be used. Since there are two antennas, there will be two data matrices from which $\Phi_A$ and $\Phi_B$ will be obtained.

For a given range and elevation angle, all possible target directions lie on a circle centered on the vertical axis, as shown in Figure 1.7. For clarity purposes, this circle will be referred to as the 'elevation circle'. Detection in azimuth will determine which exact point on the circle corresponds to the target location.

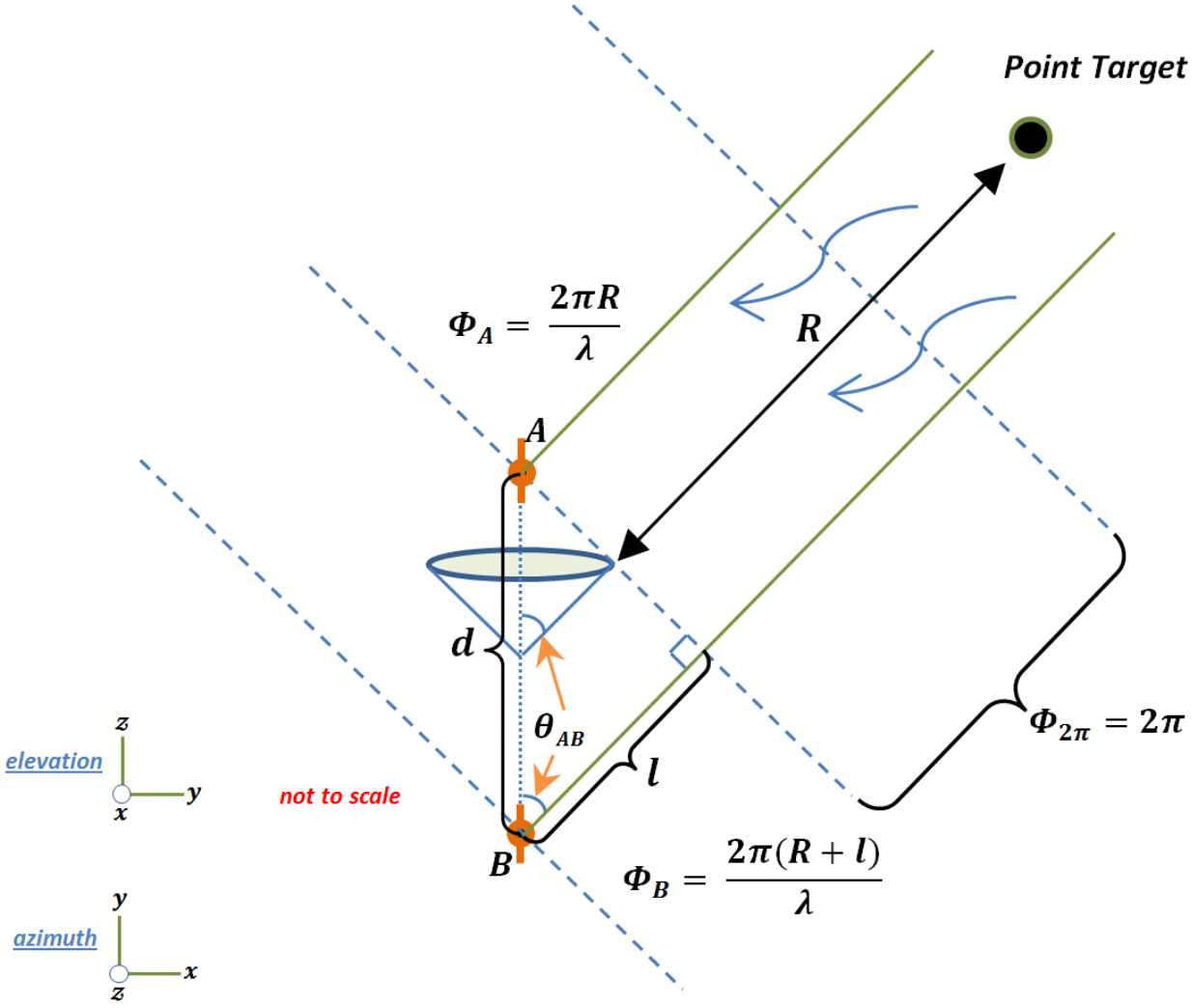


**Figure 1.7 Possible target locations for a single point target.**

Note that the distance between the tip of the cone (origin) and the circle is the range to the target and is not drawn to scale.

### 1.4.2 Azimuth Angle Detection

For analyzing AoA in the azimuth, refer to Figure 1.6 but now assuming that the antennas are located in the horizontal plane. The theory for finding the AoA in azimuth is the same as for the elevation angle. If two antennas are used (just like in the elevation measurement), there will again be a circle that corresponds to all possible target locations. A problem arises from the fact that the 'elevation circle' could (and almost always will) intersect the 'azimuth circle' at two points. Consequently, this would mean that there are two solutions (targets) when in reality there is only one (in this example). A simple way to solve this problem would be to introduce a third antenna whose 'circle' would intersect just one of

the two previous points. This is depicted in Figure 1.8, where the two azimuth circles intersect at two points. Only one of these two points will lie on the 'elevation circle'. Therefore, a total of five antennas will be used to unambiguously detect a target's location: two for determining the elevation angle and three for determining the azimuth angle. Multiple antennas will require multiple receiver channels for which reason this is a multichannel radar.

In this discussion, the term 'azimuth angle' has been used extensively, but based on its definition, its use would be grammatically correct only if the target (in this azimuth analysis) lies in the plane of the three antennas. This is important, because if the target is not in the three antennas' plane (and it usually will not be), then additional mathematical manipulation of the measured angles would be required to extract the target's true azimuth angle.

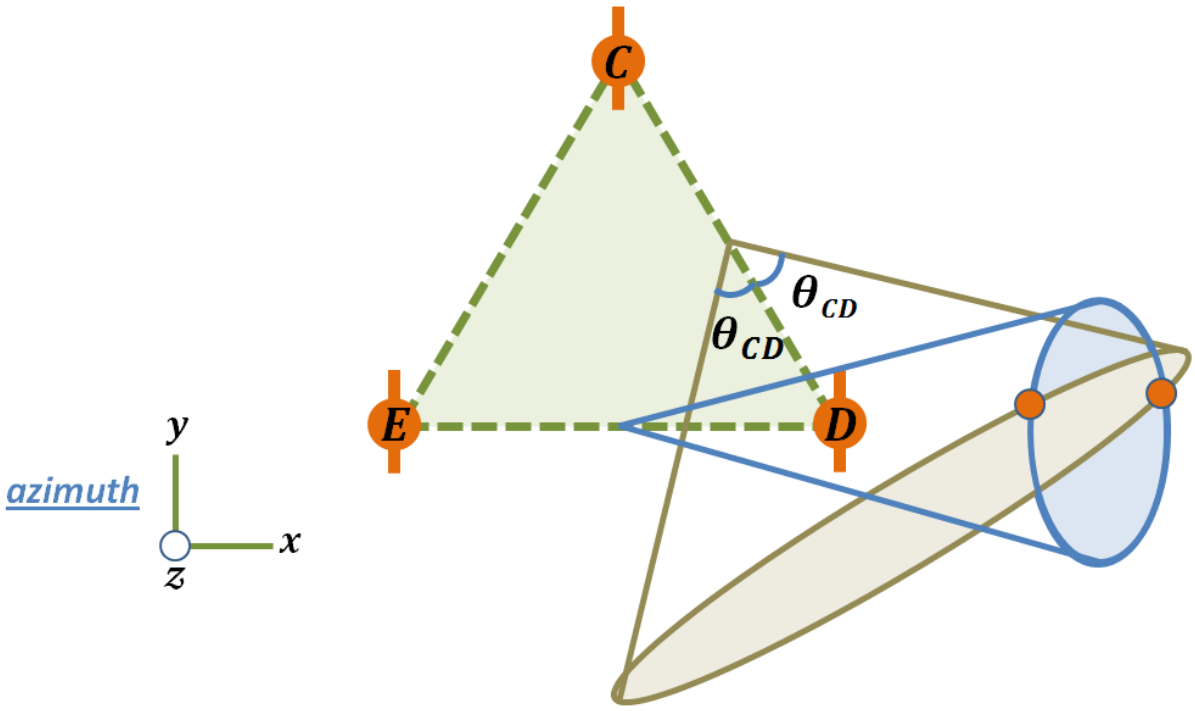


**Figure 1.8 Solving location ambiguity using three antennas.**

### 1.4.3 Angle-of-Arrival Estimation Error

A method for detecting the AoA has been presented in the previous section, however, any measurement is incomplete if the accuracy of the measured parameter is unknown. The accuracy with which this AoA can be found depends on the received signal's signal-to-noise ratio. It is important to recognize that the SNR used in calculating the AoA error is not the SNR at the receiving antennas (i.e. at the beginning of

the receiver chain) but rather the SNR of the signal right before it will be used to determine the AoA, which in the case of the FMCW radar will be after the 2-D FFT process.

If the complex voltages in every data matrix were noise free, and the inaccuracies in the array setup and error in the quantization process were ignored, then the measured AoA would be exact and errorless. This is of course a physical impossibility as a noise-free voltage would result in an infinite SNR. Since the environment surrounding the receiving antennas and the components used in creating the receiver are above absolute zero, some amount of thermal noise will be generated due to the random motion of charged particles. This type of noise is well modeled by a Gaussian random process with zero mean [7]. The existence of such noise will impact the AoA measurement by introducing an error. Therefore, a realistic representation of the voltage at any bin in a data matrix after the 2-D FFT process will be the sum of the true signal (i.e. error free) and noise as shown in Equation 1.24, where $V_S$ represents the true signal voltage, $V_N$ represents the noise voltage and where the superscripts $R$ and $I$ represent the real and imaginary components, respectively.

$$\boldsymbol{V^{FFT}} = V_S^R + jV_S^I + V_N^R + jV_N^I \tag{1.24}$$

This equation can also be represented as a sum of two complex exponentials, where the angle $\phi$ is equivalent to the inverse tangent of the imaginary part over the real part.

$$\boldsymbol{V^{FFT}} = |V_S|e^{j\phi_S} + |V_N|e^{j\phi_N},\ \ \phi = \tan^{-1}\frac{Im\{V\}}{\Re e\{V\}} \tag{1.25}$$

The phase-angle $\phi_S$ by itself corresponds to the true phase, but it is the phase-angle of the *total* voltage $V^{FFT}$ [corresponding to the phase of the received signal (e.g. $\Phi_A$ in Figure 1.6)] that will be used in Equation 1.23 to determine the AoA. Note that in actuality, the phase-angle of the total voltage (i.e., $V^{FFT}$) corresponding to the target will not be equal to the phase of the received signal ($\Phi_A$ or $\Phi_B$), since the signal had to additionally propagate through the receiver before it was digitized which would change the phase. Therefore, the actual equation that will be used in calculating the AoA is the following:

$$\boldsymbol{\theta_{AB}} = cos^{-1}\left(\frac{(\Phi_B^{FFT} - \Phi_A^{FFT})}{\pi}\right),\ \ \Phi^{FFT} = \angle\{V^{FFT}\} \tag{1.26}$$

However, it will be assumed that the (unaccounted) receiver delay is the same for all channels such that the *difference* in phase-angles (of the *total* voltages) is the same regardless of the receiver delay.

*AoA Measurement Error*

The following analysis is presented to help quantify the amount of error that can be expected for a given AoA measurement. The basic idea is to simplify the total voltage representation (Equation 1.25) by relating the signal voltage to the noise voltage, so that the necessary phase-angle can easily be found.

Signal power and noise power are related by the signal-to-noise ratio.

$$\boldsymbol{SNR} = \frac{P_S}{P_N}\ [unitless] \tag{1.27}$$

Representing both powers in terms of root-mean-square (RMS) voltages yields,

$$SNR = \frac{\frac{\left(V_S^{RMS}\right)^2}{R_S}}{\frac{\left(V_N^{RMS'}\right)^2}{R_N}} \tag{1.28}$$

Allowing $R_N$ to equal $R_S$ reduces to,

$$SNR = \frac{\left(V_S^{RMS}\right)^2}{(V_N^{RMS})^2} \tag{1.29}$$

Note the change of $V_N^{RMS}$ *prime* to just $V_N^{RMS}$. Solving for the noise voltage and letting the signal voltage to equal one for simplicity yields,

$$\boldsymbol{V_N^{RMS}} = \frac{1}{\sqrt{SNR}} \tag{1.30}$$

Since SNR is a relative parameter, any value for the signal voltage could have been used.

It can be shown that if additive complex noise follows a Gaussian distribution, then the individual quadrature (i.e. real and imaginary) components of this noise will likewise be Gaussian [7]. Therefore, the noise voltage can be fully described by the following equation,

$$\boldsymbol{V_N} = \frac{V_N^{RMS}}{\sqrt{2}}(v_N^R + jv_N^I) \tag{1.31}$$

$$= \frac{1}{\sqrt{2SNR}}(v_N^R + jv_N^I) \tag{1.32}$$

where, $v_N^R$ and $v_N^I$ are random variables having Gaussian distributions centered at zero with unity standard deviations. The square-root of two in the denominator is needed to allow the standard deviation of the magnitude of the noise voltage to equal $V_N^{RMS}$.

To represent the true signal ($V_S$), its magnitude would have to be one (since $V_S^{RMS}$ was set equal to one previously) but its phase could be any arbitrary angle. With these constraints, it is easiest to represent the true signal as a complex exponential as follows:

$$\boldsymbol{V_S} = |1|e^{j\phi_S} \tag{1.33}$$

Summing the simplified signal and noise voltages yields,

$$\boldsymbol{V^{FFT}} = |1|e^{j\phi_S} + \frac{1}{\sqrt{2SNR}}(v_N^R + jv_N^I) \tag{1.34}$$

This final equation is a representation of the voltage at any cell in the data matrix after the 2-D FFT. Note that this equation is based on the assumption that the signal RMS voltage is one and that noise follows a Gaussian distribution.

*AoA Measurement Error Example*

Suppose the true phase-angles of the received signal are 30° and 135° and that the SNR is 24 dB. The two signals can then be represented as follows:

$$\boldsymbol{V_A^{FFT}} = |1|e^{j\frac{30\pi}{180}} + \frac{1}{\sqrt{2 * 10^{2.4}}}\left(v_N^{R_A} + jv_N^{I_A}\right) \tag{1.35}$$

$$\boldsymbol{V_B^{FFT}} = |1|e^{j\frac{135\pi}{180}} + \frac{1}{\sqrt{2 * 10^{2.4}}}\left(v_N^{R_B} + jv_N^{I_B}\right) \tag{1.36}$$

where, the angles have been expressed in radians and SNR in linear "units". [The quadrature components of noise for signal *A* cannot be *exact* copies of that of signal *B* (e.g. $v_N^{R_A} \neq v_N^{R_B}$)]. Note that the magnitude of the true signals is the same (one) in both cases. This is a very accurate approximation due to the close proximity of the two antennas (i.e., the range to the target for both antennas is minutely different).

The final step is to take the angle of both signals and use the difference in the phase-angles to determine the AoA as follows:

$$\boldsymbol{\theta_{AB}} = cos^{-1}\left(\frac{\angle(V_B^{FFT}) - \angle(V_A^{FFT})}{\pi}\right) \tag{1.37}$$

where, the phase-angles of both signals are in radians.

Figure 1.9 shows results of a MATLAB simulation of the probability density of the AoA. Note how the plot follows a bell-like (Gaussian) curve. If thermal noise was excluded in the AoA calculation, the true AoA would be 54.3° which is also the mean angle of the probability density plot. This distribution has a standard deviation of 1.4°, which means that about 68% of the time the measured AoA will be within ±1.4° of the true angle (if all other sources of error are ignored).

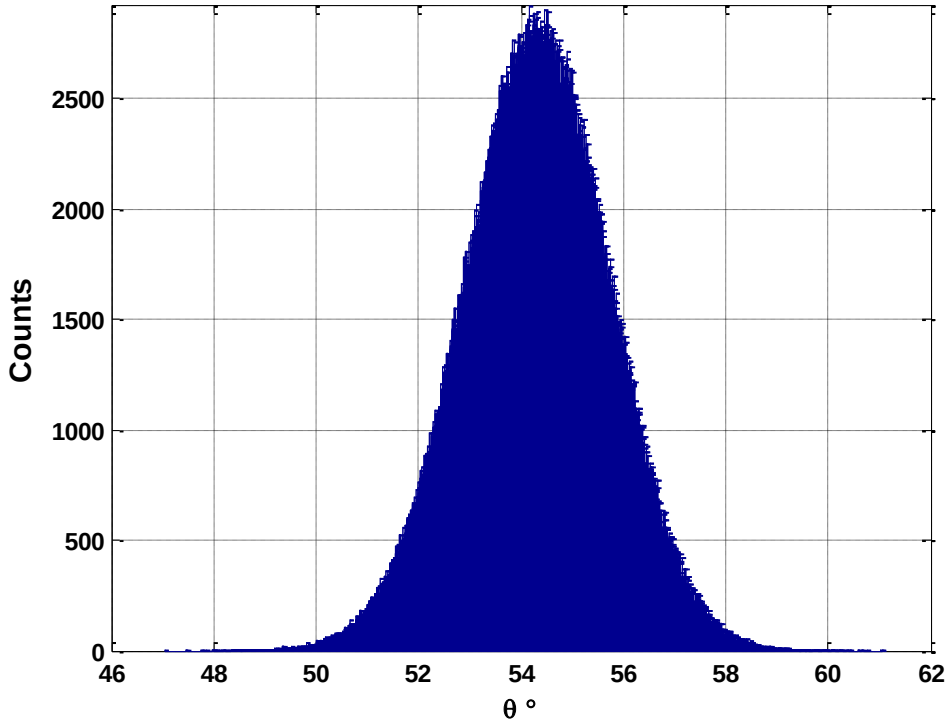


**Figure 1.9 Probability density of the AoA.**

Figure 1.10 shows the AoA error for various values of SNR. The error in this plot is equivalent to one standard deviation. Notice that a SNR of approximately 11 dB is a breakpoint after which the error diminishes by about 0.5 dB for every 1 dB increase in SNR.

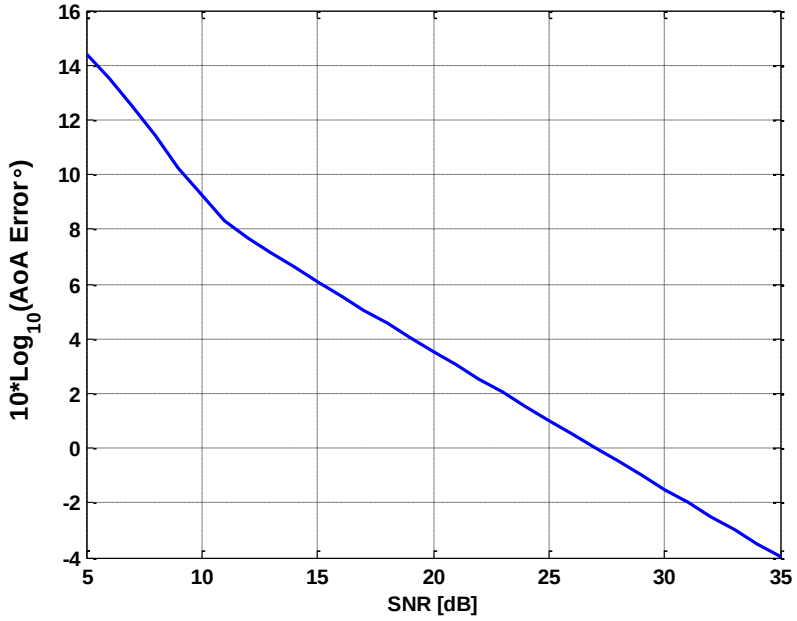


**Figure 1.10 AoA estimation error as a function of SNR.**

### 1.4.4 AoA Rate of Change

Recall that the collision avoidance radar is required to update AoA information at a rate of 10 Hz, and the measured AoA uncertainty must not exceed 3°. But is it possible to reduce the update rate to 5 Hz and still meet the required accuracy? Being able to update AoA information every other observation period (100 ms) could reduce the required number of channels in the receiver to just two. Although five antennas will still be used for AoA estimation, only one pair of antennas will be connected to the receiver at any time. For example, for the first observation period, the two elevation antennas will be connected, during the second observation two azimuth antennas will be connected and during the third observation another pair of azimuth antennas will be connected. This last pair of azimuth antennas is only needed to resolve the ambiguity in the AoA and thus need not be connected every two observations. Therefore, in steady-state, only two pairs of antennas are necessary to determine AoA information with each pair connected every other observation period.

To determine whether the AoA uncertainty requirement will still be met, there are two things that must be known namely, the measured angle's error and the maximum amount of change that the true angle could undergo in 100 ms. The first factor has already been determined and can be found by finding the corresponding angle error for a given SNR using Figure 1.10, however, the latter one will require additional analysis.

*Maximum AoA Rate of Change Simulation*

When computing the maximum AoA rate of change, it is perhaps easiest to demonstrate this maximum change with a simulation, as it can be difficult to determine analytically in which direction the target must be moving that results in maximum AoA rate of change. The guidelines for this simulation are as follows:

1. It is unacceptable for an intruder (target) to come within 100 m of the UAS as it could be considered a safety hazard. This zone will be referred to as the keep-out region.
2. All intruders move at 54 m/s.
3. The radar-carrying UAS is moving in the +$x$-direction at 36 m/s.
4. Only targets in the $xy-plane$ will be considered (for simplicity).

Since the AoA rate of change is greatest when the intruder is closest, and the lowest range that the radar is specified to detect is 300 m, we will assume a circle of potential intruders with a radius of 300 m and centered at the UAS. Although an intruder radius of 100 m (the minimum acceptable before entering the keep-out region) would result in a greater AoA rate of change, the radar is only required to detect intruders at ranges of 300 m or more, and so the 300 m radius intruder circle was chosen for the simulation. This setup can be seen in Figure 1.11 where the inner circle composed of red dots represents the keep-out region while the outer circle composed of blue dots represents potential intruders.

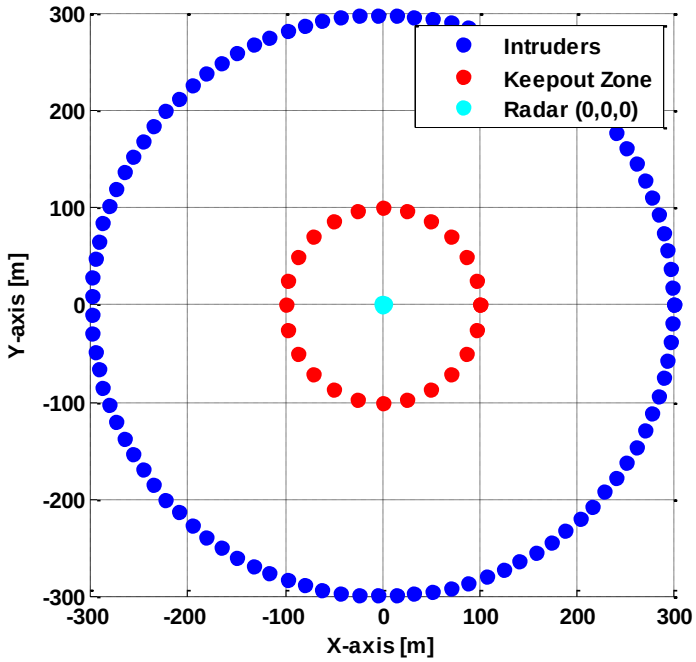


**Figure 1.11 Maximum AoA rate of change simulation setup.**

The keep-out zone (red dots) and all potential intruders (blue dots) are centered about the radar (turquoise dot) which itself is at the origin. It should be noted that this plot only represents the general setup, and for clarity reasons the number (or density) of keep-out and intruder points shown is less than what will be used in the simulation. In Figure 1.11, there are 100 intruders and 25 keep-outs while in the actual simulation there will be 2000 intruders and 500 keep-outs.

Since the maximum speed of an intruder is 54 m/s, the maximum distance that it can move in 100 ms is 5.4 m. Rather than moving the UAS in the $+x$-direction by 3.6 m (guideline #3), it is equivalent to leave the UAS at the origin and *instead* move the intruder in the $-x$-direction by 3.6 m (in addition to moving the intruder initially in its own direction by 5.4 m). As seen from the radar relative to which the AoA rate of change will be calculated, these two scenarios are identical. This latter approach will be used because it is easier to calculate the rate of change. Figure 1.12 shows graphically how the AoA rate of change is determined. Note that the figure is *not* to scale and should only be used as a visual aid in the following summary: we first take a single intruder (initial) point and move it in the $-x$-direction by 3.6 m to

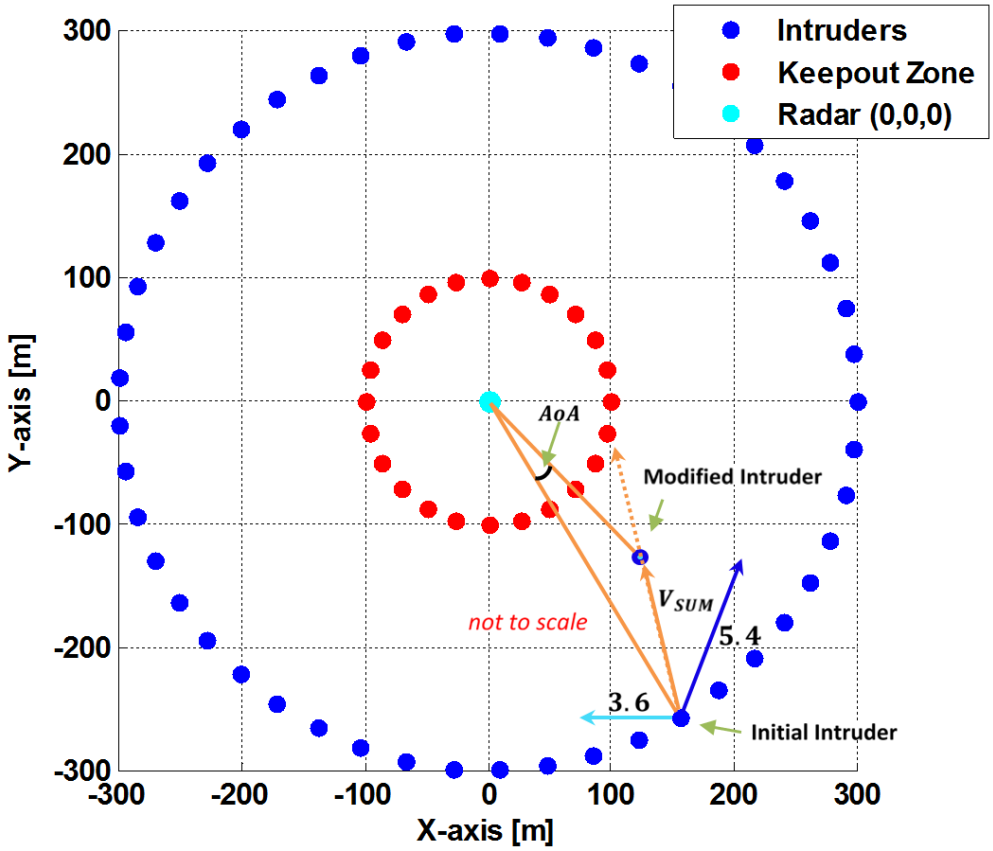


**Figure 1.12 Visual algorithm used to determine AoA rate of change (not to scale).**

simulate the radar moving in the $+x$-direction. Since we are only interested in intruder paths that result in the intruder penetrating the keep-out region (guideline #1), we move the intruder by 5.4 m in any direction such that the $V_{SUM}$ vector points toward one of the keep-out points as shown by the dashed orange arrow. To see the relationship between the angles of the intruder vector and $V_{SUM}$, see Appendix A.12. There are now three unique points (or coordinates): the intruder's original coordinate, the intruder's modified coordinate, and the radar's coordinate. A triangle is formed from these three points with the triangle's angle at the origin (where the radar is also) being the angle by which the AoA will change in one observation period.

For a single intruder point, this process is repeated for all other keep-out points allowing a single intruder to move toward any point on the keep-out circle to simulate all possible flight paths that a single intruder might take on that could result in the intruder coming within 100 m of the radar-mounted UAS. This process is then performed on the rest of the intruders. At the end, every single intruder point has been moved toward every single keep-out point with the AoAs being calculated for any given intruder/keep-out combination. Recall that the AoAs that are being found are based on the intruders' and UAS' movement in 100 ms, therefore, it is the AoA rate of change (in 100 ms) that is being simulated. The maximum AoA rate of change was found to be 0.59°/observation-period. This value, as previously mentioned, was found by simulating 2000 intruder and 500 keep-out points.

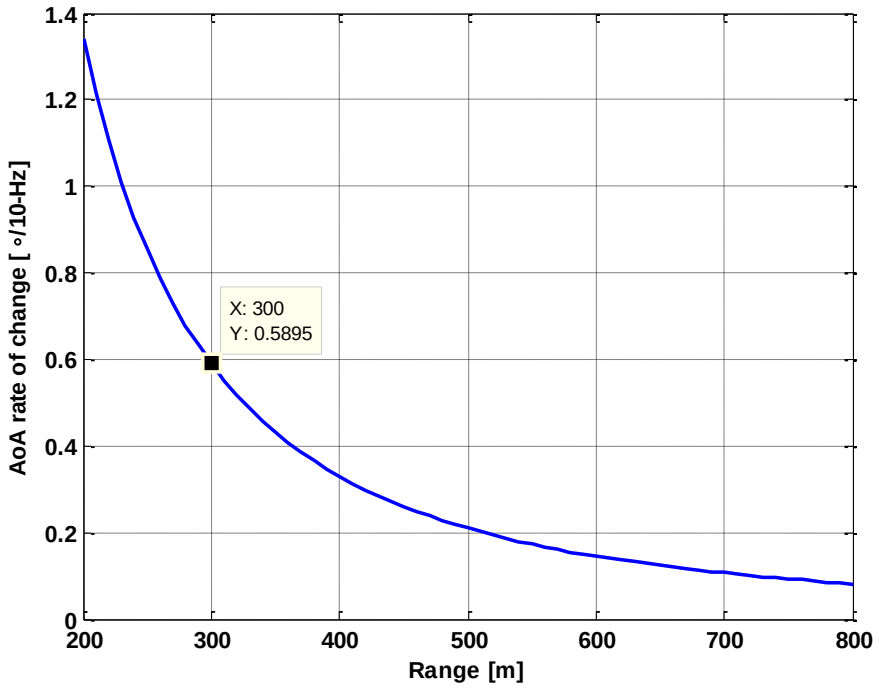


**Figure 1.13 Maximum AoA rate of change vs range.**

The AoA rate of change decreases for intruders farther away from the UAS (assuming their speeds are always 54 m/s). Figure 1.13 shows how the maximum AoA rate of change decreases with increasing range, such that at a range of 800 m the rate of change is approximately 0.08°/observation-period.

If the maximum speed of intruders was equal to that of the radar-mounted UAS, an entire circle of points representing intruders would not be necessary since certain intruders will never be able to catch up to the UAS. Figure 1.14 shows all intruder locations that could potentially penetrate the keep-out region from which we can conclude that the radar only needs to be able to detect targets within ±110° in azimuth. (However, if the speed of intruders is greater than the speed of the UAS, then the radar *must* detect targets from all directions in azimuth). According to MATLAB simulations, the maximum AoA rate of change for when the speeds of the UAS and intruders are equal was found to be 0.47°/observation-period.

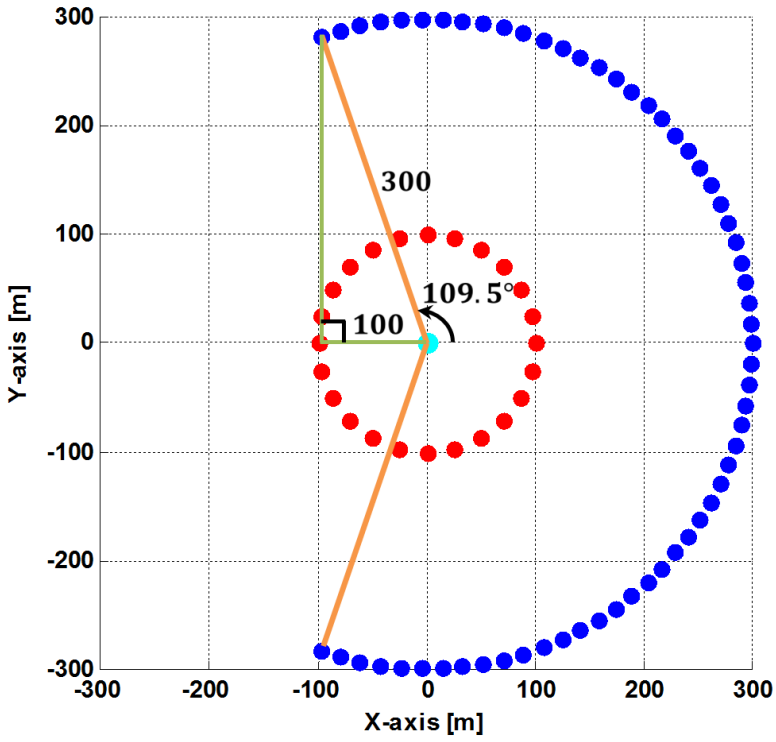


**Figure 1.14 Modified intruder locations when the speed of intruders and the UAS are equal.**

*Summary*

Recall that the radar system's AoA measurement uncertainty is required to be no greater than ±3°. Since the maximum AoA rate of change is about 0.6°/observation-period (at 300 m) and the AoA estimation error has been found to be less than 1.5° (it is 1.42 for a SNR of 24 dB), it is not strictly necessary to require an update (i.e. refresh) rate of 10 Hz. To see how this is so, refer to the diagram below while considering the following: after one observation period (100 ms) the radar system delivers its measured

AoA. The measured AoA, however, will be somewhere within ±1.5° of the true (mean) angle based on a Gaussian distribution. After the second observation period, the true AoA could maximally change by 0.6°, based on the maximum AoA rate of change simulation. At this point, the initially measured AoA will be somewhere within ±2.1° of the true angle. Therefore, if a newly measured angle (after the second observation period) is not provided, the radar system will still satisfy the required accuracy of ±3°, since the initially measured AoA is within ±2.1° of the true angle. Thus, the AoA update rate can be 5 Hz and still meet the system's angular accuracy requirement.

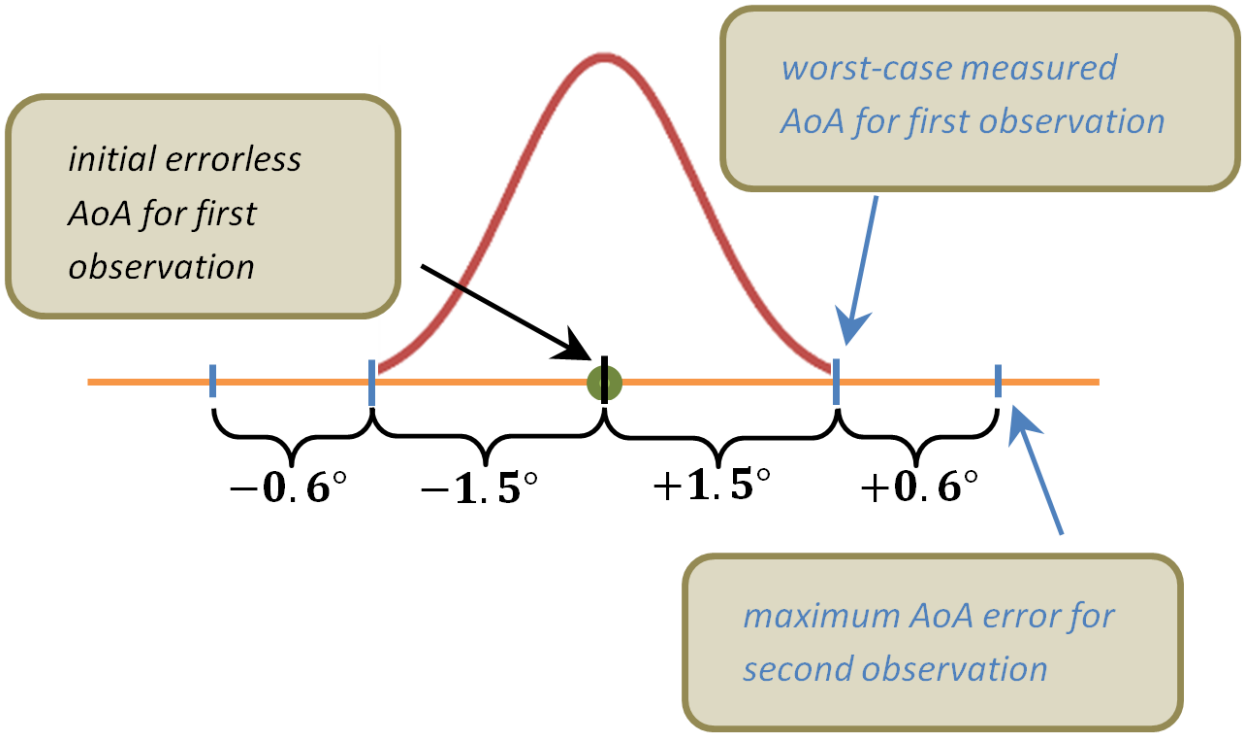


**Figure 1.15 AoA uncertainty due to estimation error and maximum AoA rate of change.**

Pushing this concept a little further, a SNR of 19.5 dB results in an AoA uncertainty of about 2.4° (see Figure 1.10 and note that the error is in dB). Thus, after the "second observation", the uncertainty will become 3° which would still satisfy the required accuracy of ±3°, although marginally. Whether 19.5 dB of SNR is enough to be able to provide an angular accuracy of 3° will depend on how much uncertainty exists in the unaccounted for potential error contributions such as imperfect antenna placement.

If the AoA update rate is 10 Hz, then the maximum uncertainty in the AoA measurement can be 3° which corresponds to about 17.5 dB in SNR according to Figure 1.10. Therefore, to satisfy the required angular accuracy of 3°, the SNR must be at least 17.5 dB.

# Chapter 2: Implementing FMCW Radar with Hardware

# (FMCW Radar Design)

## 2.1 Receiver Design

This section will present the reasoning behind the selection of components used in the receiver design. For the duration of this section, it may be helpful for the reader to refer to the following figure showing the placement and type of components used in the initial design.

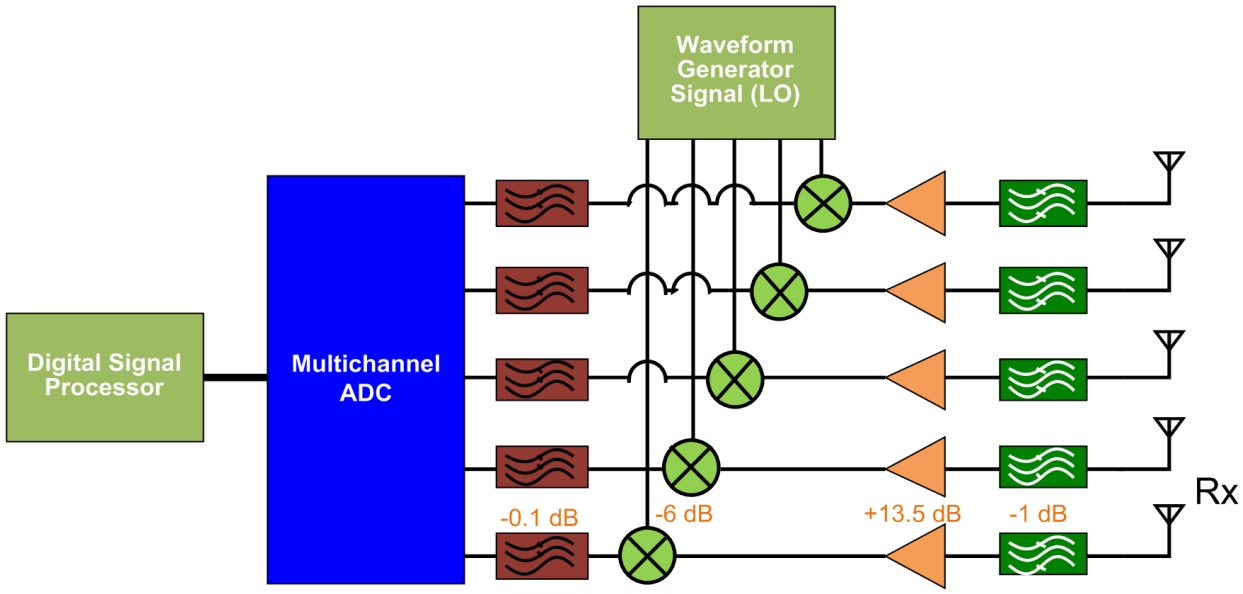


Figure 2.1 Initial receiver design.

### 2.1.1 ADC Selection

To obtain the range to a target as well as Doppler information, a 2-D FFT must be performed on the data matrix as outlined in the previous chapter. Because the data stored in a matrix must be digital, and the beat signal is analog, an analog-to-digital converter (ADC) must be incorporated in the receiver design to convert the analog beat signal into a digital sequence.

An important parameter to consider when selecting an ADC is the number of channels that it must have. Without the use of switches in the design, the number of channels required will depend on the number of antennas used. For target detection, at least two antennas will be used for detection in elevation and at least three antennas will be necessary to unambiguously detect in azimuth. Therefore, the ADC must have at least five channels. Analog Devices' 6-channel AD8283 was selected to perform the quantization process. In addition to having multiple channels, the ADC has a low noise amplifier (LNA), a

programmable gain amplifier (PGA) as well as an antialiasing filter (AAF) prebuilt into every channel. This ADC provides 12 bits of accuracy up to 80 Mega samples per second (MSPS). Unfortunately, this component did not have its own evaluation board and so it was necessary to make one.

Figure 2.2 shows the printed circuit board (PCB) created using EAGLE CAD for testing of the ADC. The SubMiniature version A (SMA) connectors allow easy access to all five channels. To verify the ADC's functionality, its digitized 12-bit output was sent to a 12-bit digital-to-analog converter (DAC) and the DAC's output analog signal was compared to the initial ADC input.

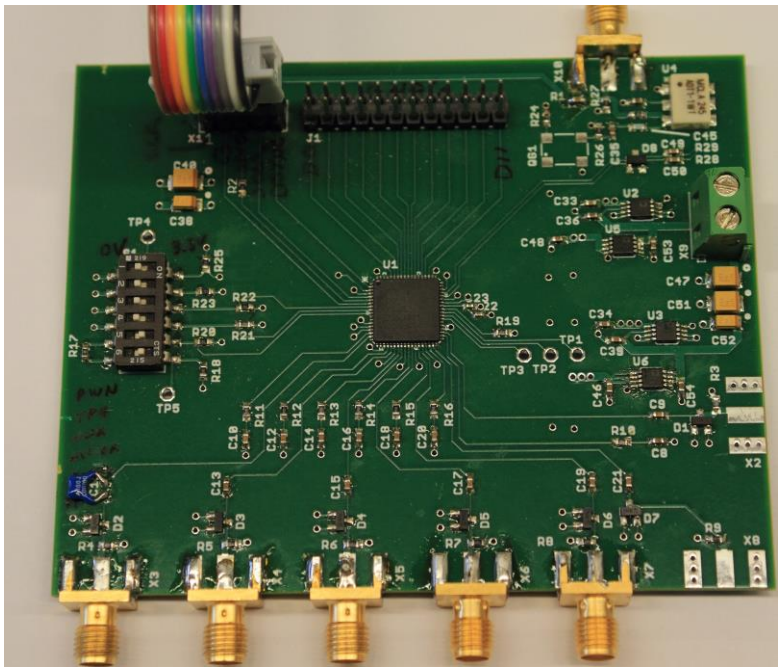

**Figure 2.2 Evaluation board for Analog Devices' ADC.**

The gain of the LNA was not provided in the datasheet, however, the datasheet did specify what the ADC's input voltages should approximately be for certain PGA gains. The PGA's gain selection varies from 16 dB to 34 dB in increments of 6 dB. The exact value will depend on how much additional gain is required in the receiver before the signal is digitized. The AAF is a third-order elliptical filter with a sharp roll off past the cutoff frequency. The cutoff frequency can be programmed to be as low as ¼ of the ADC sample clock rate and as high as 1.3 times the sampling frequency with possible cutoff frequencies ranging from 1 MHz to 12 MHz. To obtain the smallest possible cutoff frequency of 1 MHz, a sampling frequency of 4 MHz would be required.

*Selecting the SRP and the Sampling Frequency*

From the Nyquist criterion, the sampling frequency needs to be at least twice the bandwidth of the signal being sampled if aliasing is to be avoided. In practice, however, the sampling frequency must be greater than the Nyquist rate due to the non-ideal nature of the components being used.

For any given chirp duration ($SRP$) and bandwidth ($B$), Equation 2.1 can be used to determine the resulting beat frequency as a function of range.

$$\Delta f' = \frac{2Range * B}{c * SRP} \tag{2.1}$$

Note that the beat frequency will be higher for targets at a greater range. Initially, the maximum detectable range was required to be one nautical mile (1852 m). If the duration of the chirp was set to 200 µs, and knowing that the bandwidth of the chirp must be at least 15 MHz (for proper range resolution) then at a range of one nautical mile, the beat frequency would be 926 kHz (see Appendix A.4). A maximum beat frequency of 926 kHz would be desirable if the AAF's cutoff frequency is set to 1 MHz (which would require a sampling frequency of 4 MHz). Increasing the AAF's cutoff frequency while keeping the maximum beat frequency constant (926 kHz) is undesired as it would let more noise in. Therefore, a SRP of 200 µs was chosen because at a range of one nautical mile the corresponding beat frequency is close to the AAF's cutoff frequency of 1 MHz. Although the required maximum detectable range has been reduced to 800 m, the SRP was kept at 200 µs. Based on Equation 2.1, the beat frequency corresponding to 800 m is 400 kHz.

The resulting number of rows in the data matrix will equal to the product of the sampling rate (4 MHz) and the chirp duration (200 µs), a value of 800. The number of columns in the matrix will be equal to the inverse of the product of the chirp duration and the update rate. This results in 500 columns.

### 2.1.2 Mixer

A mixer is a three-port device with the ability to perform analog multiplication of two sinusoids in the time domain resulting in $\Sigma$ (sum) and $\Delta$ (delta) frequency terms. However, mixers are built with non-linear devices which introduce higher (and lower) order terms at the mixer's output port also called the intermediate-frequency (IF) port. Unwanted output terms are commonly referred to as spurious signals. When designing mixers, manufacturer's try to suppress all spurious terms while retaining only the preferred 2nd order term. Equation 2.2 shows the desired mixer's 2nd order term output when two sinusoids with different frequencies are multiplied.

$$\boldsymbol{V_{IF}(t)} = V_{RF}(t) * V_{LO}(t)$$

$$= \cos(\omega_{RF} t\ ) * \cos(\omega_{LO} t)$$

$$= \frac{1}{2}\cos(\omega_{RF} t - \omega_{LO} t) + \frac{1}{2}\cos(\omega_{RF} t + \omega_{LO} t) \quad (2.2)$$

The up-converted (Σ) frequency term in the previous equation is usually filtered out and the down-converted (Δ) term (also called the beat frequency) is retained, because higher frequencies are more difficult to process than lower ones. Recall that the fundamental principal of FMCW radar is subtracting the received echo from the current transmit chirp resulting in a beat frequency. Therefore, a mixer will be used to perform this subtractive process.

*Dechirp Analysis*

The following analysis will show mathematically how a mixer can be used to produce the necessary beat frequency in a FMCW radar, as well as provide some characteristics of the beat frequency.

Suppose a target and the radar are separated by a distance $R$, then the time duration $T$, between when the signal was first transmitted and when the echo is first received can be found using Equation 2.3.

$$\boldsymbol{T} = \frac{2R}{c} \quad (2.3)$$

Note that a factor of 2 is necessary to account for the round trip time.

The linear frequency-modulated waveform can be expressed by the widely known equation of a line as seen in Equation 2.4.

$$\boldsymbol{y} = mx + b \quad (2.4)$$

where, the dependent variable $y$ represents the changing frequency, $m$ is the slope of the line, $b$ is the $y$-intercept and $x$ is the function variable time.

If the transmitted chirp starts at time zero, then the $y$-intercept ($b$) will be the starting frequency (shown as $f_l$ in Figure 1.3) of the chirp, and the slope will be the chirp rate as presented in Equation 2.5.

$$\boldsymbol{m} = \frac{f_2 - f_1}{SRP} \quad (2.5)$$

Replacing the variables $y$ with $f_{chirp}$, $m$ with $k$, $x$ with $t$ and the $y$-intercept with $f_i$ (initial frequency) results in Equation 2.6.

$$\boldsymbol{f_{chirp}} = kt + f_i \tag{2.6}$$

To express the chirp signal as a *cosine* function whose argument is phase, the integral of the chirp signal with respect to time must be found, since the integral of frequency is phase (and the derivative of phase is frequency).

$$\boldsymbol{\Phi} = 2\pi \int f_{chirp} dt = 2\pi \int (kt + f_i)\, dt$$

$$= 2\pi \left(\frac{1}{2} kt^2 + f_i t\right) + \varphi_i \tag{2.7}$$

where,

$\varphi_i$ is the initial phase (rad)

A linear frequency-modulated signal can, therefore, be expressed sinusoidally as shown in Equation 2.8.

$$\boldsymbol{s(t)} = A_T \cos\left(2\pi \left(f_i t + \frac{1}{2} kt^2\right) + \varphi_i\right), \qquad 0 \leq t \leq SRP \tag{2.8}$$

where,

$A_T$ is the transmitted wave's amplitude (V)

$k$ is the chirp rate (Hz/s)

$SRP$ is the sweep repetition period (s)

The received signal will be time delayed by the round trip time $T$ and can be expressed using Equation 2.9.

$$\boldsymbol{s(t-T)} = A_R \cos\left(2\pi \left(f_i(t-T) + \frac{1}{2} k(t-T)^2\right) + \varphi_i\right), \qquad T \leq t \leq SRP + T \tag{2.9}$$

$$= 0, \qquad t \leq T$$

The output of the mixer will be the product of the received and transmitted signals and can be found as follows with Equation 2.10.

$$\boldsymbol{s(t)s(t-T)} = A_T \cos\left(2\pi \left(f_i t + \frac{1}{2} kt^2\right) + \varphi_i\right) * A_R \cos\left(2\pi \left(f_i(t-T) + \frac{1}{2} k(t-T)^2\right) + \varphi_i\right)$$

$$= \frac{A_T A_R}{2}\left\{cos\left[\left(2\pi\left(f_i t + \frac{1}{2}kt^2\right) + \varphi_i\right) + \left(2\pi\left(f_i(t-T) + \frac{1}{2}k(t-T)^2\right) + \varphi_i\right)\right]\right.$$

$$\left. +\cos\left[\left(2\pi\left(f_i t + \frac{1}{2}kt^2\right) + \varphi_i\right) - 2\pi\left(f_i(t-T) + \frac{1}{2}k(t-T)^2\right) + \varphi_i\right]\right\}$$

$$= \frac{A_T A_R}{2}\left\{(\cos(2\pi ktT + 2\pi f_i T - \pi kT^2) + cos\left[2\pi\left(kt^2 + 2f_i t - ktT + \frac{1}{2}kT^2\right) + 2\varphi_i\right]\right\} \quad (2.10)$$

Low-pass filtering the output of the mixer leaves only the down-converted term [recall that only the down converted sinusoid (the Δ term) is of interest] reducing the beat frequency to that of Equation 2.11.

$$\boldsymbol{b(t)} = \frac{A_T A_R}{2}\cos(2\pi ktT + 2\pi f_i T - \pi kT^2)$$

$$= \frac{A_T A_R}{2}\cos\left[2\pi(ktT + f_i T - \frac{1}{2}kT^2)\right] \quad (2.11)$$

Note that the mathematical representation of the beat frequency is a sinusoid with a linear time dependent phase resulting in a constant frequency. Also, the initial phase of this wave is a function of time $T$ and therefore, range (implicitly). As mentioned in the signal processing section, the initial phase is range dependent and will change if there is relative motion between the radar and target, thus allowing through the FFT process (in the slow time), the measurement of the Doppler frequency.

*Mixer Selection*

Some of the most important parameters that must be considered when selecting a mixer are conversion loss, port matching, port isolation, mixer compression and local oscillator (LO) power.

Conversion loss specifies the amount by which the desired signal's power will decrease (if the mixer is passive) as the signal passes through the mixer. It will be seen later that minimizing this attenuation will increase the SNR.

Port isolation is the amount of coupling that is present between any two ports. Isolation between the LO port and the RF port needs to be maximized to reduce coupling from the high power transmit chirp (connected to the LO port) to the weak echo (entering the RF port).

If the characteristic impedance of a port is not matched to that of the transmission line connecting it, signal reflections will inevitably occur, leading to a loss in delivered signal power as well as signal distortion. The amount of reflection is often times specified as return loss in datasheets which is the

magnitude squared of the ratio of the reflected power to the incident power. Generally, mixer ports are difficult to match resulting in relatively significant signal reflection.

Mixer compression signifies that there is a maximum limit on the input signal power beyond which the mixer's conversion loss starts (or appears) to increase. The 1 dB compression point ($P^{1dB}$) of a mixer relates to an input power that results in a conversion loss that appears to be 1 dB greater than the mixer's normal conversion loss. It was mentioned previously that a real mixer in addition to multiplying its two input signals will produce many undesired higher order terms (or spurious signals) and that manufacturers try to minimize their power (or weight) when designing mixers. When a mixer compresses, the output and input signal power relationship is not linear anymore such that increasing the input power will not increase the output power. However, the higher order term outputs (which have been designed to be much weaker than the 2nd order term), *will* increase with an increase in input power.

The LO port of a mixer must be supplied a signal with a certain minimum amount of power known as the LO drive power, if the mixer is to perform to its specifications. Supplying the LO port with a signal below the LO drive power inevitably increases the mixer's conversion loss.

Mini-Circuits' ZX05-30W frequency mixer was chosen to perform the down-conversion process and its specifications are presented in the following table. These parameters are usually specified in decibels

**Table 2.1 Mini-Circuits' mixer specifications.**

| Parameters | Value |
|---|---|
| **Model** | ZX05-30W+ |
| **Frequency (MHz)** | LO/RF: 300 to 4000<br>IF: DC to 950 |
| **Conversion Loss (dB)** | 6 |
| **LO-RF Isolation (dB)** | 40 |
| **RF Port Return Loss (dB)** | 6 |
| **LO Port Return Loss (dB)** | 8 |
| **1 dB Compression Point (dBm)** | 1 |
| **LO Drive Power (dBm)** | 7 |
| **Max. Input Power (dBm)** | 17 |

(dB), which results when a mathematical operator is performed on a unitless value such as a ratio or coefficient. Values and plots in dB can be especially useful when data (not in dB) can span a large range of values. Equations 2.12 and 2.13 can be used to convert to dB from linear "units" and vice versa.

$$\boldsymbol{A(dB)} = 10\log_{10} A \tag{2.12}$$

$$\boldsymbol{A} = 10^{\frac{A(dB)}{10}} \tag{2.13}$$

### 2.1.3 Low-Pass Filter

Placing a low-pass filter (LPF) at the mixer's output will guarantee that only the beat frequency is retained since the up-converted term will be heavily attenuated. It was mentioned previously that for a range of 800 m, the beat frequency will be 400 kHz, thus, the LPF's 3-dB cutoff frequency would need to be a little greater than 400 kHz (to prevent signal attenuation by 3 dB). However, if for any reason in the future the radar's maximum detection range is increased, the maximum beat frequency will be greater than 400 kHz. To have plenty of margin in the case that the detection range is increased, Mini-Circuits' SLP-1.9 with a 3-dB cutoff frequency of 2.5 MHz was chosen. Its specifications are provided in Table 2.2.

**Table 2.2 Specifications of Mini-Circuits' low-pass filter used to reject the up-converted signal component.**

| Parameters | Value |
|---|---|
| **Model** | SLP-1.9+ |
| **Passband (MHz) (Loss < 1 dB)** | DC to 1.9 |
| **3-dB Cutoff Frequency (MHz)** | 2.5 |
| **Insertion Loss @ 0.4 MHz (dB)** | 0.1 |
| **Max. Input Power (dBm)** | 27 |

### 2.1.4 Receiver Amplifier

Properly selecting an RF amplifier (and other components) can be a difficult task without understanding the ever pervasive impact of thermal noise. This section will show the importance of not only selecting the proper amplifier but that its placement in the receiver chain can have a substantial effect on the performance of the receiver.

#### *Noise Figure*

One way that manufacturers specify the amount of noise inherent in a device is by providing the component's noise figure. Noise figure is a unitless factor and is dependent on the physical temperature of a device ($T_p$) as well as the equivalent (input) noise temperature ($T_e$) of a component which is a device parameter that tells how noisy the device is. It is typically assumed that the physical temperature of a device is the standard 290 K, which is around room temperature. The following equation can be used to calculate the noise figure from a device's equivalent noise temperature and physical temperature.

$$\boldsymbol{F} = \frac{T_e}{T_p} + 1 \tag{2.14}$$

The noise figure of a device tells how much additional noise will be added to a signal as it propagates through the device (with a physical temperature of 290 K) and is always greater than or equal to one, which means that the amount of noise at the output of any device will always be greater than or equal to the input amount.

The presence of noise in a device is generally an undesired reality and must be taken into account when selecting components for any receiver design. When a design is completed, it is possible to calculate the overall noise figure of the receiver, by treating the entire receiver as a single device and determining by how much greater is noise at the receiver (now considered a single device) output than at its input assuming that the physical temperature of the receiver is 290 K. Equation 2.15 can be used to calculate the overall noise figure of a receiver with $N$ number of components, where the first component is considered to be at the input to the receiver.

$$\boldsymbol{F} = F_1 + \frac{F_2 - 1}{G_1} + \frac{F_3 - 1}{G_1 G_2} + \frac{F_4 - 1}{G_1 G_2 G_3} + \cdots + \frac{F_N - 1}{\prod_1^{N-1} G_N} \tag{2.15}$$

It can be seen that the noise figure of the first device ($F_1$) has the most weight in comparison to any other device that follows, since the noise figures of all other components are divided by some amount of gain. Moreover, maximizing the gain of the first device ($G_1$) will lessen the significance of all other noise figures. Therefore, to minimize the overall receiver noise figure, it is important that the first component in the receiver chain have a small noise figure and a high gain.

### *Low Noise Amplifiers*

Low noise amplifiers (LNAs), as their name suggests, are a certain category of amplifiers that have been designed to have a very small noise figure. LNAs generally have a noise figure of around 1.5 dB, although there are some under 1 dB. Using a LNA as the first component in a receiver will most definitely minimize the receiver's noise figure, however, it will also make the design more sensitive to outside interference, since the LNA will amplify *all* received signals within its bandwidth. A solution is to precede the LNA with a filter that will pass only the desired spectrum (i.e., only the bandwidth of the signal of interest). Just as mixers have a maximum input signal power rating before they compress, LNAs (and all amplifiers in general) have a maximum input signal power before they compress or saturate. A band-pass filter is used to condition the received signal without which the LNA will be more prone to saturation from signals outside the desired spectrum but within the amplifier's bandwidth.

*LNA Selection and Contending With the Leakage Signal*

It has been shown that to minimize the overall receiver noise figure, (and thus increase SNR) there must be a component at the beginning of the receiver chain with a low noise figure and high gain such as an LNA. But is there an upper limit on the amplifier's gain for this FMCW radar? The gain of the amplifier must be as high as possible without the amplifier compressing (or saturating) the mixer which follows it. To prevent mixer saturation, the LNA's gain can be at most the difference between the mixer's ($P^{1dB}$) (in dB) and the maximum anticipated input power (in dB) into the LNA. Recall that the leakage signal will be the most powerful received signal due to the close proximity of the transmitter and receiver. If the transmitted signal power is 25 dBm, then based on Equation 1.18 (one-way range equation) the received leakage signal was previously calculated to be -11 dBm. Therefore, the maximum gain of the LNA can be 12 dB without saturating the mixer whose $P^{1dB}$ is 1 dBm (see Table 2.1). Note that this means that the isolation (due to free space) between the transmit and receive antennas is 36 dB (see Appendix A.5). However, since this prototype radar will initially be tested on board a Cessna C172, with the receiving antenna located inside the cockpit and the transmitting antenna under a dome and outside the aircraft, the exact isolation between the antennas will be slightly different than that calculated using the one-way range equation. The best way to determine this isolation would be to physically measure the strength of the received signal for a given transmit signal power. If the transmit antenna is considered to be the input of this system and the receiving antenna the output, then the ratio of the output signal power to the input is often called the $S_{21}$ scattering parameter. These measurements are usually accomplished using a network analyzer. To determine the worst case (minimum) isolation, the receiving antenna was moved to different locations inside the cockpit and the worst case isolation was recorded and is shown in Figure 2.3. The second marker corresponds to the radar's center frequency of 1.445 GHz. For a bandwidth of 15 MHz, the isolation curve is fairly flat and even increases slightly in both directions. Note that each cell is 20 MHz wide. Based on the measured antenna isolation, the gain of the LNA can be increased to 15 dB since the actual isolation is about 3 dB greater than the initially calculated isolation of 12 dB. 15 dB of gain would, therefore, result in a signal power that is equivalent to the mixer's $P^{1dB}$. Note that this will result only if the receiving antenna will in the end be positioned exactly in the location that results in the lowest (worst case) isolation. Most likely, when the antennas will be placed inside the aircraft, the actual isolation will be greater, which is good since it is undesirable to have the mixer compress.

The insertion loss of the band-pass filter preceding the amplifier will also attenuate the received signal slightly (by ~1 dB). Therefore, the maximum gain of the LNA should not exceed 16 dB.

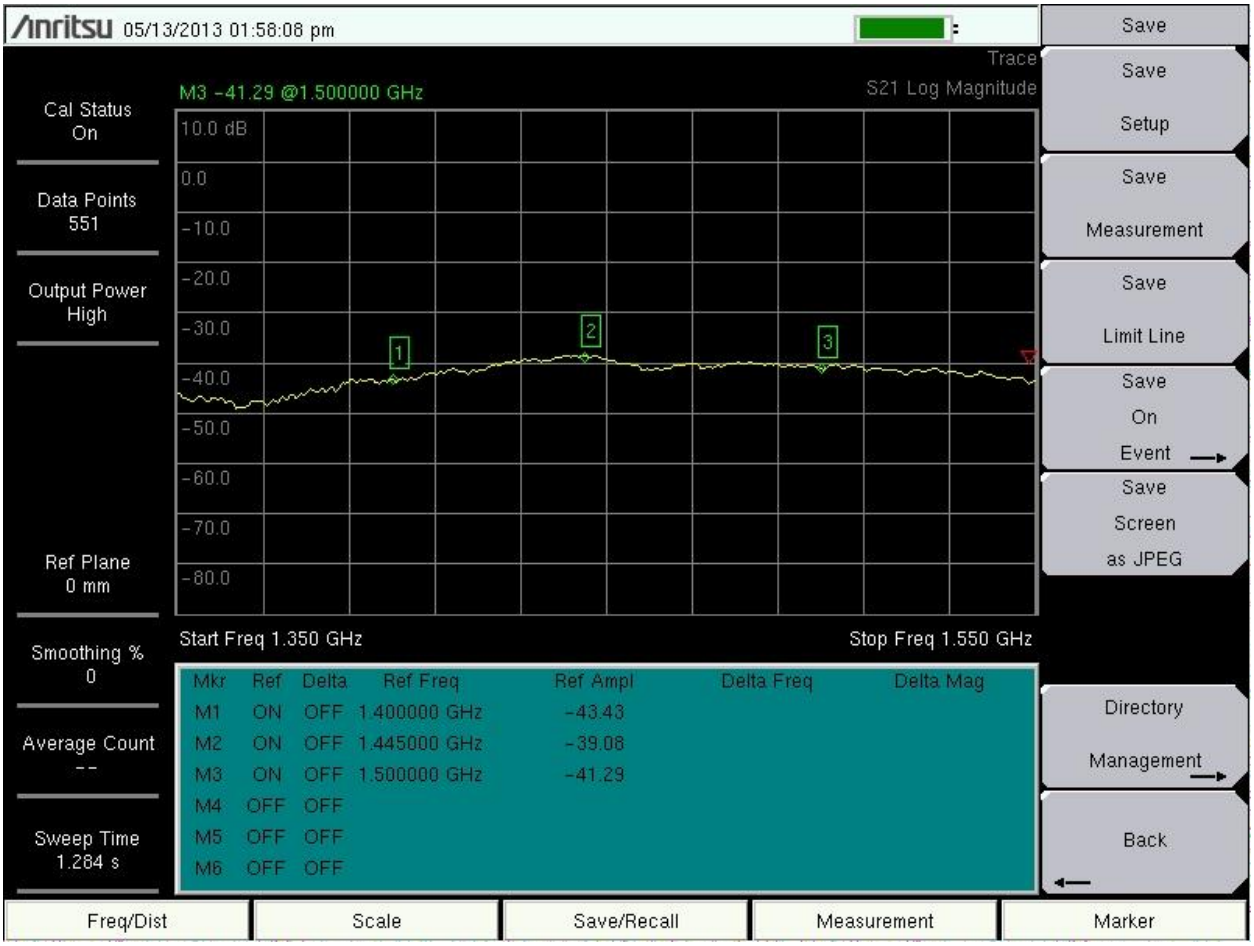


**Figure 2.3 Measured isolation between the Rx and Tx antennas onboard the Cessna-172.**

Mini-Circuits' ZX60-3011 LNA was chosen due to its low noise figure and a gain of 13.5 dB, which will ensure that the mixer's input signal power is further away from its $P^{1dB}$. Table 2.3 shows the LNA specifications.

**Table 2.3 Mini-Circuits' low-noise amplifier (LNA) specifications.**

| Parameters | Value |
|---|---|
| **Model** | ZX60-3011+ |
| **Frequency Range (MHz)** | 400 to 3000 |
| **Gain (dB)** | 13.5 |
| **Noise Figure (dB)** | 1.5 |
| **Input Return Loss (dB)** | 12 |
| **Output Return Loss (dB)** | 13 |
| **Output 1 dB Compression Point (dBm)** | 19.5 |
| **Max. Input Power (dBm)** | 15 |
| **DC Supply (V)** | 12 |

### 2.1.5 Receiver Input Filter

The purpose of placing a filter at the beginning of the receiver is to suppress all out of band signals and retain only the desired range of frequencies. In RF receivers, a band-pass filter is usually used to reject frequencies above and below the desired frequency range. When selecting a filter, there are three important specifications that must be considered namely, maximum input power, insertion loss and the filter's frequency response.

The maximum input power, usually given in dBm in datasheets, limits the input power which if exceeded could possibly destroy the component. The necessary maximum input power of a filter will depend on the maximum anticipated input power which will depend on the power of the desired spectrum as well as the environment in which the filter is used. The environment can be highly polluted, a term that signifies that there is a presence of many undesired high power signals, in which case a filter with a higher maximum input power value might be needed.

Insertion loss is the amount of attenuation that a signal undergoes as it passes through a device. For signals in the passband, this value is small and typically can range from about 0.5 dB to 2.5 dB, depending on the filter type. Insertion loss increases for frequencies in the stopband, thus attenuating undesired frequencies. However, when the term insertion loss is used, it is implied that the attenuation mentioned is for frequencies in the passband. It is understood from a previous section that the noise figure of the first element in a receiver has the most impact on the overall receiver noise figure. For filters, the noise figure is numerically equal to the insertion loss, therefore, it is important to select a filter will the smallest attenuation in the passband.

The shape of the frequency response can give insight as to how steep the roll off is past the upper and below the lower cutoff frequencies (in band-pass filters). Furthermore, a frequency plot can show how attenuation varies in the passband and stopbands. In general, we want the attenuation in the passband to be as small as possible and in the stopband to be as high in value and as long in bandwidth as possible (e.g. the upper stopband extends all the way to daylight). Looking only at the attenuation values provided in a datasheet's table can sometimes be deceiving, because at times, the attenuation in the stopband can significantly decrease (i.e. attenuate less) in certain frequency ranges which are not specified in the table.

TriQuint's surface acoustic wave (SAW) filter was selected as the input receiver band-pass filter and its specifications are shown in the table below. The maximum input power was not specified in the datasheet.

Table 2.4 TriQuint's SAW filter specifications.

| Parameters | Value |
|---|---|
| **Model** | 856928 |
| **Center Frequency (MHz)** | 1445.4 |
| **Bandwidth (MHz)** | 35 |
| **Insertion Loss (dB)** | 1.25 |
| **Return Loss (dB)** | 12 |
| **Output 1 dB Compression Point (dB)** | 19.5 |
| **Max. Input Power (dBm)** | Unknown |

The surface mount technology (SMT) required building an evaluation board with SMA connectors so that the filter could be easily connected to all other SMA connectorized components. The evaluation board designed and built by Lei Shi is shown in Figure 2.4

.

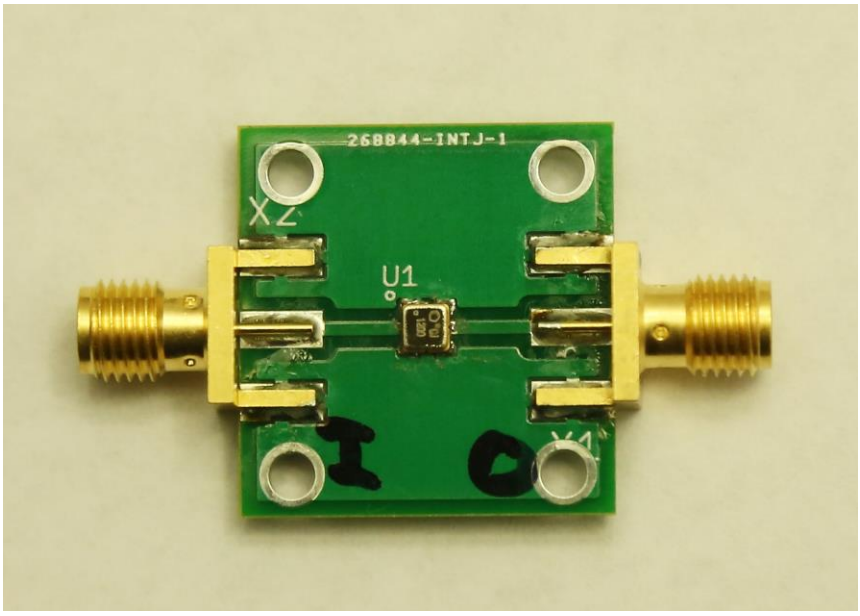


Figure 2.4 Evaluation board for TriQuint's SAW filter.

### 2.1.6 Summary

For the following summary, refer to Figure 2.1. The received echo is first band-pass filtered which makes the receiver less prone to saturation due to out of band signals. The signal is then amplified by the LNA but only enough to keep the mixer from saturating. The LNA's low noise figure and fairly high gain have the impact of substantially reducing the overall receiver noise figure. As the signal passes through the

mixer, it is mixed with the current transmit signal which produces the necessary beat frequency at the mixer's output. The signal is then low-pass filtered so that only the down-converted (beat frequency) component is retained. Finally, the beat signal is sampled and the quantized data is stored in a data matrix before digital signal processing takes place.

## 2.2 Transmitter Design

### 2.2.1 FMCW Waveform Generation

A common method for generating high frequency CW signals is to use a tunable voltage-controlled oscillator (VCO). For a given input voltage, a VCO will output a single frequency tone. Tunable VCOs allow a certain range of input voltages and thus result in a specific range of frequencies that can be generated at the output. By properly controlling the input voltage, it is possible to generate different kinds of waveforms. Figure 2.5 shows how a linearly increasing input voltage produces a linearly increasing output frequency. Note that real (i.e. non ideal) VCOs cannot jump in frequency instantaneously as shown in Figure 2.5 because the input voltage cannot change instantaneously.

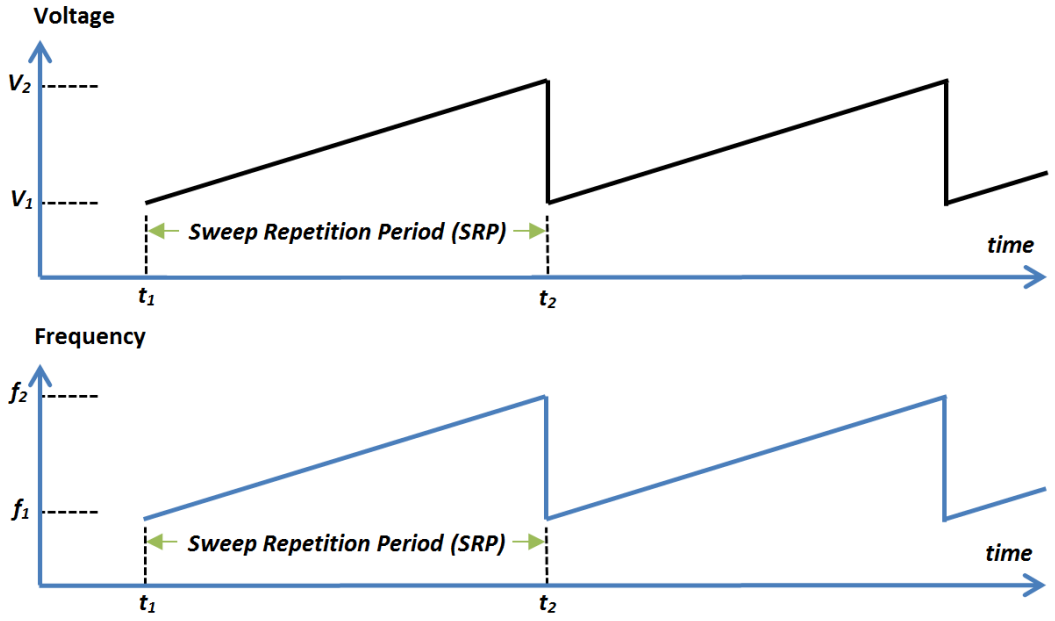


**Figure 2.5 A range of input VCO voltages corresponding to a range of output frequencies.**

Shown in Figure 2.6 is an ADF4158 FMCW synthesizer evaluation board from Analog Devices that was chosen for generating the required linear frequency-modulated waveform. The original 5.8 GHz VCO on the board was replaced with a VCO from Z-Communications capable of generating frequencies from 1400 to 1624 MHz. The FMCW radar's center frequency was chosen to be 1.445 GHz, because it falls

within the mobile aeronautical telemetering band. The software used to program the synthesizer allows the user to simply select the desired waveform from a drop down menu and define parameters such as the start and stop frequencies as well as the duration of each chirp.

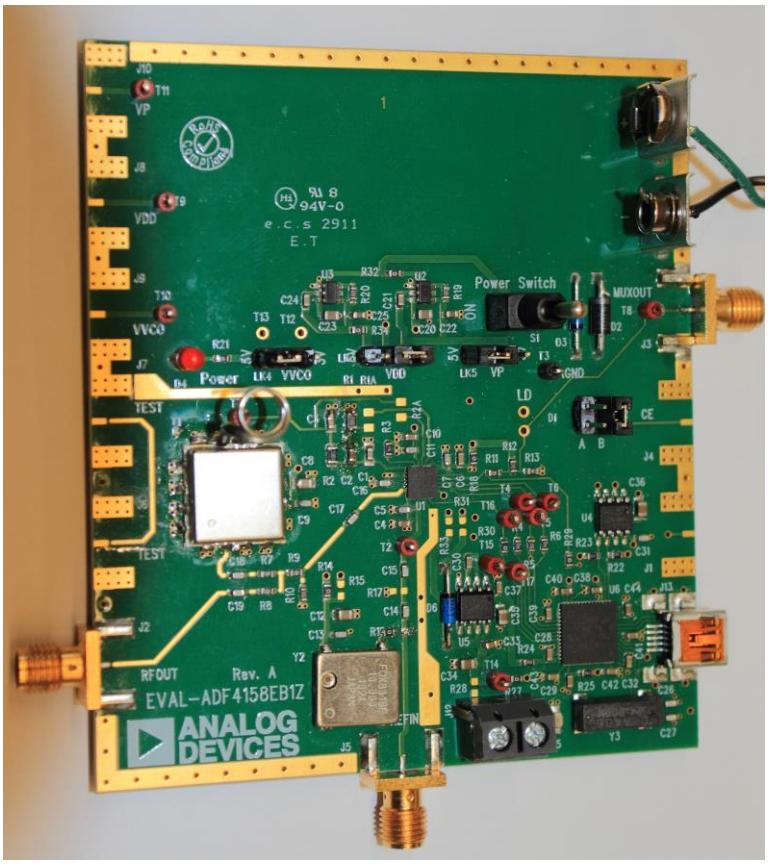


**Figure 2.6 Waveform generator evaluation board.**

Figure 2.7 shows the VCO input voltage for generating a sawtooth wave with a center frequency of 1.445 GHz and a bandwidth of 15 MHz. Notice that at the end of a chirp when the voltage drops to begin generating the next chirp, there is about 40 µs of ringing before the input voltage becomes linear again. The VCO has no way of knowing whether the input voltage is linear or not and will therefore continue generating a signal proportional to the input voltage, thus introducing a nonlinearity in the chirp for a duration of 40 µs. To reduce the magnitude and duration of ringing, the onboard snubber circuit (a frequency filter) was modified to filter out the high frequency components of the input voltage. Figure 2.8 shows the new VCO input voltage with the transition time reduced to 27 µs. Note that it is impossible to reduce the transition time to zero due to the presence of capacitance in the circuit as well as a bandlimited feedback response that does not allow voltage to change instantaneously. This means that the generated chirp will always be nonlinear for approximately 27 µs at the beginning of each cycle.

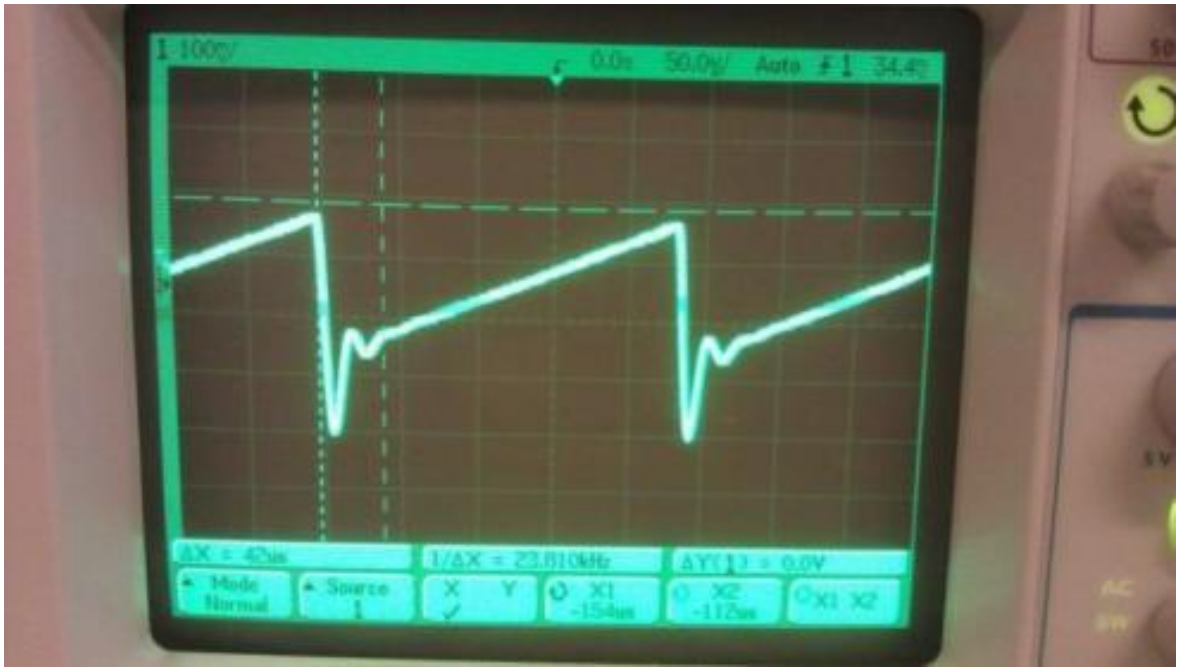


**Figure 2.7 VCO input voltage with 42 µs of ringing.**

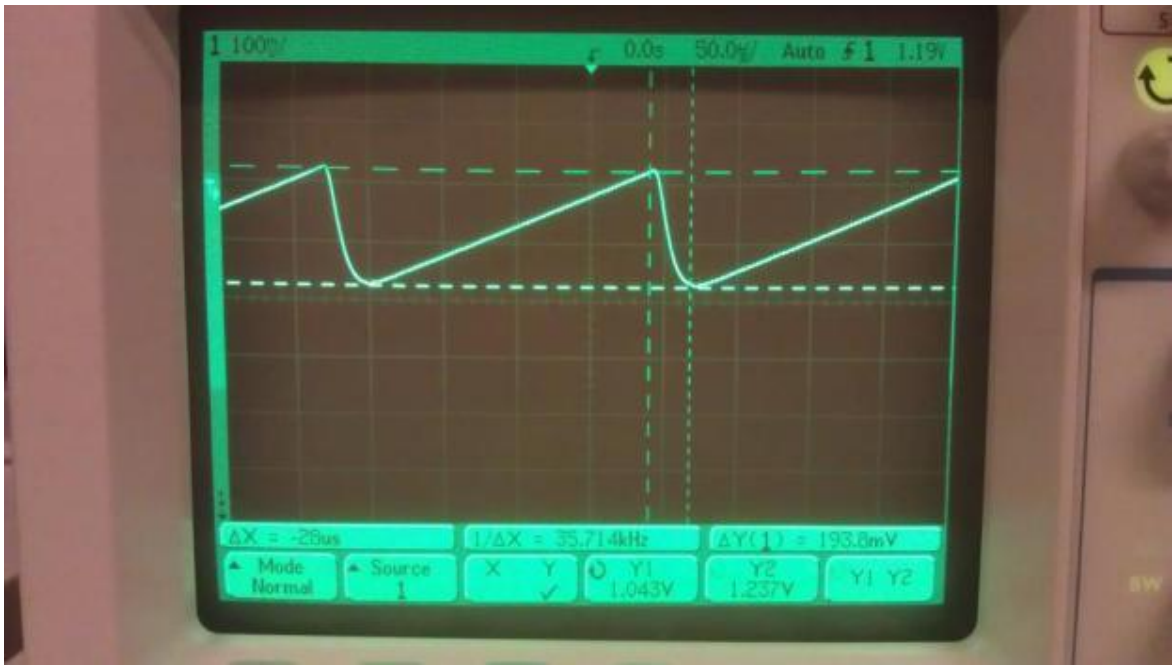


**Figure 2.8 VCO input voltage due to a modified snubber circuit.**

One way to counter this problem is to simply disregard 27 µs worth of samples at the beginning of each frequency sweep and not use them at all in signal processing.

The spectrum of the sawtooth waveform was measured with a spectrum analyzer and is shown in Figure 2.9. Signal power for marker 3 is shown as -10.75 dBm, however, a coaxial cable with about 1.5 dB of insertion loss was used to connect the waveform generator to the spectrum analyzer which means that the waveform generator is actually outputting about -9 dBm. This value is important to know because it will help determine how much additional gain will be required to be able to transmit a certain amount of power.

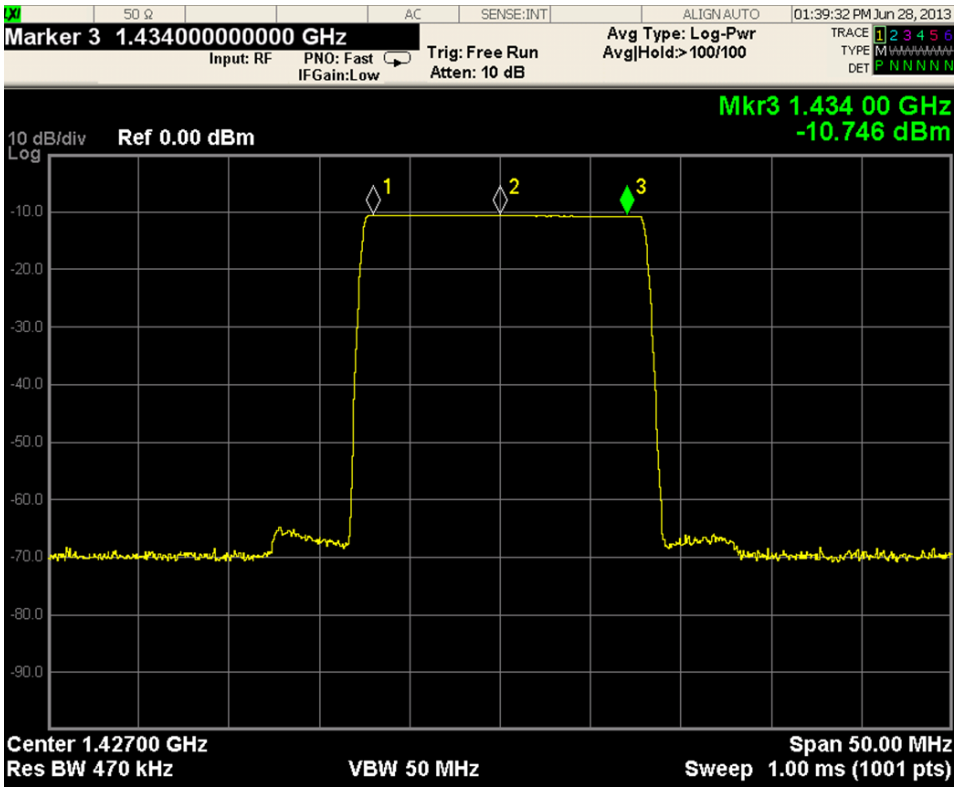


**Figure 2.9 Spectrum of the linear frequency-modulated waveform.**

### 2.2.2 Duplicating the Sawtooth Waveform

Recall that one of the fundamental principles behind FMCW operation is that the frequency of the received signal must be subtracted from the signal that is currently being transmitted resulting in a beat frequency from which range and Doppler information can be found. It was shown that a mixer can be used to perform this subtraction process if a copy of the transmitted signal is input into the mixer's LO port. Therefore, it is necessary to divide the generated sawtooth waveform into two identical copies so that one copy will be sent to the transmit antenna and the other copy sent to the LO port of the mixer.

*2-Way Splitter*

In general, a RF signal can easily be divided into $N$ number of copies by using a $N$-way splitter. In reality, of course, a splitter can only produce signals that are very similar to one another but not exactly identical. There will always be some finite amount of amplitude and phase variation between any two signals. Ideally, the power of the divided signals will be at most the input signal power divided by the number of copies ($N$) produced (unavoidable splitting loss due to Conservation of Energy), but due to insertion loss (inherent in all devices) the output signal power is slightly less.

For the purpose of creating two copies of the sawtooth waveform, a 2-way splitter was chosen, although a $N$-way splitter could be used, provided that all unused ports are terminated with a matched load. Mini-Circuits' ZAPD-23+ was selected because of its low insertion loss and minimal amplitude and phase variation between the two output signals. Its specifications are found in the following table.

**Table 2.5 Mini-Circuits' 2-way splitter specifications.**

| Parameters | Value |
|---|---|
| **Model** | ZAPD-23+ |
| **Frequency Range (MHz)** | 700 to 2000 |
| **Isolation (dB)** | 30 |
| **Insertion Loss (dB)** | 0.5 |
| **Total Loss (dB)** | 3.5 |
| **Amplitude Unbalance (dB)** | 0.01 |
| **Phase Unbalance (deg.)** | 0.5 |
| **Input Return Loss (dB)** | 29 |
| **Output Return Loss (dB)** | 29 |
| **Max. Input Power (dBm)** | 40 |

*6-Way Splitter*

It was mentioned earlier that five antennas will be used to unambiguously determine AoA information, for which reason a multichannel ADC was selected to individually quantize the beat signal for each channel. Every channel will contain the same components such as a band-pass filter at the beginning of each channel, a LNA and a mixer. To produce the desired beat frequency for each channel, all five mixers' LO ports must receive a copy of the current transmit signal, thus requiring an additional multi-way splitter after the 2-way splitter. Since the frequency range of the 5-way power splitters from Mini-Circuits did not include the required operating center frequency of 1.445 GHz, a 6-way splitter was used instead with one (unused) port terminated in a matched (50 Ω) load. The specifications for this 6-way

Table 2.6. Mini-Circuits' 6-way splitter specifications.

| Parameters | Value |
|---|---|
| **Model** | ZB6PD-17 |
| **Frequency Range (MHz)** | 600 to 1700 |
| **Isolation (dB)** | 23 |
| **Insertion Loss (dB)** | 0.5 |
| **Total Loss (dB)** | 8.3 |
| **Amplitude Unbalance (dB)** | 0.14 |
| **Phase Unbalance (deg.)** | 2.56 |
| **Input Return Loss (dB)** | 20 |
| **Output Return Loss (dB)** | 30 |
| **Max. Input Power (dBm)** | 40 |

splitter are provided in Table 2.6. Note that the insertion loss of this splitter is approximately the same as of the 2-way splitter, but since the parent signal's power is divided by 6 (as opposed to 2 in the 2-way splitter), the total loss is greater, where total loss is defined as the sum of the insertion loss (in dB) and the splitting loss (in dB).

In summary, the FMCW synthesizer generates a linear frequency-modulated signal which is then sent through a 2-way splitter. One copy of the signal will be amplified and transmitted through an antenna, while the other copy will be sent through a 6-way splitter and the resulting signals into each mixer's LO port.

### 2.2.3 Transmit Signal Integrity

Generally, all systems or devices that transmit signals must do so without transmitting relatively powerful signals outside of their operating frequency range. Typically, a band-pass filter will be added in the transmit chain to accomplish this. Although the spectrum of the frequency modulated signal shown in Figure 2.9 does not extend beyond the operating frequency range, it is still a good idea to have the signal pass through a filter before the signal is transmitted into free space or sent to the LO ports of the mixers, to reduce any chances of the signal extending beyond the operational frequency range. To keep the number of different components to a minimum, the bandpass filter was chosen to be the same one that is used in the receiver.

Ideally, a filter would be placed right before the transmit antenna and after the power (transmit) amplifier so that any spurious signals generated by the power amplifier can be attenuated by the filter. However, placing a filter after the power amplifier can be unreliable if the power of the signal coming from the amplifier is comparable to the filter's maximum input power. If for any reason the filter gets damaged

and results in an open circuit, the reflection coefficient will approach unity and reflect all of the signal power back into the amplifier and possibly damage the expensive power amplifier. Since the chosen band-pass filter's datasheet did not specify the maximum input power for safe operation, it would be safer to place the filter before the power amplifier. To avoid having to use 2 filters, one filter for the transmit signal and one for the LO signals (after the 2-way splitter but before the 6-way splitter), a single filter can be placed before the 2-way splitter.

### 2.2.4 RF Amplifier Selection

*Transmit Power Amplifier*

Since it is known that the radar being designed will transmit approximately 0.5 W (or 27 dBm), it is important to choose a transmit amplifier that will be able to transmit such signal power without compressing (very much). Recall that when an amplifier operates in saturation mode, the weight of higher order terms (harmonics) will increase while the strength of the desired signal remains constant. If these harmonics are not filtered out, then the system could possibly not pass certain Federal Communications Commission (FCC) requirements since the transmit signal's spectrum will extend beyond the designated radar's spectrum.

In the transmit chain, the -9 dBm generated FM signal will be attenuated by the band-pass filter's insertion loss and the 2-way splitter's total loss. Therefore, if the radar is to transmit 27 dBm, then at least 41 dB of gain is required (see Appendix A.6). Due to slight impedance mismatches in any device's ports or in interconnections, it is good practice to design a system with more gain than necessary because extra gain can always be attenuated with an attenuator.

Unlike mixers, whose $P^{1dB}$ is specified as the *input* power that results in a conversion loss that appears to be 1 dB higher than the normal conversion loss, amplifier datasheets typically relate the $P^{1dB}$ to the *output* power of the amplifier that results when the gain appears to have been decreased by 1 dB. Mini-Circuits' ZHL-42W was selected as the power amplifier, because it had the highest $P^{1dB}$ of 27 dBm, a high gain of 36 dB, and because it was capable of running off of a 12 V power supply. Table 2.7 shows the specifications of this power amplifier.

**Table 2.7 Mini-Circuits' power amplifier specifications.**

| Parameters | Value |
|---|---|
| **Model** | ZHL-42W+ |
| **Frequency Range (MHz)** | 10 to 4200 |
| **Gain (dB)** | 36 |
| **Noise Figure (dB)** | 7 |
| **Input Return Loss (dB)** | 13 |
| **Output Return Loss (dB)** | 11 |
| **Output 1 dB Compression Point (dBm)** | 27 |
| **Max. Input Power (dBm)** | 0 |
| **DC Supply (V)** | 12 |

*Pre-Amplifier*

Recall that the -9 dBm generated FM signal must be amplified by at least 41 dB if the system is to transmit 27 dBm. Since the gain of the power amplifier is only 36 dB, a pre-amplifier with a gain of at least 5 dB will be necessary. Mini-Circuits' ZX60-3011 with a gain of 13.5 dB was chosen to provide the extra amplification. Note that this amplifier is the same as the LNA in the receiver whose specifications are shown in Table 2.3. The gain of this amplifier was intentionally selected to be greater than 5 dB which will make the system more tolerable to unexpected reflections or other system losses.

All amplifiers that were selected up to this point can be powered by a 12 V supply. It is convenient to have all amplifiers (and/or other devices) run off of the same DC supply because it eliminates the need for extra voltage regulation.

*Amplifier Saturation at $P^{1dB}$*

The phenomenon of higher order terms gaining in power relative to the signal of interest can be seen in Figure 2.10, where the input power to the power amplifier is -8 dBm and results in an output power equal to the amplifier's $P^{1dB}$. [The -8 dBm input power was determined by measuring the amplifier's $S_{21}$ (amplifier gain) parameter and increasing the input power until the gain decreased by 1 dB]. Here, the first marker corresponds to the fundamental frequency, and the second marker has been placed at the first harmonic [i.e., twice the fundamental (center) frequency]. The fundamental frequency component appears to be approximately 30 dB greater than the first harmonic. Contrast this with Figure 2.11 where the input power is -16 dBm such that the amplifier is further away from compression. Here, harmonics are present, but they are of much less power than the fundamental frequency and all but the first harmonic are down below the noise floor. The fundamental frequency is almost 40 dB greater than the first harmonic. Note that since an amplifier enters compression gradually, harmonics will still be prevalent

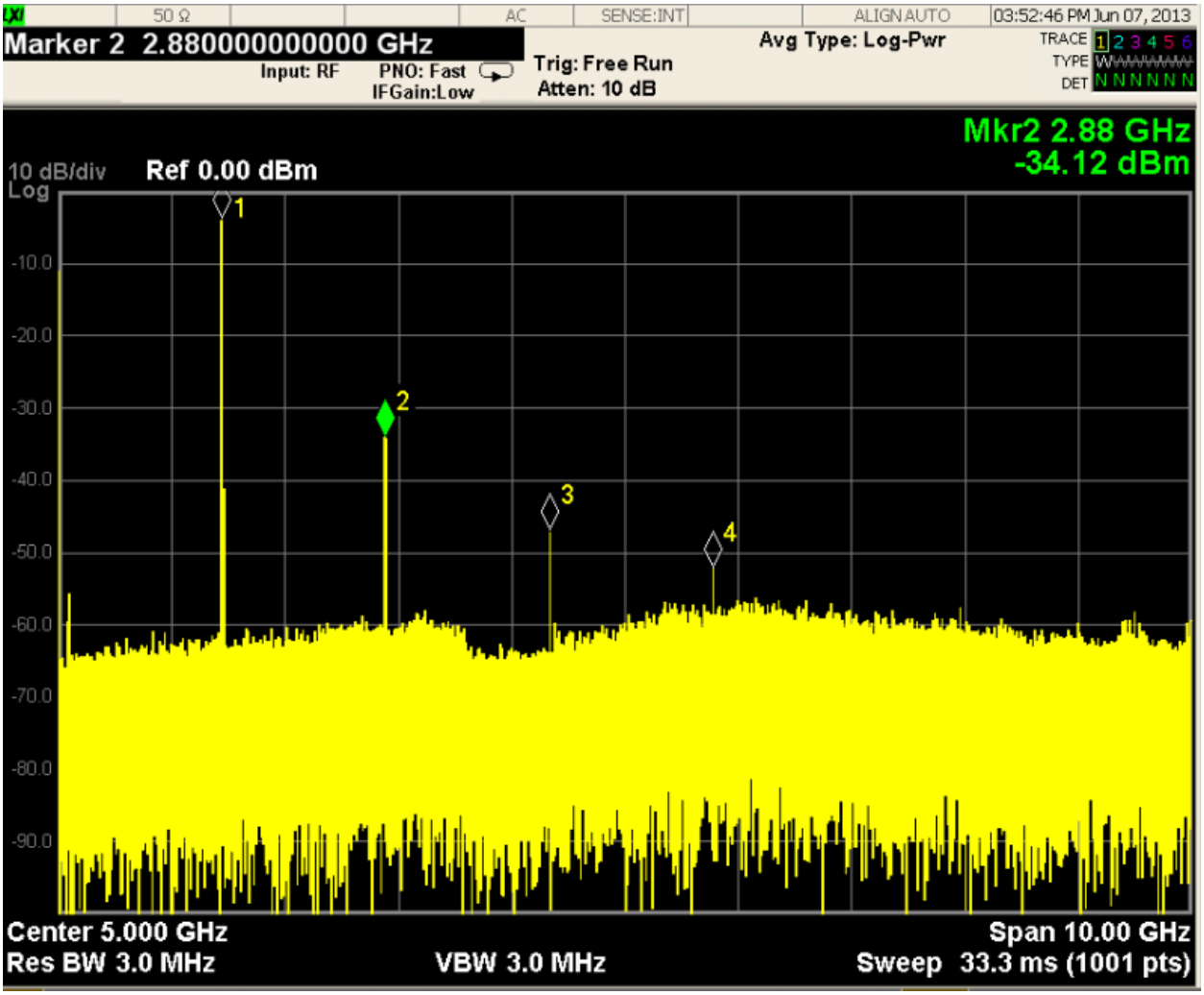


**Figure 2.10 Stronger harmonics due to amplifier saturation.**

even when the output power is +25 dBm, which is about 2 dB less than $P^{1dB}$. The only way to reduce these harmonics would be either to low-pass filter the signal or to reduce the output signal power. The latter option would require an output power that is much less than +25 dBm, which would negatively impact the SNR at the receiver, since according to Equation 1.14 the received signal power is directly proportional to the transmit power. Thus, it will be necessary to add a low-pass filter after the power amplifier. Mini-Circuits' VLF-1700 7$^{th}$ order low-pass filter with a 3-dB cutoff frequency of 2050 MHz was selected due to its sharp roll off and for tolerating a maximum input signal power of 40 dBm. Figure 2.12 shows the spectrum of the transmit signal when a 27 dBm signal from the amplifier is sent through a low-pass filter. According to the filter's datasheet, the first harmonic (at about 2890 MHz) would have been attenuated by about 50 dB. Recall that without the filter, the fundamental frequency was about 30 dB greater than the first harmonic (see Figure 2.10) which means that with the filter, the fundamental component will be about 80 dB greater.

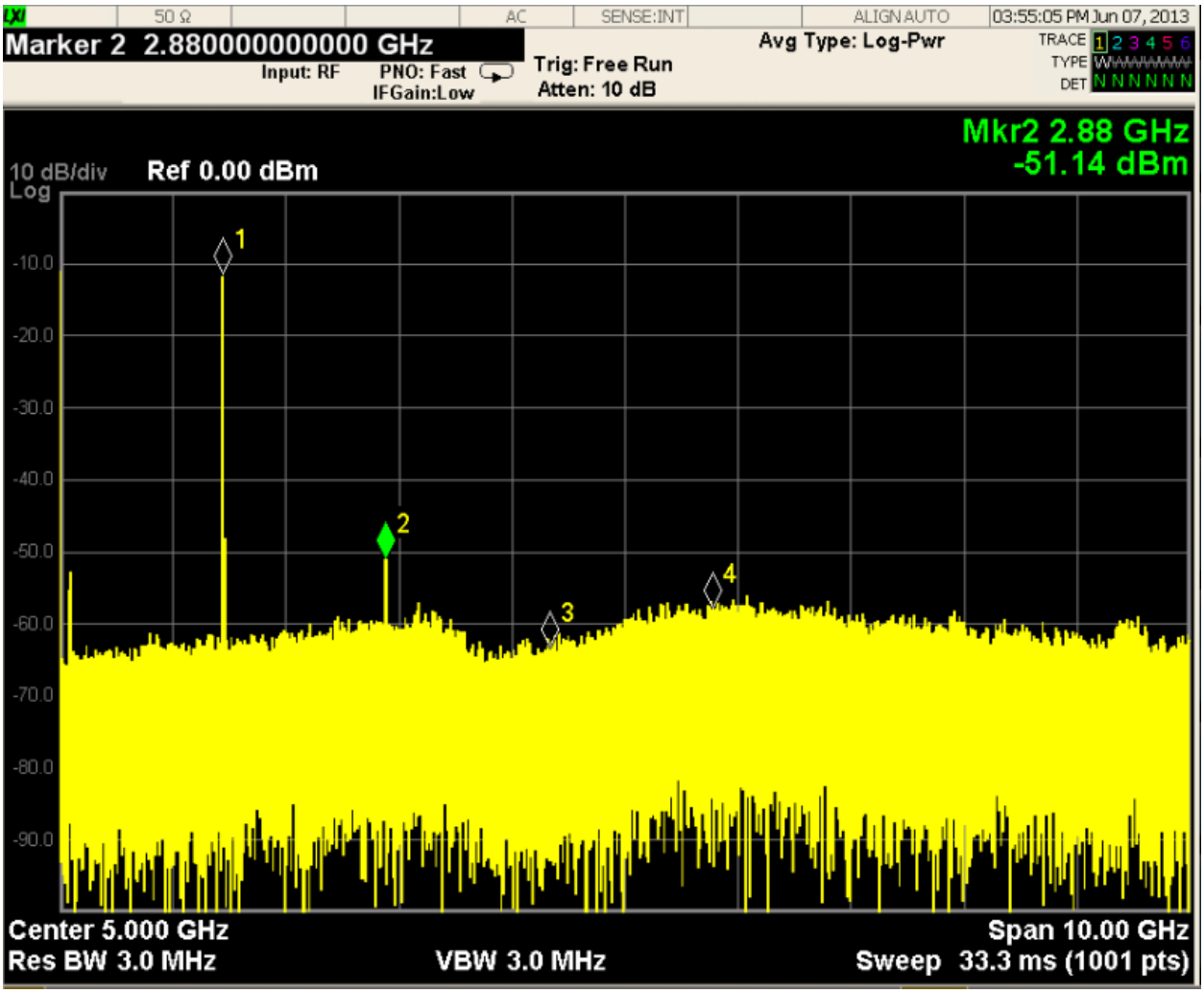


**Figure 2.11 Amplifier output when not operating in compression mode.**

**Table 2.8 Mini-Circuits' low-pass filter specifications.**

| Parameters | Value |
|---|---|
| **Model** | VLF-1700+ |
| **Passband (MHz) (Loss < 1.2 dB)** | DC to 1700 |
| **3-dB Cutoff Frequency (MHz)** | 2050 |
| **Insertion Loss @ 1445 MHz (dB)** | 0.5 |
| **Max. Input Power (dBm)** | 40 |
| **Number of Sections** | 7 |

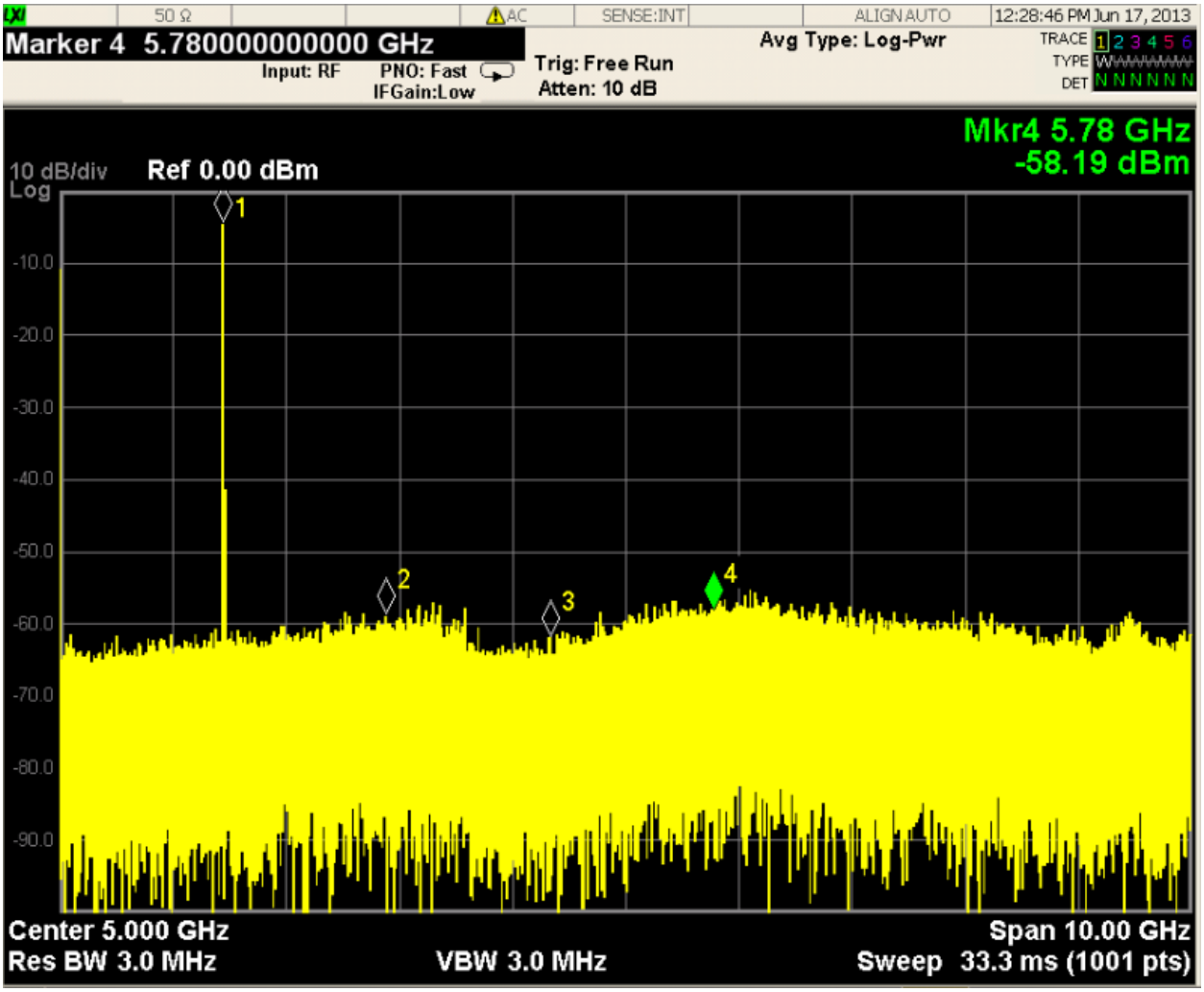


Figure 2.12 The effect of a low-pass filter on harmonics.

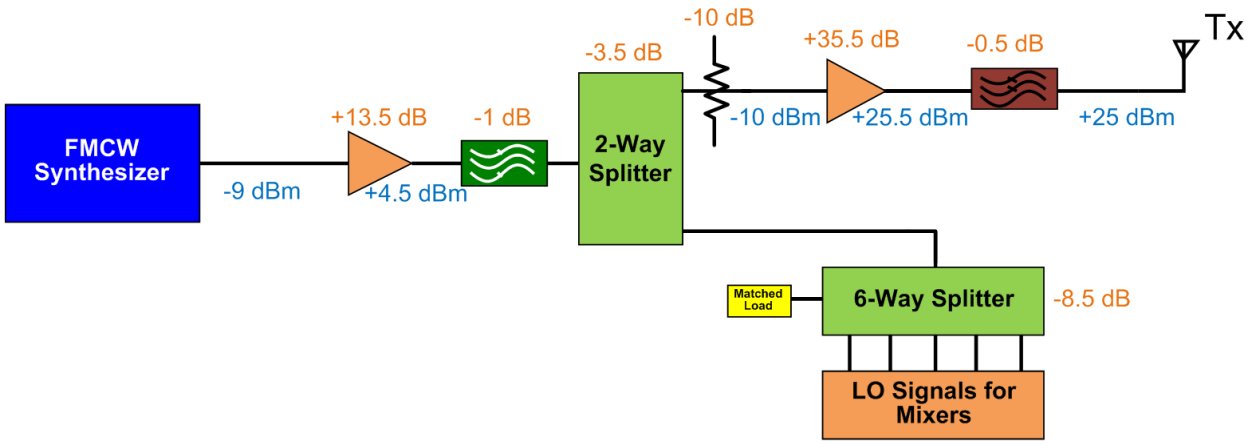


Figure 2.13 Initial design of the FMCW transmit chain.

Figure 2.13 shows the transmit chain design. Note that the included attenuator pad can be used to adjust the signal power entering the power amplifier, and thus the output signal power. Signal power at various stages is shown in blue, and the gains of devices is shown in orange.

*LO Amplifier*

The mixers chosen for the down-conversion process require a LO drive power of at least +7 dBm (see Table 2.1). It is also known that the waveform generator outputs a signal power of -9 dBm, and that the signal before reaching any mixer's LO port will be additionally attenuated by the total loss of both splitters as well as by the insertion loss of the filter (placed before the 2-way splitter). Therefore, if the -9 dBm signal is amplified by 30 dB, then at the LO ports the signal power will be exactly +8 dBm (see Appendix A.7). Since an amplifier with 13.5 dB of gain has already been placed before the 2-way splitter, at least 16.5 dB of gain is necessary to result in +8 dBm of signal power at the LO port. This amplifier would also need to have a $P^{1dB}$ that is much greater than +8 dBm to keep the amplifier from compressing. Mini-Circuits' ZRL-2150 was selected whose specifications can be found in Table 2.9.

**Table 2.9 Mini-Circuits' LO amplifier specifications.**

| Parameters | Value |
|---|---|
| **Model** | ZRL-2150+ |
| **Frequency Range (MHz)** | 950 to 2150 |
| **Gain (dB)** | 25.5 |
| **Noise Figure (dB)** | 1.4 |
| **Input Return Loss (dB)** | 13 |
| **Output Return Loss (dB)** | 11 |
| **Output 1 dB Compression Point (dBm)** | 23 |
| **Max. Input Power (dBm)** | 10 |
| **DC Supply (V)** | 12 |

Note that the extra gain can always be attenuated which allows the LO signal power to be adjusted to a desired value. It is normal to allow the LO signal power to exceed the LO drive power by a couple of dB. This ensures that the transistors in the mixer turn fully on and off and has the effect of slightly reducing the conversion loss of the mixer.

### 2.2.5 Summary

For the following summary of the initial radar design, refer to Figure 2.14.

The FMCW synthesizer generates a linear frequency-modulated signal which is then amplified and bandpass filtered to ensure that any out of band frequencies are suppressed. The signal is then divided

into two copies where one copy is amplified by the power amplifier (36 dB of gain). This amplifier becomes slightly compressed and so its output signal is sent through a low-pass filter to attenuate the harmonics (especially the first harmonic) before the signal is sent into free space through the transmit antenna. The attenuator preceding the power amplifier can be used to adjust the transmit power. The other copy from the 2-way splitter is amplified and split so that all five mixers' LO ports can receive the same transmit signal.

When the transmitted signal reflects off of a target, the received echo is received by all five receive antennas. The received signals are first bandpass filtered to make sure that only the desired signal is retained and all out of band signals are attenuated. The signals then pass through an LNA whose high gain and low noise figure have the greatest weight in reducing the overall receiver noise figure. The signals are then mixed with the current transmit signal which results in up and down converted terms at the mixer's output. The low-pass filter following the mixer attenuates the up-converted component and retains the desired down-converted term which is the desired beat frequency. The signal then is amplified by a built-in programmable gain amplifier and sent through a built-in antialiasing filter before the signal is sampled and stored in the data matrix upon which a 2-D FFT is performed.

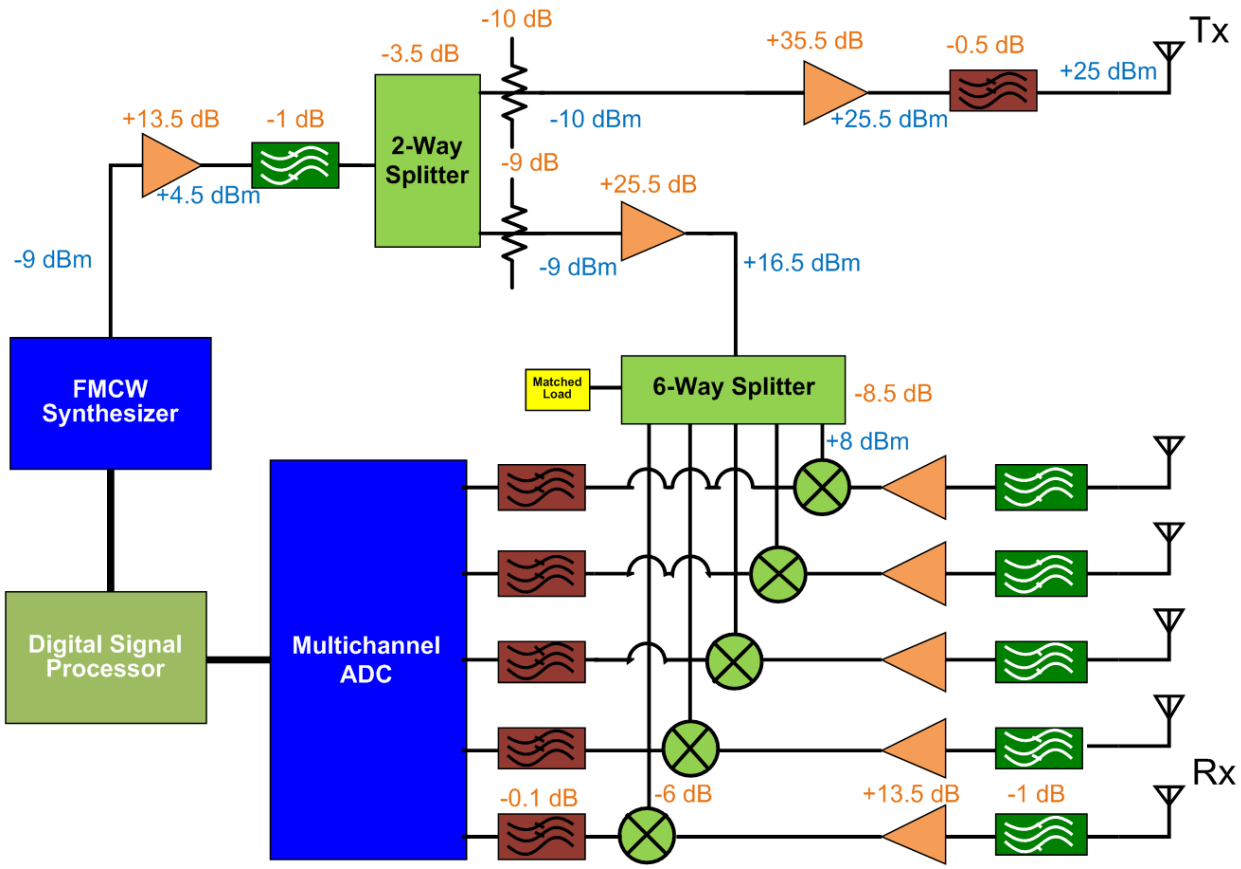


**Figure 2.14 Initial radar design.**

## 2.3 Antenna Design

An antenna is a device that is capable of radiating an electrical signal into free space, as well as converting a radio wave into an electrical signal, where the first results when an antenna is used to transmit and the latter if an antenna is used to receive. From basic microwave theory, it is known that when the medium in which an electrical signal travels in changes impedance, part of the signal will reflect at the boundary of impedance mismatch. An antenna can be thought of as an impedance transformer (or a matching network) that transforms the characteristic impedance of the transmission line to that of free space, a constant of about 377 Ω. If carefully designed, an antenna can be made to have a very small reflection coefficient which is commonly termed as the antenna's $S_{11}$ parameter. The radiation pattern of an antenna can be designed such that its sensitivity is direction dependent which allows an antenna to be used as a spatial filter.

### 2.3.1 Receive Antenna

Since the sense-and-avoid radar is being designed for small UASs, the size and weight of this radar is limited. It is, therefore, of major importance to design an antenna that would be light and small in size while still meeting all performance requirements. From a cost and complexity perspective, the antenna would need to be inexpensive and simple to manufacture.

*Azimuth Antennas*

Monopole and half-wave dipole antennas are probably two of the most basic antennas that are non-expensive and easy to fabricate. Their radiation patterns are very similar (identical above the *z-plane* if the antenna is at the origin) in that they both have an omnidirectional radiation pattern in the azimuth plane. In the elevation plane, an omnidirectional pattern's gain decreases with elevation and approaches zero at zenith. Monopole antennas are usually half the height of dipole antennas, and have a maximum gain that is about 3 dB greater. For these reasons, a monopole type was chosen to be used as the receive antennas for measuring the AoA in the azimuth plane. For more information on how and why a monopole antenna was selected, refer to Neto [6].

Figure 2.15 (*left*) shows an array of three monopole antennas (recall that there should be three antennas for azimuth AoA detection) made on a PCB. The three monopoles have been arranged symmetrically such that there is 120° between any two antennas. The circular plate on which the antennas are seated is the ground plane that is required if the antennas are to have an omnidirectional radiation pattern (above

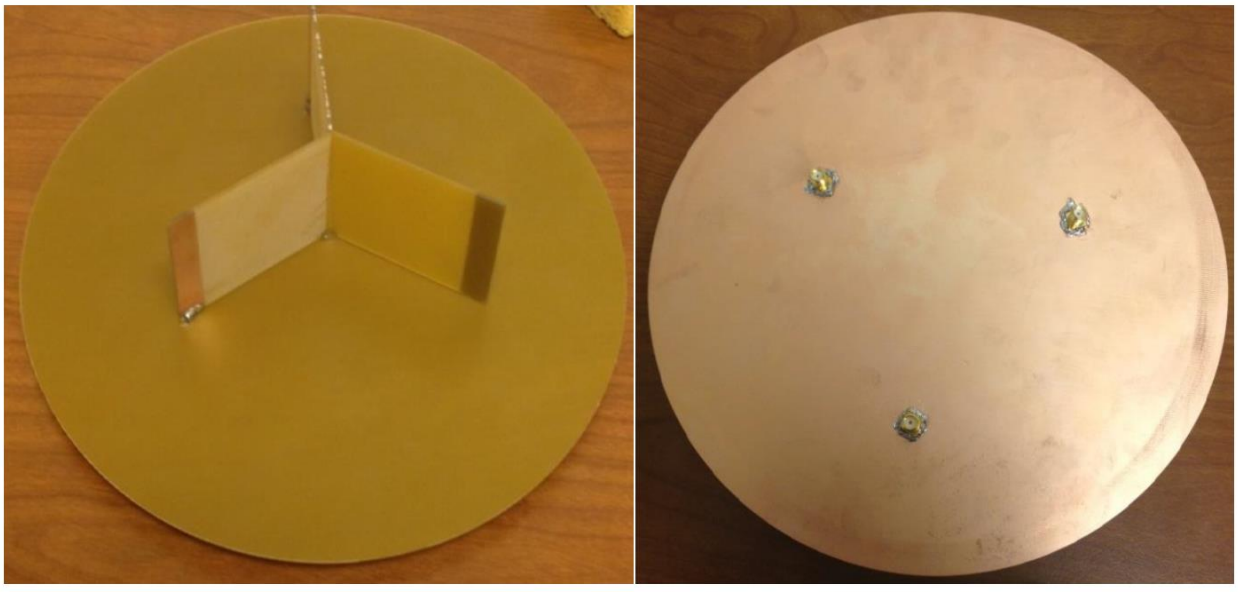

**Figure 2.15 Top view of the receiving antenna array (*left*), bottom view of antenna array (*right*).**

the *z-plane*). Figure 2.15 (*right*) shows the bottom side of the plate. Tiny holes have been drilled to allow the inner conductor of SMA connectors to be connected to each antenna.

Figure 2.16 shows the magnitude of the reflection coefficient of about -14 dB which is also the lowest of all three antennas. The $S_{11}$ parameter of an antenna is generally considered acceptable if it is at least 10 dB.

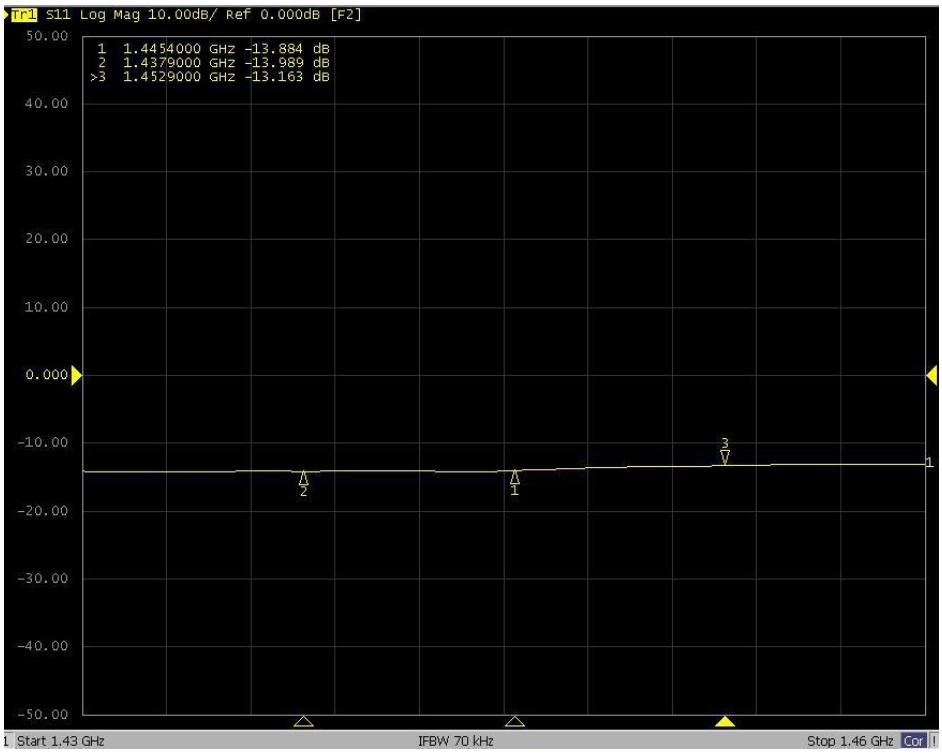


**Figure 2.16 Magnitude of $S_{11}$ between 1430 MHz and 1460 MHz.**

## *Elevation Antennas*

One of the system's requirements is that it must be able to detect targets within ±15° in elevation. To do this, two antennas need to be placed vertically. This cannot be (easily) accomplished with a monopole array because the required ground planes will "sandwich" one antenna. Therefore, dipole antennas were used instead. Figure 2.17 shows the dipole antennas designed and built by Nahal Niakan that will be used for measuring the elevation angle. The back side containing the other half of the dipoles is not shown. These antennas were made on a PCB just as the azimuth antennas were.

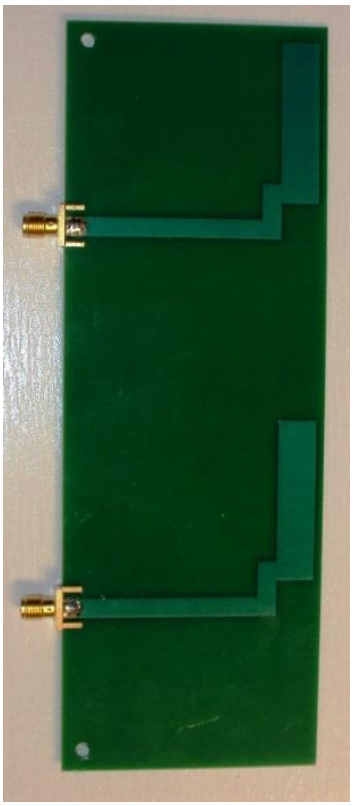

**Figure 2.17 Dipole antenna array for measuring the elevation angle.**

### 2.3.2 Transmit Antenna

The prototype radar system will be eventually tested on board a Cessna, however, the transmit antenna will be placed outside of the aircraft. To ensure mechanical rigidity/stability at high speeds, it is important to enclose the antenna in a radome. Since the aircraft was already equipped with a monopole antenna inside an ABS plastic radome, that antenna was chosen. An image of the radome mounted on top of one of Cessna's wings is shown in Figure 2.18 and its specifications are provided in Table 2.10. Note that this antenna's horizontal (azimuth) and vertical (elevation) angular coverage suffices the required field of view.

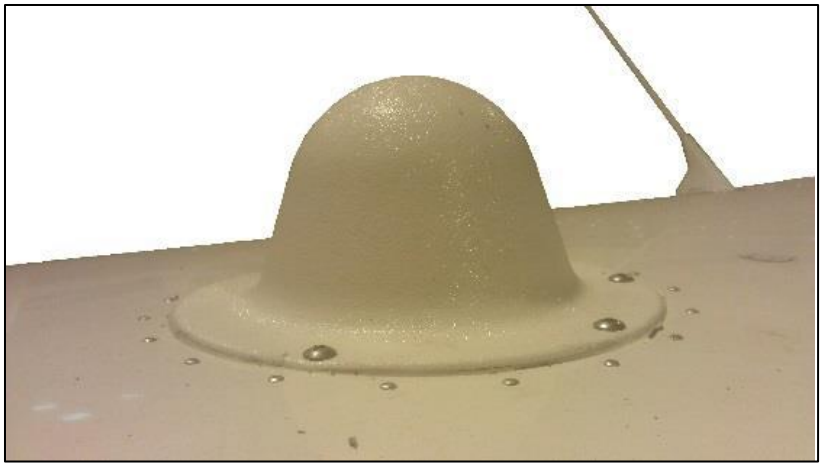

**Figure 2.18 Transmit antenna underneath a radome on top of a Cessna's wing.**

**Table 2.10 Pasternack transmit antenna specifications.**

| Parameters | Value |
|---|---|
| **Model** | PE51057 |
| **Frequency Range (MHz)** | 800 to 3000 |
| **Gain (dBi)** | 3 to 6.5 |
| **Horizontal 3-dB Bandwidth (°)** | 360 |
| **Vertical 3-dB Bandwidth (°)** | 75 |
| **Impedance (Ω)** | 50 |
| **Output 1 dB Compression Point (dBm)** | 23 |
| **Max. RF Power (W/dBm)** | 100/50 |

This concludes the initial radar design.

# Chapter 3: FMCW Radar Analysis

## 3.1 Loopback Test Setup

Preliminary ground tests are generally conducted before a radar system is tested in its final environment. Testing a FMCW radar would require time-delaying the received signal. By varying the duration of the delay, various ranges of a static target can be emulated. Dynamic targets can be simulated by introducing a Doppler shift in the time-delayed received signal. Finally, to completely simulate a FMCW radar, the leakage signal must also be included in the received signal.

### 3.1.1 Emulating Range

One way to delay a high frequency signal is to send it through a long coaxial cable. However, a delay corresponding to the radar's maximum detection range of 800 m would require hundreds of meters of cable length. If RG-174 coaxial cable is used, the resulting spool of cable will be quite heavy and expensive.

Another approach would be to use a fiber-optic delay line. This method, though, requires an optical transmitter which will modulate an optical frequency with the RF signal, and a receiver which will demodulate the signal back to an RF frequency. Since all of the necessary equipment was at hand, this method was chosen.

The relationship between the length ($\ell$) of the fiber-optic delay line and time ($T$) that it takes for a signal to propagate through is shown in Equation 3.1, where $v_p$ is the speed of propagation.

$$\boldsymbol{T} = \frac{\ell}{v_p} \ [s] \tag{3.1}$$

Substituting the previous equation into Equation 1.2 and solving for $\ell$ results in the following equation which can be used to solve for the length of fiber-optic line needed to simulate a certain target range, where $\epsilon_r$ is the relative dielectric constant of the line which is approximately 2.13.

$$\boldsymbol{\ell} = \frac{2R}{\sqrt{\epsilon_r}} \ [m] \tag{3.2}$$

Therefore, if the transmitted signal is sent through a delay line of length $\ell$, then the received signal at the end of the delay line would have a delay corresponding to range $R$, based on Equation 3.2.

### 3.1.2 Emulating a Doppler Shift

Introducing a Doppler shift in the received signal can be done either before the signal enters the delay line or after, it doesn't matter. However, if the Doppler shift is generated before the signal is delayed, then at least two splitters would be required as opposed to three if the shift is introduced after the delay line.

One way to generate a Doppler shift is to modulate the transmitted RF signal with a Doppler frequency. In the analog world, a mixer is normally used for modulation purposes. A simple balanced mixer, however, will produce double sidebands of equal power. If this approach is followed, then there always will be a positive and negative Doppler shift which means that for a given range (delay), a 2-D FFT process will always show two targets having the same range but opposite Doppler frequencies. Therefore, simulating a single target would require single-sideband modulation.

*Single-Sideband Modulation*

One way to achieve single-sideband modulation is to combine two double-sideband signals with a 90° splitter. A 90° splitter splits the input signal such that the two output signals are both copies of the parent signal but are 90° out of phase relative to one another. One unique property of such a device is that it can be used as a summer. When used as a combiner, the signal entering the 90° port will first be delayed by 90° before the summation takes place. By properly adjusting the phase of one Doppler signal, either the upper or lower sidebands will destructively combine leaving only one sideband. Figure 3.1 shows the setup used for achieving single-sideband modulation. The same input transmit signal is connected to the

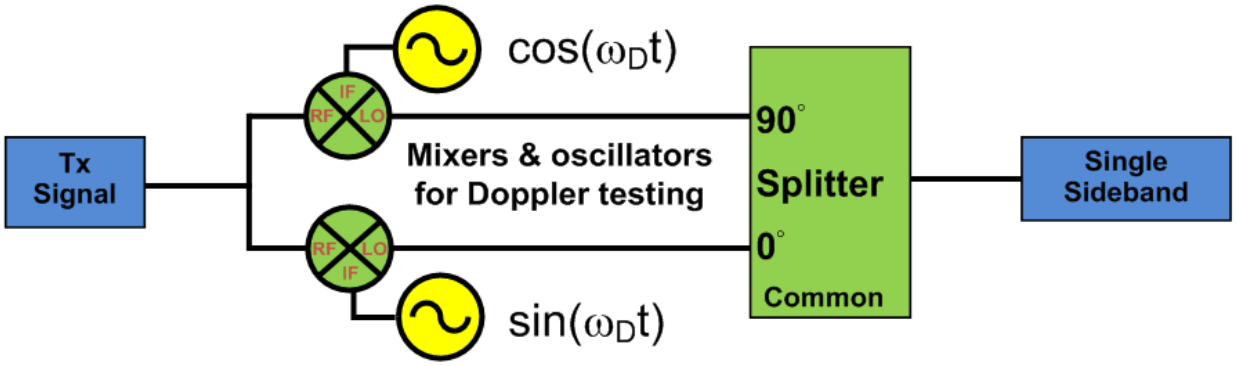


**Figure 3.1 Single-sideband modulation setup.**

RF ports of both mixers. The local oscillators (yellow) are sinusoids representing the Doppler frequency. These sinusoids have been referred to as LOs but are connected to the mixer's IF ports (and not the LO ports), because from an earlier section, the maximum Doppler frequency was found to be 694 Hz, and

only the IF port of the mixers used supported such low frequencies. Note that the upper LO is shown as a *cosine* term while the lower is a *sine* function which can be achieved by delaying the phase of the upper LO by 90°. In practice, properly adjusting the phase requires that the signal generators that are used to generate the Doppler frequencies be phase-locked.

To show mathematically how a single-sideband can be accomplished with this setup, allow (for simplicity) the mixers' input to be a tone with a frequency of $\omega_C$, or the carrier frequency. The output of the mixers will be the product of the carrier frequency and the mixers' LO signal (i.e. the Doppler frequency), as shown in the following equations:

$$\boldsymbol{cos(\omega_C t)} * \boldsymbol{cos(\omega_D t)} = \frac{1}{2} cos(\omega_C t + \omega_D t) + \frac{1}{2} cos(\omega_C t - \omega_D t) \qquad (Upper\ Product) \tag{3.3a}$$

$$\boldsymbol{cos(\omega_C t)} * \boldsymbol{sin(\omega_D t)} = \frac{1}{2} sin(\omega_C t + \omega_D t) - \frac{1}{2} sin(\omega_C t - \omega_D t) \qquad (Lower\ Product) \tag{3.3b}$$

Before the two signals are combined, the upper product will undergo a phase delay of 90°, as shown in Equation 3.4.

$$\mathbf{90°\ Phase\ Delay} \Longrightarrow \frac{1}{2}\cos(\omega_C t + \omega_D t - 90°) + \frac{1}{2} cos(\omega_C t - \omega_D t - 90°) \tag{3.4}$$

Rewriting the previous equation in terms of *sine* yields,

$$\mathbf{90°\ Phase\ Delay} \Longrightarrow \frac{1}{2}\sin(\omega_C t + \omega_D t) + \frac{1}{2} sin(\omega_C t - \omega_D t) \tag{3.5}$$

The sum of Equations 3.3b and 3.5 will be the output of the combiner $S(t)$ which in this case is an upper sideband.

$$\boldsymbol{S(t)} = \sin(\omega_C t + \omega_D t) \tag{3.6}$$

### 3.1.3 Emulating the Leakage Signal

It has been shown that introducing a Doppler shift using single-sideband modulation requires two mixers and two identical mixer inputs. To simulate the leakage signal, an additional (third) copy of the transmit signal is needed. Although a 3-way splitter can accomplish this, a 4-way splitter was used since it was readily available.

To combine the leakage signal with the delayed and Doppler shifted signal, a 2-way splitter can be used. Recall that a splitter can also be used as a combiner. The combined signal must then be split into five

copies, one for each receive channel. Also, testing all five receive channels simultaneously is only required when measuring the AoA, however, the loopback setup being presented is intended to simulate only range and Doppler and not AoA. The combined signal was split with a 4-way splitter since it was already bought.

### 3.1.4 Summary

Figure 3.2 shows the resulting test setup that can be used to emulate range, Doppler and the leakage signal. Note that the leakage signal must be properly attenuated so that the leakage signal's power at the receiver input corresponds to what it would be in reality. (Therefore, an attenuator was placed at one of the 4-way splitter's outputs). For example, if the transmit power is +25 dBm and the antenna isolation is 39 dB (see Figure 2.3), then the received signal power needs to be -14 dBm. The attenuator pad right after the delay line is also necessary for the same reason. There is also an attenuator placed right before the 4-way splitter which can be used to adjust the incoming mixer's drive power.

Also, shown in the setup is an additional delay for the leakage signal as well as the transmitted signal (before the power amplifier). Being able to vary the delay of only the leakage or transmitted (or both) signals can be helpful during testing.

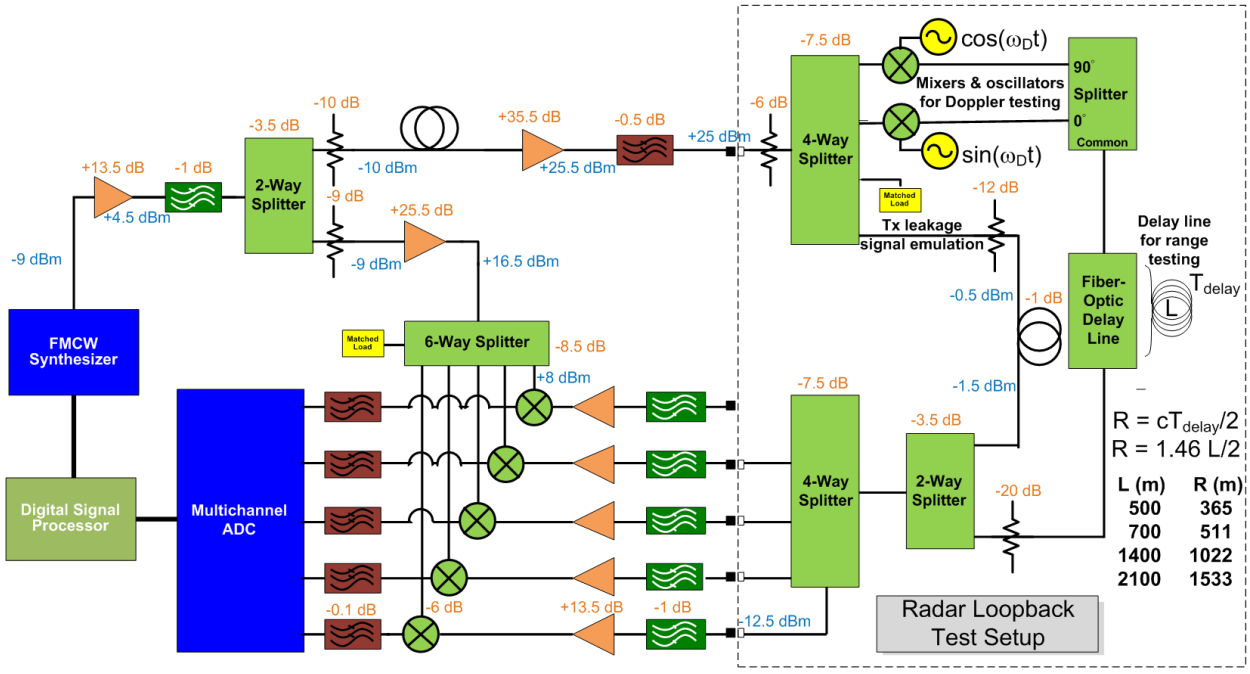


**Figure 3.2 Loopback setup for testing an FMCW radar.**

## 3.2 Loopback Test Results

To simulate the maximum range of 800 m using the loopback test setup that was presented in the previous section, an 1100-m fiber-optic delay line was used based on Equation 3.2. To simulate a single Doppler frequency of 600 Hz, two 600 Hz tones from two synchronized function generators were input into the mixers' IF ports. To make sure that single-sideband modulation was achieved, the output of the 90° splitter (used as combiner) was monitored with a spectrum analyzer while the phase of one of the sinusoids was increased until only one sideband was left on the analyzer. The resulting 2-D FFT of this single sideband modulated carrier (transmit chirp) is shown in Figure 3.3. The carrier signal that exists is a result of the test setup and will not be present when the system is tested in the air onboard the Cessna. The signal has a fast-time (range) frequency of about 400 kHz which corresponds to a range of about 800 m based on Equation 3.2. The slow-time (Doppler) frequency of 600 Hz corresponds to a Doppler frequency of about 600 Hz as it should. Notice the powerful leakage signal at zero Doppler and low range frequencies as predicted by theory. It is important to make sure that the leakage signal does not saturate the ADC since doing so will render the 2-D FFT results useless. Note that the leakage signal is present for all range frequencies. At this point, a question might be asked. What if a target is mapped to some bin on the range (fast-time) axis but is undetected because the leakage power happens to be greater

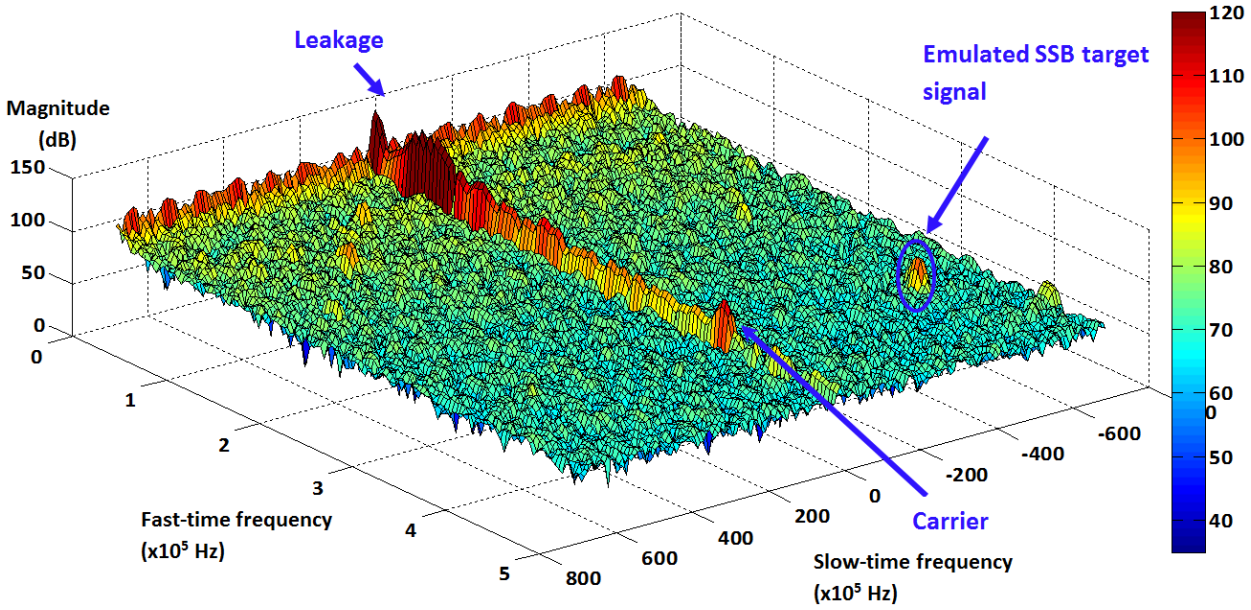


**Figure 3.3 2-D FFT result due to a simulated range of 800 m and a Doppler frequency of 600 Hz.**

than the signal power at that bin? Could that lead to an unexpected collision? To answer this question, it needs to be understood that the fast-time axis corresponds to all range bins with zero Doppler, which

means that the radial velocity for any such range bin is zero. Therefore, a collision cannot occur since the radar and target are not moving toward each other.

The rest of what makes up this 2-D image is noise. When the SNR of a signal is to be determined, it is measured based on the power of this noise floor.

### 3.2.1 ADC Noise

When the SNR of the signal was measured, it was found to be tens of dB lower than what theory predicted. After numerous different tests, it was determined that the reason behind such a loss in SNR was due to the relatively high noise contribution of the ADC resulting from the quantization process. Since the selected ADC has a 12-bit accuracy, the magnitude of the noise voltage is equivalent to the voltage corresponding to the least significant bit (LSB). To better understand the impact of ADC noise, consider the following example: Assume that the signal power right *before* the ADC is -60 dBm, and the noise power is -30 dBm. The SNR before the ADC, therefore, is -30 dB. If the coherent integration process results in 50 dB of SNR improvement, then the final SNR should be +20 dB. Such reasoning is only possible if the noise of the ADC is much smaller than the thermal noise (-30 dBm) relative to which the +20 dB SNR was determined. Consider now the ADC to have a noise power of -15 dBm. Since the ADC noise is much stronger than the thermal noise now, the SNR must be measured relative to the ADC noise power. Right after the ADC (but before the 2-D FFT) the SNR would now be -45 dB, and after the integration process it would increase to +5 dB (assuming again an SNR improvement of 50 dB).

One way to solve this problem is by simply adding additional amplifiers in the IF chain before the ADC to the point where the thermal noise is made equivalent to the noise of the ADC. Note that these amplifiers will also increase signal power, and since they will be placed in the IF chain (i.e., far from the receiver front end), the increase in the overall receiver noise figure due to the added amplifiers' inherent noise will be minimal as conveyed through Equation 2.15. Therefore, the SNR (before the ADC) will remain about the same as before the introduction of additional amplifiers.

Placing more amplifiers in the receiver chain, however, will inevitably increase the power of the leakage signal at the input to the ADC. This is a problem because the leakage signal could saturate the ADC. To decrease the leakage power while keeping the desired signal power constant, a high-pass filter (HPF) can be inserted in the IF chain. Recall that the leakage signal maps to a very low fast-time (range) frequency and so a proper HPF will be able to attenuate the low frequency leakage signal while passing the signal of interest.

*Selecting a HPF*

The cutoff frequency of the HPF will depend on the lowest anticipated beat frequency, which will depend on the lower range detection requirement. For a range of 300 m, the corresponding beat frequency ($\Delta f$) is 150 kHz, based on Equation 1.9 (see Appendix A.8). Therefore, the 3-dB cutoff frequency of the HPF needs to be lower than 150 kHz so as not to attenuate the 150 kHz signal.

The HPF must have a steep roll-off, because according to Figure 3.3, the leakage signal is quite powerful up to about 100 kHz and it was mentioned previously that the 3-dB cutoff frequency would need to be less than 150 kHz. Mini-Circuits' ZFHP-0R12 was chosen due to its high rejection of signals below 90 kHz and its specifications can be seen in the following table. According to the datasheet, this filter has an insertion loss of over 30 dB at 85 kHz and more than 70 dB at 50 kHz.

**Table 3.1 Mini-Circuits' IF high-pass filter specifications.**

| Parameters | Value |
|---|---|
| **Model** | ZFHP-0R12+ |
| **Stopband (MHz) (Loss > 12 dB)** | DC to 0.090 |
| **3-dB Cutoff Frequency (MHz)** | 0.096 |
| **Insertion Loss @ 0.150 MHz (dB)** | 0.4 |
| **Max. Input Power (dBm)** | 5 |

*IF Amplifier*

Determining the amount of additional amplification needed to raise the thermal noise to the ADC's noise level, can easily be accomplished using a variable gain amplifier. By slowly increasing its gain while constantly monitoring the 2-D FFT results, the noise floor at some point will start to rise. Once the noise floor is raised by 3 dB, at that point the thermal noise will be equivalent (in power) to the ADC noise. If a variable amplifier is not available, a fixed amplifier with a variable attenuator can be used which was the case in this project. The specifications of the amplifier used are provided in Table 3.2.

The test revealed that an additional 24 dB of gain would increase the thermal noise enough to be comparable to the ADC noise power. It should be mentioned that this additional gain was found when the built-in PGA was set to 34 dB of gain. Tests also showed that at least two of the HPFs would be necessary to sufficiently attenuate the leakage signal.

Table 3.2 Mini-Circuits' IF amplifier specifications

| Parameters | Value |
|---|---|
| **Model** | ZFL-500LN+ |
| **Frequency Range (MHz)** | 0.1 to 500 |
| **Gain (dB)** | 24 |
| **Noise Figure (dB)** | N/A |
| **Input Return Loss (dB)** | 20 |
| **Output Return Loss (dB)** | 22 |
| **Output 1 dB Compression Point (dBm)** | ~7 |
| **Max. Input Power (dBm)** | 5 |
| **DC Supply (V)** | 12 |

Figure 3.4 shows the modified radar design that includes the IF amplifier as well as two HPFs. The filters have been placed before the amplifier to keep the leakage signal from saturating the amplifier. Recall that the worst case coupling between the transmit and receive antenna was -39 dB, which means that if +25 dBm of transmit power is used, the leakage power at the receiving antennas will be -14 dBm and about -8 dBm at the output of the mixer. Had the IF amplifier been placed right after the mixer, this -8 dBm leakage signal would have saturated the amplifier since the gain of the amplifier is 24 dB and its $P^{1dB}$ is about +7 dBm.

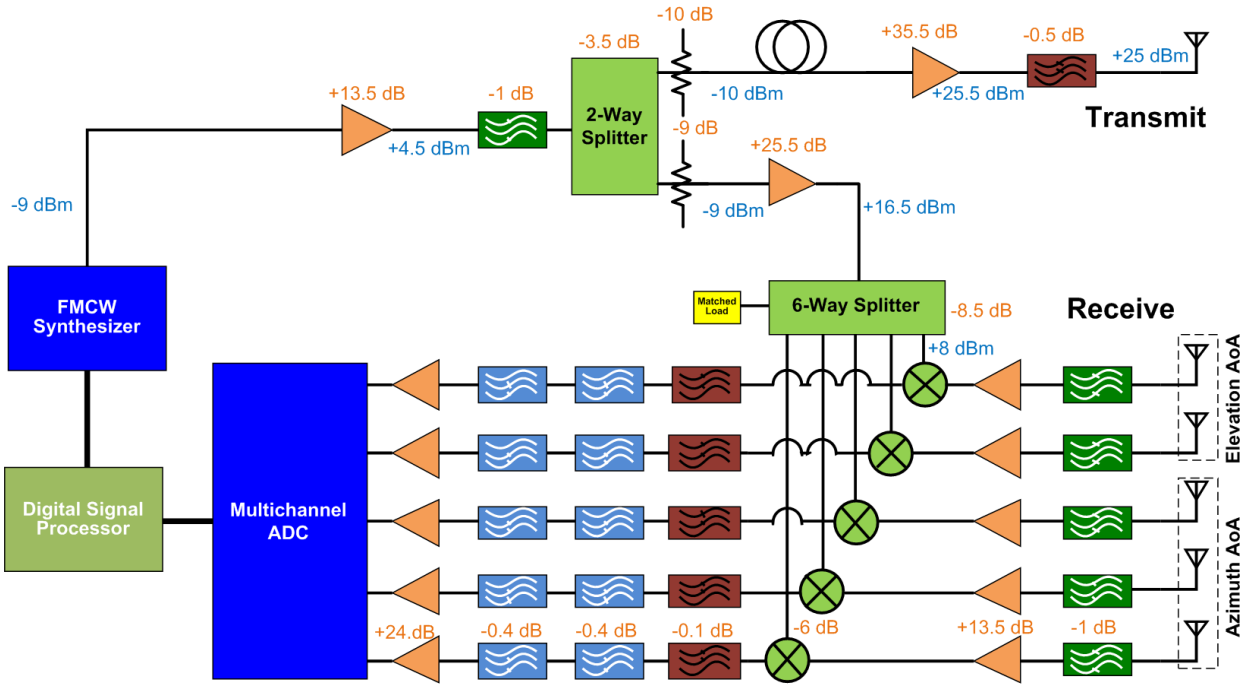


Figure 3.4 Final FMCW radar design.

### 3.2.2 Loopback Test with Additional IF Gain and HPFs

With the additional IF amplifier and two HPFs, the 2-D FFT result for a simulated range of 584 m is shown in Figure 3.5. The loopback setup was configured to simulate a range is of 584 m. Note that the familiar carrier signal is an artifact of the test setup and will not be present during an actual flight test. There are now two targets present (enclosed in blue circles) with equal range but opposite Doppler frequency. This is due to double-sideband modulation and in reality would represent two targets of equal range with one moving toward the radar and the other moving away from it. Note also how much the leakage signal is suppressed with the additional HPFs in the IF chain by comparing this figure to Figure 3.3. An interesting anomaly appears in the 2-D plot whose presence also existed for other range and Doppler simulations. This anomaly is expected to disappear during actual flight tests.

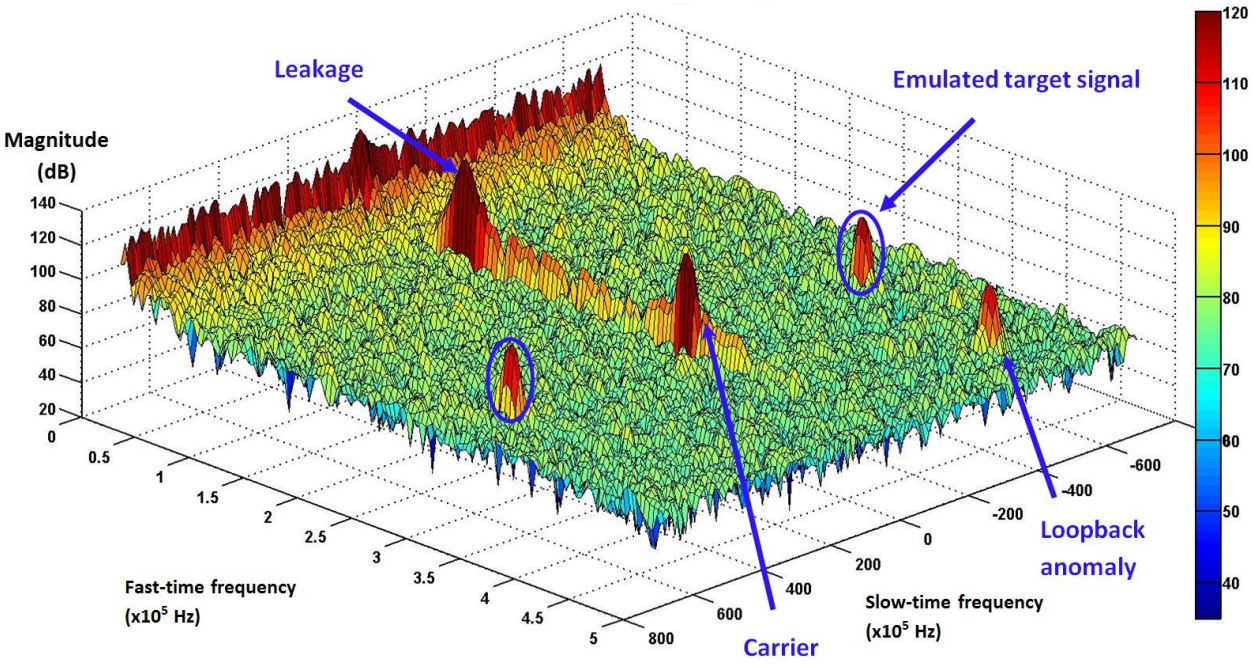


**Figure 3.5 2-D FFT result for a simulated range of 584 m based on the final FMCW radar design.**

*System Performance*

The fast-time (range) frequency of the emulated target in this simulation was measured to be 305.9 kHz while the predicted frequency was 305.6 kHz. In this particular range simulation, the uncertainty in the measurement is 300 Hz which is equivalent to about 0.6 m in terms of range (see Appendix A.9). Note that the bandwidth of the signal was programmed to be 15.7 MHz (not 15 MHz) which is the value used in calculating the range uncertainty of 0.6 m. It is worth mentioning that the uncertainty of 0.6 m is not the true and final range accuracy of the system. The true range accuracy will be found by measuring the

length of time that it takes for the signal to pass through a given length of fiber-optic delay line and comparing the delay's corresponding (range) frequency with the 2-D FFT target's (range) frequency.

To determine the maximum detectable range, the input receiver power was decreased to the point where the resulting SNR of the emulated target after the FFT process was 10 dB. A SNR of 10 dB is a widely accepted signal-to-noise ratio for proper detection. This resulted in a minimum detectable signal (MDS) of -125 dBm. Based on the radar range equation and assuming a RCS of 1 $m^2$, the maximum detectable range was found to be 430 m. It is important to note that this range corresponds to a SNR of 10 dB and not 24 dB that resulted in 1.5° of accuracy in the AoA error analysis. A SNR of 10 dB at a range of 430 m is quite low when compared to the theoretical SNR of around 28.7 dB at a range of 800 m (see Appendix A.10).

The total gain and noise figure of the modified receiver design (shown in Figure 3.4) was calculated to be 63.6 dB and 3.5 dB, respectively (see Appendix A.10). Table 3.3 summarizes the radar specifications based on the design in Figure 3.4.

**Table 3.3 Final radar specifications.**

| Parameters | Value |
|---|---|
| **Type** | FMCW |
| **Center Frequency (GHz)** | 1.445 |
| **Bandwidth (MHz)** | 15 |
| **Sweep Repetition Period (μs)** | 200 |
| **Transmit Power (W/dBm)** | 0.316/25 |
| **Receiver Gain (dB)** | 63.6 |
| **Receiver Noise Figure (dB)** | 3.5 |
| **Transmit Antenna** | single monopole |
| **Receive Antenna** | 3 element azimuth array<br>2 element elevation array |
| **Range Resolution (m)** | 10 |
| **Doppler (radial velocity) Resolution (Hz)** | 10 |
| **Update Rate (Hz)** | 10 |
| **Sampling Frequency (MHz)** | 4 |
| **Power Consumption** | 12 V @ 1.66 A (20 W) |

Figure 3.6 shows the assembled FMCW radar on an aluminum plate. The PCB in the upper-left corner is a field-programmable gate array (FPGA) used to perform the 2-D FFT. The device in the lower-right hand corner is the power amplifier. It is much bigger than any other amplifier due to the size of the required heat sink. The entire system can be powered by a 12 V supply. Note that the assembled radar is big and heavy and certainly will not be flown onboard the Yak-54 model plane. However, the system's

size and weight is not a constraint since this is only a prototype design and one that will be tested onboard a pilot flown Cessna.

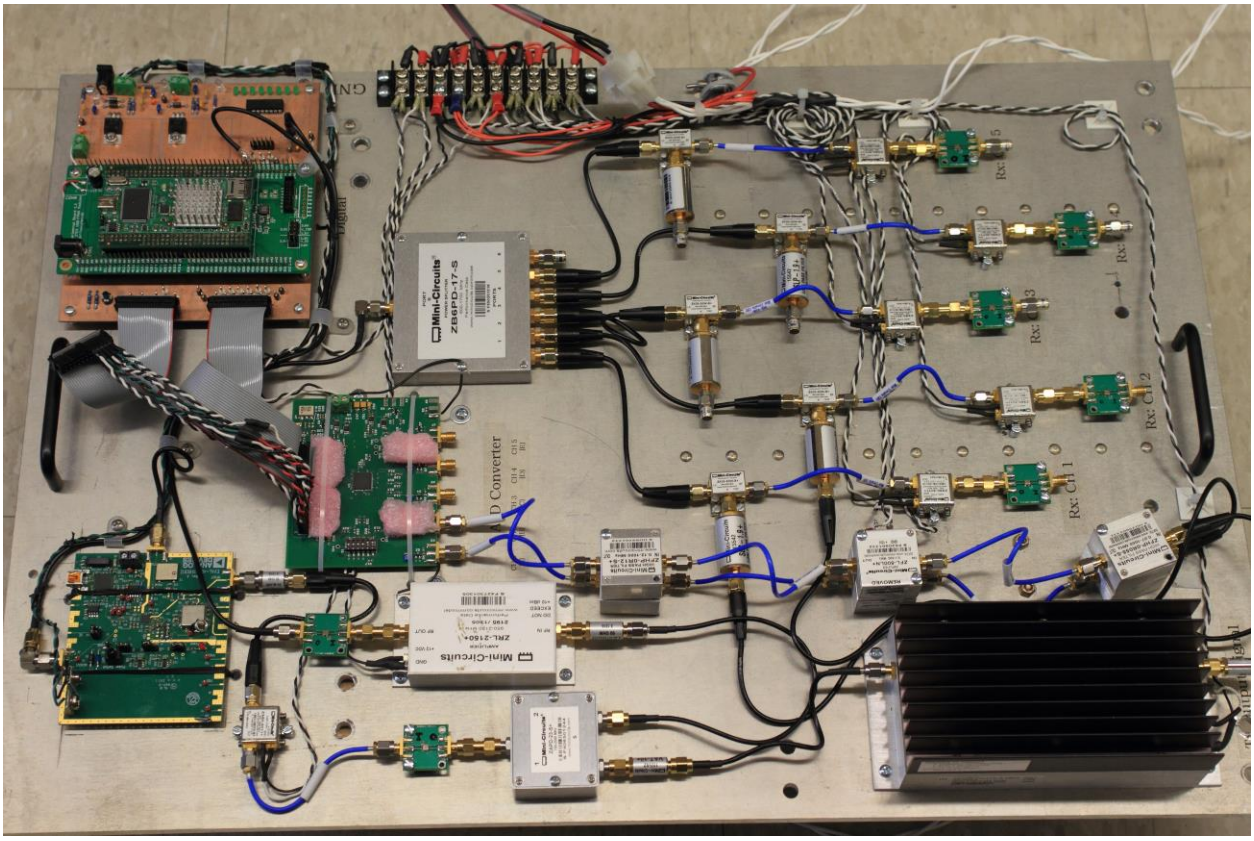


**Figure 3.6 Prototype radar on an aluminum plate (26 in x 18.5 in).**

# Chapter 4: Conclusions and Future Work

## 4.1 Conclusions

In this thesis, the analysis of a prototype sense-and-avoid FMCW radar system was presented as well as the justification for the components used in the system design. Based on the latest tests and an SNR of 10 dB, the radar was found to have a minimum detectable signal of -125 dBm corresponding to a maximum detectable range of 430 m assuming the target's RCS is 1 $m^2$. AoA error (due to thermal noise) simulation revealed that at least 17.5 dB of SNR is required to achieve the required angular accuracy of 3° if the AoA update rate is 10 Hz, and at least 19.5 dB of SNR is required if the update rate is 5 Hz. The maximum AoA rate of change simulation showed that if both the radar and intruder are moving at their maximum speeds of 36 m/s and 54 m/s, respectively, then the maximum possible change in the AoA will be 0.59° in a period of 100 ms (one observation period).

## 4.2 Future Work

The maximum detectable range of 430 m is based on a SNR of 10 dB which does not meet the minimum 17.5 dB necessary to achieve the required angular accuracy, let alone the possibility of updating the AoA at 5 Hz which requires a minimum of 19.5 dB of SNR. If the maximum detectable range is to be 800 m, the SNR must be higher yet by approximately an additional 12 dB (with a doubling in range, the received signal power is 12 dB lower). Therefore, if the sensor is to detect up to 800 m *and* meet the required angular accuracy, the minimum SNR would need to be 29.5 dB for an AoA update rate of 10 Hz, and 31.5 dB if the refresh rate is 5 Hz. However, based on theoretical calculations, the SNR after the 2-D FFT process for a range of 800 m should have been about 23 dB and at a range of 430 m it should have been about 34 dB (see Appendix A.11). The exact reason why there is a loss of 24 dB at a range of 430 m remains to be found.

The only target detection test that the system has underwent thus far is the loopback ground test. The system has yet to be tested onboard an aircraft where the performance of the system's antennas will come into play.

Once the prototype system is made functional such that all requirements are met, the system needs to be miniaturized so that it can be tested onboard a UAS. The miniaturization aspect will involve replacing all SMA connectorized components on the aluminum plate with just the necessary integrated chips (ICs) on a PCB. It might also be of interest to increase the center frequency (consequently decreasing the wavelength) to reduce the size of antennas.

AoA estimation can theoretically be done with four antennas: Three in the horizontal plane for azimuth detection (as described in this paper) with the fourth antenna directly on top of one of the three azimuth antennas such that there is a pair of antennas in the vertical plane for elevation detection.

# References


[1] Cox, V., Gilligan, M., & Grizzle, D. (2012, Sept. 28). *Integration of unmanned aircraft systems into the national airspace system.* Federal Aviation Administration, Retrieved Dec. 15, 2013, from: http://www.suasnews.com/wp-content/uploads/2012/10/FAA-UAS-Conops-Version-2-0-1.pdf

[2] EIA. (2007, June). *About U.S. natural gas pipelines – Transporting natural gas.* Independent Statistics & Analysis. Retrieved Dec. 17, 2013, from: http://www.eia.gov/pub/oil_gas/natural_gas/analysis_publications/ngpipeline/index.html

[3] Garcia, G., Keshmiri, S., & Stastny T. (2013, July). Collision and obstacle avoidance in unmanned aerial systems using morphing potential field navigation and nonlinear model predictive control. *ASME Journal of Dynamic Systems, Measurements and Control*, Under Review.

[4] Huerta, M. (2013, Nov. 7). *Integration of civil unmanned aircraft systems (UAS) in the national airspace system (NAS) roadmap.* Federal Aviation Administration, Retrieved Dec. 19, 2013, from: http://www.faa.gov/about/initiatives/uas/media/uas_roadmap_2013.pdf

[5] Mullarkey, B. (2008, Dec. 7). *The differences between pulse radars and FMCW ones*. Retrieved Dec. 18, 2013, from http://www.slideshare.net/Nguynng11/fmcw-vs-pulse-radar

[6] Neto, J. F. F. (2013). *Receiver antenna array for a multichannel sense-and-avoid radar for small UAVs.* (ITTC-FY2013-TR-70093-01). Lawrence, Kansas: University of Kansas, Information & Telecommunication Technology Center. Retrieved from http://www.ittc.ku.edu/publications/documents/neto2013_TR_70093-01.pdf

[7] Shanmugan, S., & Breipohl, A. (1988). *Random signals: Detection, estimation and data analysis.* New York: John Wiley & Sons, Inc.

[8] Silva, G. (2013, Sept. 12). *Unmanned aerial vehicles for precision agriculture.* Michigan State University, Retrieved Dec. 15, 2013, from http://msue.anr.msu.edu/news/unmanned_aerial_vehicles_for_precision_agriculture

# Appendix A

**A.1:** *Received Signal Power for a Range of* $800\ m$

$$P_S^{Rx} = \frac{P_T G^2 \lambda^2 \sigma}{(4\pi)^3 R^4} \quad (Monostatic\ Geometry)$$

$$\boldsymbol{P_S^{Rx}(dBm)} = P_T(dBm) + 2 * G(dBi) + 2 * \lambda(\text{dB}) + \sigma(dBsm) - 3 * 4\pi(\text{dB}) - 4 * R(dB)$$

$$= 25dBm + 2 * 0dBi - 2 * 6.83dB + 0dBsm - 3 * 11dB - 4 * 29.03dB$$

$$= 25dBm - 13.65dB - 33dB - 116.12dB$$

$$= \boldsymbol{-137.8\ dBm}$$

**A.2:** *Noise Power at Receiving Antenna*

$$P_N^{Rx} = kTB_{RF} \quad (Using\ 15\ MHz\ for\ bandwidth\ at\ Rx)$$

$$\boldsymbol{P_N^{Rx}(dBm)} = k\left(\frac{dBm}{K-Hz}\right) + T(dBK) + B(dB-Hz)$$

$$= -198.6\frac{dBm}{K-Hz} + 24.6dBK + 71.8dB-Hz$$

$$= \boldsymbol{-102.2\ dBm}$$

**A.3:** *Received Leakge Power*

$$P_R = \frac{P_T G^2 \lambda^2}{(4\pi)^2 R^2} \quad (One\ Way\ with\ a\ range\ of\ 1\ m)$$

$$\boldsymbol{P_R\ (dBm)} = P_T(dBm) + 2 * G(dBi) + 2 * \lambda(\text{dB}) - 2 * 4\pi(\text{dB}) - 2 * R(dB)$$

$$= 25dBm + 2 * 0dBi - 2 * 6.83dB - 2 * 11dB - 2 * 0dB$$

$$= 25dBm - 13.66dB - 22dB$$

$$= \boldsymbol{-10.66\ dBm}$$

**A.4:** *Beat Frequency for a Range of* $1852\ m$

$$\Delta \boldsymbol{f'} = \frac{2Range * B}{c * SRP}$$

$$= \frac{2 * 1852 * 15 * 10^6}{3 * 10^8 * 200 * 10^{-6}}$$

$$= \boldsymbol{926\ kHz}$$

**A.5:** *Transmit and Receive Antenna Isolation* (see also A. 3)

$$\boldsymbol{Loss} = \frac{P_T}{P_R}$$

$$\boldsymbol{Loss(dB)} = P_T(dBm) - P_R(dBm)$$

$$= 25dBm - (-10.66dBm)$$

$$= \boldsymbol{35.66\ dB}$$

**A.6:** *Minimum Gain Required to Transmit* 27 *dBm*

$$\boldsymbol{Gain(dB)} = P_T(dBm) + Splitter\ Loss(dB) + BPF\ Insertion\ Loss(dB) - Input\ Power(dBm)$$

$$= 27dBm + 3.5dB + 1.25dB - (-9\ dBm)$$

$$= \boldsymbol{40.8dB}$$

**A.7:** *Minimum Gain Required to Achieve LO Power of* 8 *dBm*

$$\boldsymbol{Gain(dB)} = P_{LO}(dBm) + BPF\ Insertion\ Loss(dB) + Splitter\ Loss(dB) - Input\ Power(dBm)$$

$$= 8dBm + 1.25dB + 3.5dB + 8.3dB - (-9dBm)$$

$$= \boldsymbol{30.05dB}$$

**A.8:** *Beat Frequency for a Range of* 300 *m*

$$\Delta \boldsymbol{f'} = \frac{2Range * B}{c * SRP}$$

$$= \frac{2 * 300 * 15 * 10^6}{3 * 10^8 * 200 * 10^{-6}}$$

$$= \boldsymbol{150\ kHz}$$

**A.9:** *Range Uncertainty for an Emulated Range of* 584 *m*

$$\boldsymbol{Range} = \frac{c * \Delta f * SRP}{2B}$$

$$= \frac{3 * 10^8 * 300 * 200 * 10^{-6}}{2 * 15 * 10^6}$$

$$= \boldsymbol{0.6\ m}$$

## **A.10:** *Theoretical SNR after the FFT process for a range of 800 m*

*Signal Power at Receiving Antenna*

$$\boldsymbol{P_s^{Rx}(dBm) = -137.8\ dBm} \quad (see\ A.1)$$

*Noise Power at Receiving Antenna*

$$P_N^{Rx} = kTB_{IF} \quad (Using\ 1\ MHz\ for\ IF\ bandwidth\ )$$

$$\boldsymbol{P_N^{Rx}(dBm)} = k\left(\frac{dBm}{K-Hz}\right) + T(dBK) + B(dB-Hz)$$

$$= -198.6\frac{dBm}{K-Hz} + 24.6dBK + 60dB-Hz$$

$$= \boldsymbol{-114\ dBm}$$

*SNR at Receiving Antenna*

$$SNR^{Rx} = \frac{P_S^{Rx}}{P_N^{Rx}}$$

$$\boldsymbol{SNR^{Rx}(dB)} = P_S^{Rx}(dBm) - P_N^{Rx}(dBm)$$

$$= -137.8dBm - (-114dBm)$$

$$= \boldsymbol{-23.8\ dB}$$

*Receiver Noise Figure*

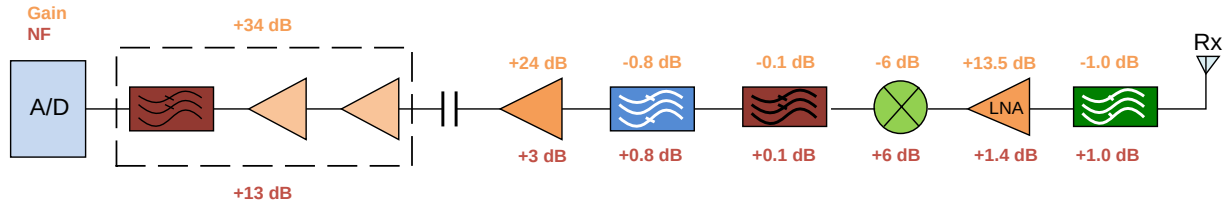


| | |
|---|---|
| $G_1$ = -1.0 dB = .79, $F_1$ = 1.0 dB = 1.26 | $G_5$ = -0.8 dB = 0.83, $F_5$ = 0.8 dB = 1.2 |
| $G_2$ = 13.5 dB = 22.39, $F_2$ = 1.4 dB = 1.38 | $G_6$ = 24 dB = 251.19, $F_6$ = 3 dB = 2.00 |
| $G_3$ = -6 dB = .25, $F_3$ = 6 dB = 4 | $G_7$ = 34 dB = 2511.89, $F_7$ = 13 dB = 19.95 |
| $G_4$ = -0.1 dB = 0.98, $F_4$ = 0.1 dB = 1.02 | |

$$\boldsymbol{G_{eff}} = G_1G_2G_3G_4G_5G_6G_7, \quad = 2.269 * 10^6 \quad = \boldsymbol{63.6\ dB}$$

$$\boldsymbol{F_{eff}} = F_1 + \frac{F_2-1}{G_1} + \frac{F_3-1}{G_1G_2} + \frac{F_4-1}{G_1G_2G_3} + \frac{F_5-1}{G_1G_2G_3G_4} + \frac{F_6-1}{G_1G_2G_3\,G_4G_5} + \frac{F_7-1}{G_1G_2G_3\,G_4G_5G_6}$$

$$= 1.26 + 0.48 + 0.17 + 0.0045 + 0.046 + 0.278 + 0.021$$

$$= 2.26$$

$$= 3.5\ \boldsymbol{dB}$$

*SNR at Input to ADC*

$$SNR^{ADC} = \frac{SNR^{Rx}}{F_{eff}}$$

$$\boldsymbol{SNR^{ADC}(dB)} = SNR^{Rx}(dB) - F_{eff}(dB)$$

$$= -23.8(dB) - 3.5$$

$$= \boldsymbol{-27.3(dB)}$$

*SNR after 2-Dimensional FFT*

$$SNR^{FFT} = \frac{SNR^{ADC} G_{coh}^{FFT}}{Loss_{Window}} \quad (800x500\ Data\ Matrix)$$

$$\boldsymbol{SNR^{FFT}} = SNR^{ADC}(dB) + G_{coh}^{FFT}(dB) - Loss_{Window}(dB)$$

$$= -27.3(dB) + 56.02(dB) - 6(dB)$$

$$\therefore \boldsymbol{SNR^{FFT}} = \boldsymbol{22.72(dB)}$$

## A.11: *Theoretical SNR after the FFT process for a range of 430 m*

*Signal Power at Receiving Antenna for a range of 430 m*

$$\boldsymbol{P_s^{Rx}(dBm)} = P_T(dBm) + 2 * G(dBi) + 2 * \lambda(\mathrm{dB}) + \sigma(dBsm) - 3 * 4\pi(\mathrm{dB}) - 4 * R(dB)$$

$$= 25dBm + 2 * 0dBi - 2 * 6.83dB + 0dBsm - 3 * 11dB - 4 * 26.33$$

$$= 25dBm - 13.65dB - 33dB - 105.32dB$$

$$= \boldsymbol{-127\ dBm}$$

*SNR at Receiving Antenna*

$$\boldsymbol{SNR^{Rx}(dB)} = P_s^{Rx}(dBm) - P_N^{Rx}(dBm) \quad (see\ A.10\ for\ P_N^{Rx})$$

$$= -127dBm - (-114dBm)$$

$$= \boldsymbol{-13\ dB}$$

*SNR after 2-Dimensional FFT*

$$\boldsymbol{SNR^{FFT}(dB)} = SNR^{Rx}(dB) - F_{eff}(dB) + G_{coh}^{FFT}(dB) - Loss_{Window}(dB)$$

$$= -13dB - 3.5 + 56.02(dB)$$

$$\therefore \boldsymbol{SNR^{FFT}(dB)} = \boldsymbol{33.52(dB)}$$

**A.12:** *Find angle $\phi$ of the intruder vector such that $V_{SUM}$ is directed toward a keep − out point*

- *All angles are measured from the positive $x-$ axis which corresponds to zero degrees*

$V_R\angle\alpha - Radar\ (UAS)\ vector$

$V_I\angle\phi - Intruder\ vector$

$V_{SUM}\angle\theta - Sum\ vector$

$$V_{SUM}\angle\theta = V_R\angle\alpha + V_I\angle\phi$$

$$V_{SUM}(\hat{\boldsymbol{a}}_{\boldsymbol{x}}cos\theta + \hat{\boldsymbol{a}}_{\boldsymbol{y}}sin\theta) = V_R(\hat{\boldsymbol{a}}_{\boldsymbol{x}}cos\alpha + \hat{\boldsymbol{a}}_{\boldsymbol{y}}sin\alpha) + V_I(\hat{\boldsymbol{a}}_{\boldsymbol{x}}cos\phi + \hat{\boldsymbol{a}}_{\boldsymbol{y}}sin\phi)$$

*grouping like terms,*

$$V_{SUM}(\hat{\boldsymbol{a}}_{\boldsymbol{x}}cos\theta) = V_R(\hat{\boldsymbol{a}}_{\boldsymbol{x}}cos\alpha) + V_I(\hat{\boldsymbol{a}}_{\boldsymbol{x}}cos\phi)$$

$$V_{SUM}(\hat{\boldsymbol{a}}_{\boldsymbol{y}}sin\theta) = V_R(\hat{\boldsymbol{a}}_{\boldsymbol{y}}sin\alpha) + V_I(\hat{\boldsymbol{a}}_{\boldsymbol{y}}sin\phi)$$

*solving for $V_{SUM}$,*

$$V_{SUM} = \frac{V_R(\hat{\boldsymbol{a}}_{\boldsymbol{x}}cos\alpha) + V_I(\hat{\boldsymbol{a}}_{\boldsymbol{x}}cos\phi)}{(\hat{\boldsymbol{a}}_{\boldsymbol{x}}cos\theta)} = \frac{V_Rcos\alpha + V_Icos\phi}{cos\theta}$$

$$V_{SUM} = \frac{V_R(\hat{\boldsymbol{a}}_{\boldsymbol{y}}sin\alpha) + V_I(\hat{\boldsymbol{a}}_{\boldsymbol{y}}sin\phi)}{(\hat{\boldsymbol{a}}_{\boldsymbol{y}}sin\theta)} = \frac{V_Rsin\alpha + V_Isin\phi}{sin\theta}$$

*Equating the previous two equations and solving for $\phi$,*

$$\frac{V_Rcos\alpha + V_Icos\phi}{cos\theta} = \frac{V_Rsin\alpha + V_Isin\phi}{sin\theta}$$

$$V_Rcos\alpha sin\theta + V_Icos\phi sin\theta = V_Rsin\alpha cos\theta + V_Isin\phi cos\theta$$

$$V_I(sin\phi cos\theta - cos\phi sin\theta) = V_R(cos\alpha sin\theta - sin\alpha cos\theta)$$

$$sin\phi cos\theta - cos\phi sin\theta = \frac{V_R}{V_I}(cos\alpha sin\theta - sin\alpha cos\theta)$$

*Using a trigonometric identity,*

$$\frac{1}{2}\sin(\phi+\theta) + \frac{1}{2}\sin(\phi-\theta) - \left(\frac{1}{2}\sin(\phi+\theta) - \frac{1}{2}\sin(\phi-\theta)\right) = \frac{V_R}{V_I}(cos\alpha sin\theta - sin\alpha cos\theta)$$

$$sin(\phi-\theta) = \frac{V_R}{V_I}(cos\alpha sin\theta - sin\alpha cos\theta)$$

$$\phi - \theta = \sin^{-1}\left(\frac{V_R}{V_I}(cos\alpha sin\theta - sin\alpha cos\theta)\right)$$

$$\phi = \sin^{-1}\left(\frac{V_R}{V_I}(cos\alpha sin\theta - sin\alpha cos\theta)\right) + \theta$$

*Radar will be traveling in the positive* $x-$ *direction*

*To keep radar at the origin, intruder will instead move additionally by* 3.6 $m$ *in the minus* $x-$ *direction* $\Rightarrow\ \alpha = 180°$

$$\therefore \boldsymbol{\phi = \sin^{-1}\left(-\frac{V_R}{V_I}sin\theta\right) + \theta}$$

# Appendix B

## B.1: *AoA Estimation Error MATLAB Code*

```
clc, clear all, close all
% Purpose:
% Determine the standard deviation of the angle-of-arrival (AoA) error,
% given a certain signal-to-noise ratio (SNR).
%
% Assumptions:
% Two dipole antennas are used to determine the AoA (elevation angle) of
% the reflected signal.  The AoA will be determined from the two antennas'
% signal's phase difference.
% The two antennas are located along the z-axis (vertical).
% The distance separating the two antennas is one half of a wavelength.
% The returned signal power (excluding noise) is 0 dBw.  Its RMS voltage is
% therefore: 1 Vrms, assuming a 1 Ohm resistance.
% ========================================================================
% ************************************************************************
% Given a SNR of 24 dB and a signal power of 0 dBw, determine the
% corresponding RMS noise voltage.
SNRdB = 24;                 % signal-to-noise ratio [dB]
% ind = 1;                  % index used when varying SNR (see line # 66)
% for SNRdB = 5:35          % vary the SNR to produce a plot
SNR = 10^(SNRdB/10);        % SNR in linear 'units'
Vn = 1/sqrt(SNR);           % RMS noise voltage, iff, Ps = 0 dBw and R = 0 Ohm.
% ========================================================================
% ************************************************************************
% Generate a complex vector for antenna 1, and a complex vector for
% antenna 2.  These vectors will include both the true signal and
% gaussian noise.  When added together, the resulting complex signal will
% resemble the signal that will in actuallity result from the FFT process.

% gaussian distributions centered at 0 with n samples
n = 1e6;
r1 = randn(1,n);
r2 = randn(1,n);
r3 = randn(1,n);
r4 = randn(1,n);
% true voltage signals (withough any noise)
    % unity magnitude (iff Ps = 0dBw) signal with true phase of 30 degrees
    Vs1 = exp(j*30*pi/180);
    % unity magnitude (iff Ps = 0dBw) signal with true phase of 135 degrees
    Vs2 = exp(j*135*pi/180);
% complex signals resembling gaussian noise
Vgn1 = (Vn/sqrt(2)*(r1+j*r2));  % complex gaussian noise from antenna 1
Vgn2 = (Vn/sqrt(2)*(r3+j*r4));  % complex gaussian noise from antenna 2
% complex vectors with true signals and gaussian noise
V1 = Vs1 + Vgn1;    % complex vector from antenna 1 after the FFT
V2 = Vs2 + Vgn2;    % complex vector from antenna 2 after the FFT
% ========================================================================
```

```
% ************************************************************************
% Determine the phase distributions of vector 1, vector 2, and the
% difference in vector 1' and vector 2's phase distributions.
phase1 = angle(V1);         % phase of complex vector from antenna 1 [rad]
phase2 = angle(V2);         % phase of complex vector from antenna 2 [rad]
phase3 = phase2 - phase1;   % phase difference [rad]
% ========================================================================
% ************************************************************************
% Determine the AoA distribution as well as the standard deviation of the
% AoA distribution, given the phase difference distribution.
AoA = acosd(phase3/pi);    % AoA distribution [degrees]
stdev = std(AoA)           % standard deviation of AoA distribution [degrees]
% ========================================================================
%%%%%%%%%%%%%%%%%%%%%%%%%%%%%%%%%%%%%%%%%%%%%%%%%%%%%%%%%%%%%%%%%%%%%%%%%%%
% By varying the SNR (top) the standard deviation (sigma) of the AoA will
% change. To plot sigma vs SNR, uncomment the following as well as lines 23
% and 24.

% stdev_m(ind) = std(AoA);    % multiple standard deviations for various SNR
% x1(ind) = SNRdB;            % x-axis (needed for plot)
% ind = ind + 1;              % increment the index by 1
% end
%
% figure
% plot(x1,pow2db(stdev_m))    % uncomment this line to plot AoA error in dB
% %plot(x1,(stdev_m))         % comment this line out to plot in dB
% title('AoA Deviation vs SNR')
% title('')
% xlabel('SNR [dB]')
% ylabel('10*Log_10(AoA Error \circ)')
% grid on
%%%%%%%%%%%%%%%%%%%%%%%%%%%%%%%%%%%%%%%%%%%%%%%%%%%%%%%%%%%%%%%%%%%%%%%%%%%
% ************************************************************************
% Plot the AoA distribution
x2 = min(AoA):1e4/n:max(AoA);
figure
hist(AoA,x2)
title('Probability Density of AoA')
%title('')
xlabel('\theta \circ')
ylabel('\Psi_\sigma(\theta)')
ylabel('Counts')
axis([46, 62, 0, max(hist(AoA,x2)),])
grid on

% %normalized PDF
% y = hist(AoA,x2)/max(hist(AoA,x2))*0.3989;
% figure
% bar(x2,y)
% ========================================================================
```

```
% ************************************************************************
% Verify that the noise power is 24 dB below signal power.  Recall that the
% signal power is 0 dBw.
for ind = 1:numel(Vgn1)
    if ind == 1
        Esum = abs(Vgn1(ind))^2;
    else
        Esum = abs(Vgn1(ind))^2 + Esum;
    end
end
Psum = Esum/numel(Vgn1);        % noise power assuming a resistance of 1 ohm
Psum_dBw = pow2db(Psum)         % noise power [dBw]
```

## **B.2:** *Maximum AoA Rate of Change MATLAB Code*

```
clc, clear all, close all
% Purpose:
%Simulate the maximum rate of change of the AoA for a period of 100 ms
%for all targets that could potentially come within 100 m of the radar.
%
% Assumptions:
%Radar is moving toward +X direction.
%Targets (intruders) cannot come within 100 m of the radar
%UASs fly at max speed of 36 m/s.
%Intruder trajectories will always be linear.
%
% Definitions:
%theta:    Angle (measured from 0 deg. from +x-axis) corresponding to the
%(sum) vector that is the sum of the radar vector and UAS vector
%phi:      Angle (measured from 0 deg. from +x-axis) corresponding to the
%UAS vector only.
%Sum Vector:   Resulting vector when adding UAS and intruder vectors
%
% Procedure:
%A radar is placed at the origin (0,0).  Points around the radar are
%created (all) having a radius of 100 m. These points will correspond to
%the "keepout" zone. A circle made of points (all) having a radius of 300
%m will also be centered at the origin.  This circle will represent
%potential intruders. If the radar and all intruders are traveling at the
%same speed, a little more than half of the points on the intrduer circle
%will actually need to be considered, since the other (slightly less than)
%half of points (intrduders) will never catch up with the radar.
% ========================================================================
V_r = 36;               % radar speed [m/s]
V_t = 54;               % target (intruder) speed [m/s]
radar = [0,0];          % initial radar location (X,Y) [m]
%Angle EXACTLY opposite of desired radar movement/direction.  This angle
%is measured if 0 [deg] is the positive x-axis. To keep the radar at the
%origin, the intruder will instead move EXACTLY opposite of radar
%direction
gamma = pi;
%Rate of change depends on the refresh rate (observation period)
refresh_rate = 10;      % samples/sec [Hz]
% ************************************************************************
%Create a keepout 2-D circle with any # of points
numPoints_k = 25;       % # of points in circle (between 0 and 2pi)
radius_k = 100;         % radius of cirlce [m]
x_center_k = 0;         % x coordinate of center of cirlce
y_center_k = 0;         % y coordinate of center of circle
%Using a function that generates a circle
[X_k,Y_k] = circle(x_center_k,y_center_k,radius_k,numPoints_k);

%Create an intruder 2-D circle with any # of points
numPoints_t = 100;      % # of points in circle (between 0 and 2pi)
radius_t = 300;         % radius of cirlce [m]
```

```
%%%%%%%%%%%%%%%%%%%%%%%%%%%%%%%%%%%%%%%%%%%%%%%%%%%%%%%%%%%%%%%%%%%%%%%%%%%%
% ind = 1;                % uncomment when plotting max. AoA vs range
% for radius_t = 200:25:800   % plot AoA rate of change vs range
%%%%%%%%%%%%%%%%%%%%%%%%%%%%%%%%%%%%%%%%%%%%%%%%%%%%%%%%%%%%%%%%%%%%%%%%%%%%
x_center_t = 0;         % x coordinate of center of cirlce
y_center_t = 0;         % y coordinate of center of circle
[X_t,Y_t] = circle(x_center_t,y_center_t,radius_t,numPoints_t);
% ========================================================================
% ************************************************************************
%Find the angle "theta" that corresponds to the "sum vector" for every
%intruder-keepout combination. These angles will result in the intruder
%comining within 100 m of the radar.
theta = total_ang(X_k,Y_k,X_t,Y_t);
%Find the angle of the intruder vector. This is the direction toward which
%only the intruder is moving. (The total (intruder and UAS) angle is theta)
phi = asin(V_r/V_t*(cos(gamma)*sin(theta)-sin(gamma)*cos(theta)))+theta;
 %Find the magnitude (velocity) of the "sum" vector
 for R = 1:numel(X_t)
     for C = 1:numel(X_k)
         V_sum(R,C) = (V_r*cos(gamma) + V_t*cos(phi(R,C)))/cos(theta(R,C));
     end
 end
 %Find the coordinates of the intruder relative to (origin/radar) after one
 %observation period (100 ms). (New coordinates will have two t's (tt)).
 %This is done by treating a keepout point as the origin and finding the
 %location of the intruder in polar coordinates.  The range (magnidude) of
 %the intruder's location is reduced by "V_sum" and the intruder's polar
 %coordinates are mapped back to cartesian coordinates which are modified
 %by adding the location of the keepout so that the intruder coordinate is
 %relative to the origin (basically undo what was done in line #87)
 for R = 1:numel(X_t)
     for C = 1:numel(X_k)
             [theta_ik(R,C),range(R,C)] = cart2pol(X_t(R)-X_k(C),Y_t(R)-Y_k(C));
             range_dV(R,C) = range(R,C) - V_sum(R,C)/refresh_rate;
             [X_tt(R,C),Y_tt(R,C)] = pol2cart(theta_ik(R,C),range_dV(R,C));
             X_tt(R,C) = X_tt(R,C) + X_k(C);
             Y_tt(R,C) = Y_tt(R,C) + Y_k(C);
     end
 end
 %The AoA rate of change will be determined from a triangle whose three
 %points are: Origin (0,0),Intruder initial location, Intruder modified
 %location.
  for R = 1:numel(X_t)
      for C = 1:numel(X_k)
        % Find distance between radar and intruder coordinate after 0.1 s.
        range_rt_dV(R,C) = sqrt((X_tt(R,C))^2 + (Y_tt(R,C)^2));
        % distance between initial and after 0.1 s coordinates of intruder
        dV(R,C) = V_sum(R,C)/refresh_rate;
        % subtended angle (angle opposite of side dV) from Law of Cosines
        alpha(R,C) = subt_angle(range_rt_dV(R,C),radius_t,dV(R,C));   % in degrees
        %alpha(R,C) = real(alpha(R,C));
      end
  end
```

```
%Determine which intruder and toward which keepout point the "sum" vector
%points that results in the maximum subtended angle. "alpha_values" are
%the maximum alpha values per column and the "Row_A_vector" keeps track of
%which row the maximum alpha (in a column)was taken from.
[alpha_values,Row_t_vector] = max(alpha);
%alpha_max is the final single maximum alpha value and Col_A represents
%the column from which this maximum alpha came from.  Col_A corresponds to
%a specific keepout point, the movement toward which maximizes alpha.
[alpha_max,Col_k] = max(alpha_values);
%Determine the row (specific intruder) that generated this maximum alpha.
Row_t = Row_t_vector(Col_k);
%%%%%%%%%%%%%%%%%%%%%%%%%%%%%%%%%%%%%%%%%%%%%%%%%%%%%%%%%%%%%%%%%%%%%%%%%%%
% uncomment the following section and lines 57 & 58 to plot the AoA rate of
% change vs various intruder ranges.

% alpha_maxx(ind) = alpha_max;
% distance(ind) = radius_t;
% ind = ind + 1;
% end
% figure
% plot(distance,alpha_maxx)
% %title('AoA Rate of Change vs Range')
% xlabel('Range [m]')
% ylabel('AoA rate of change [\circ/10-Hz]')
% grid on
%%%%%%%%%%%%%%%%%%%%%%%%%%%%%%%%%%%%%%%%%%%%%%%%%%%%%%%%%%%%%%%%%%%%%%%%%%%
%Plot the intruder and keepout circles as well as the radar location. Show
%in red the specific intruder and keepout points that result in max. AoA.
figure
hold on
scatter(X_t,Y_t,'b','fill');
scatter(X_k,Y_k,'r','fill');
scatter(radar(1),radar(2),75,'c','fill')      % radar
scatter(X_t(Row_t),Y_t(Row_t),125,'b')
scatter(X_k(Col_k),Y_k(Col_k),125,'r')
scatter(X_k(Col_k),Y_k(Col_k),1,'w','fill')

hold off
xlabel('X-axis [m]')
ylabel('Y-axis [m]')

legend('Intruders','Keepout Zone','Radar (0,0,0)','Worst Case Intruder',...
    'Corresponding Keepout',['Max \angle =  ',num2str(alpha_max,3),'\circ'])
grid on
axis square
```